UNIVERSIDADE ESTADUAL DE CAMPINAS

Faculdade de Engenharia Química

HELOISA PEREIRA DE SÁ COSTA

APLICAÇÃO DO RESÍDUO DA EXTRAÇÃO SÓLIDO-LÍQUIDO DE ALGINATO DA ALGA *SARGASSUM FILIPENDULA* PARA BIOADSORÇÃO DE ÍONS ALUMÍNIO

APPLICATION OF SOLID-LIQUID ALGINATE EXTRACTION WASTE FROM ALGAE *SARGASSUM FILIPENDULA* FOR ALUMINUM ION BIOADSORPTION

Campinas – São Paulo

2021

HELOISA PEREIRA DE SÁ COSTA

APLICAÇÃO DO RESÍDUO DA EXTRAÇÃO SÓLIDO-LÍQUIDO DE ALGINATO DA ALGA *SARGASSUM FILIPENDULA* PARA BIOADSORÇÃO DE ÍONS ALUMÍNIO

APPLICATION OF SOLID-LIQUID ALGINATE EXTRACTION WASTE FROM ALGAE *SARGASSUM FILIPENDULA* FOR ALUMINUM ION BIOADSORPTION

Dissertação apresentada à Faculdade de Engenharia Química da Universidade Estadual de Campinas (UNICAMP) como parte dos requisitos exigidos para obtenção do título de Mestra em Engenharia Química.

Orientadora: Profa. Dra. Melissa Gurgel Adeodato Vieira

ESTE EXEMPLAR CORRESPONDE À VERSÃO FINAL DA DISSERTAÇÃO DEFENDIDA PELA ALUNA HELOISA PEREIRA DE SÁ COSTA, ORIENTADA PELA PROF.ª. DR.ª. MELISSA GURGEL ADEODATO VIEIRA.

Campinas – São Paulo

2021

Ficha catalográfica
Universidade Estadual de Campinas
Biblioteca da Área de Engenharia e Arquitetura
Rose Meire da Silva - CRB 8/5974

C823a

Costa, Heloisa Pereira de Sá, 1994-
Application of solid-liquid alginate extraction waste from algae Sargassum filipendula for aluminum ions bioadsorption / Heloisa Pereira de Sá Costa. – Campinas, SP : [s.n.], 2021.

Orientador: Melissa Gurgel Adeodato Vieira.
Dissertação (mestrado) – Universidade Estadual de Campinas, Faculdade de Engenharia Química.

1. Adsorção. 2. Alumínio. 3. Sargassum. 4. Resíduos. 5. Biotecnologia. 6. Biotecnologia. I. Vieira, Melissa Gurgel Adeodato, 1979-. II. Universidade Estadual de Campinas. Faculdade de Engenharia Química. III. Título.

Informações para Biblioteca Digital

Título em outro idioma: Aplicação do resíduo da extração sólido-líquido de alginato da alga Sargassum filipendula para bioadsorção de íons alumínio
Palavras-chave em inglês:
Adsorption
Aluminum
Sargassum
Residue
Biotechnology
Seaweed
Área de concentração: Engenharia Química
Titulação: Mestra em Engenharia Química
Banca examinadora:
Melissa Gurgel Adeodato Vieira [Orientador]
Marcelino Luiz Gimenes
Lucas Meili
Data de defesa: 05-03-2021
Programa de Pós-Graduação: Engenharia Química

Identificação e informações acadêmicas do(a) aluno(a)
- ORCID do autor: https://orcid.org/0000-0003-3765-043X
- Currículo Lattes do autor: http://lattes.cnpq.br/2147758335809075

Folha de Aprovação da Dissertação de Mestrado da aluna HELOISA PEREIRA DE SÁ DA COSTA e aprovada em 05 de março de 2021 pela comissão examinadora da defesa constituída pelos doutores:

Profa. Dra. Melissa Gurgel Adeodato Vieira - Presidente e Orientadora

FEQ / UNICAMP

Videoconferência

Dr. Marcelino Luiz Gimenes

UEM/Maringá

Videoconferência

Dr. Lucas Meili

Universidade Federal de Alagoas/Maceió

Videoconferência

A Ata de defesa com as respectivas assinaturas dos membros encontra-se no SIGA/Sistema de Fluxo de Tese e na Secretaria do Programa da Unidade.

AGRADECIMENTOS

Agradeço primeiramente à toda a minha família, em especial aos meus pais Henrique e Elaine (em memória), pelo amor incondicional e por terem sempre oferecido todo o suporte necessário não só para a obtenção desse título, que foi um sonho que sonhamos juntos, mas no desenvolvimento de tudo que me trouxe até aqui. Ao meu irmão Fábio, minha cunhada Ana Flávia e meus amados sobrinhos Fábio Jr. e Renato, por todo amor, pela compreensão dos momentos longe e pelos ótimos momentos passados perto.

Agradeço especialmente a minha grande amiga Cinthia, que entrou nessa jornada junto comigo na Unicamp e foi meu porto seguro em todos os momentos sejam eles difíceis ou alegres.

Agradeço à professora Melissa Gurgel Adeodato Vieira pela oportunidade, pela orientação e por todos os ensinamentos divididos nesta caminhada.

Agradeço a todos os amigos feitos durante este período no LEA/LEPA, em especial ao Talles por toda a ajuda, troca de ideias, risadas, choros e companhia noites adentro no laboratório. Não poderia deixar de mencionar também a Giani e o Thiago que me ajudaram muito sendo com as caracterizações ou com discussão de resultados. Todos vocês foram fundamentais para que essa pesquisa tenha chegado até aqui.

Agradeço aos meus amigos de Três Lagoas, que sempre compreenderam a minha ausência em momentos importantes, mas nunca deixaram de me apoiar, com uma união que transcende qualquer distância.

Agradeço a todos os funcionários da Unicamp, em especial aos da Faculdade de Engenharia Química, pela disposição e auxílio no desenvolvimento desta pesquisa.

À Coordenação de Aperfeiçoamento de Pessoal de Nível Superior (CAPES) - Código de Financiamento 001.

À Fundação de Amparo à Pesquisa do Estado de São Paulo – FAPESP (Proc. 2017/18236-1 e 2019/11353-8).

Ao Conselho Nacional de Desenvolvimento Científico e Tecnológico – CNPq (Proc 308046/2019-6) pelo financiamento do projeto de pesquisa, tornando possível a produção desta dissertação.

RESUMO

O alumínio é um metal classificado como tóxico e seu extensivo uso em processos industriais gera grandes quantidades de efluentes contaminados. Estes efluentes usualmente são descartados em corpos hídricos, porém a legislação exige seu pré-tratamento antes de seu descarte. Com isso, neste trabalho visou-se analisar a eficácia do resíduo proveniente da extração sólido-líquido de alginato (aqui denominado como RES) na remoção de íons alumínio. O planejamento experimental de Delineamento Composto Central Rotacional (DCCR) associado à Metodologia de Superfície de Resposta foi realizado para determinar valores ótimos de fatores operacionais e mostrou que a agitação não tem impacto significativo no processo. Já a concentração de alumínio na solução e a dosagem da biomassa tem relação diretamente proporcional entre si. Por isso, a dosagem de RES otimizada foi definida em 2 g/L, enquanto a concentração inicial de alumínio em até 3 mmol/L revela favorecer o processo. O pH apresentou grande influência no processo de bioadsorção de alumínio por RES e melhores resultados de remoção foram obtidos em pH 4. O estudo cinético revelou que o tempo de equilíbrio do processo (60 min) não foi influenciado pelo aumento da concentração inicial. A modelagem matemática indicou a ocorrência de mais de um mecanismo de remoção, estando associada a interações físicas e químicas como a troca iônica. Além disso, os ajustes do modelo de equilíbrio revelaram que o resíduo possui uma superfície energeticamente heterogênea. A capacidade máxima de remoção obtida foi de 1.431 mmol/g a 25 ºC. O estudo termodinâmico revelou que o processo é exotérmico e espontâneo. O projeto simplificado em batelada mostrou que uma pequena quantidade de resíduo (140g) é necessária para tratar 10 L de solução, removendo 90% de alumínio a 1 mmol/L. O bioadsorvente foi caracterizado antes e após a adsorção de Al e as análises indicaram que o biomaterial é composto basicamente por macroporos, além de possuir considerável resistência térmica em temperaturas até 150 ºC. No comparativo de eficiência, o resíduo se destaca em relação a outros bioadsorventes derivados de algas previamente estudados para a remoção de alumínio. A avaliação da troca iônica junto com a análise SEM-EDX mostrou que os íons sódio são os principais cátions trocáveis envolvidos no mecanismo de bioadsorção do sistema Al-RES, seguido do cálcio, magnésio e uma pequena participação dos íons potássio. A análise de FTIR e o ensaio de esterificação de grupo funcional demonstraram que principalmente grupos carboxílicos, amina e sulfonato estão envolvidos no sistema de bioadsorção estudado. O estudo em leito fixo mostrou que os parâmetros otimizados da operação contínua foram obtidos à vazão de alimentação de 0,5 mL/min e concentração inicial de alumínio de 1 mmol/L. Nessas condições o tempo de ruptura foi de cerca de 200 minutos com satisfatório percentual de remoção de alumínio (93%). O eluente testado mais adequado para a regeneração do bioadsorvente foi a solução ácida de 0,1 mol/L de HNO_3. O resíduo demonstrou aplicação viável, mantendo bom desempenho por até quatro ciclos contínuos de bioadsorção/dessorção. A modelagem matemática das curvas de ruptura revelou que o modelo fenomenológico DualSD e o modelo matemático Yan et al. foram os que melhor descreveram os dados em leito fixo. O sistema de bioadsorção de alumínio utilizando RES demonstrou em geral ter um potencial viável para aplicações futuras em efluentes reais, sendo eficaz, reutilizável e de baixo custo.

Palavras-chave: Bioadsorção. Alumínio. Alga marrom. *Sargassum filipendula*. Resíduo.

ABSTRACT

Aluminum is a metal classified as toxic and its extensive use in industrial processes generates large amounts of effluents contaminated. Such effluents are usually disposed of in water bodies, but the legislation requires pre-treatment of these before their disposal. Therefore, this work aims to analyze the efficacy of the residue from the solid-liquid extraction of alginate (here called RES) in the removal of aluminum ions. The experimental design of the Rotational Central Composite Design (RCCD) associated with the Response Surface Methodology (RSM) was carried out to determine optimal values of important factors in the operation and showed that the agitation has no significant impact on the process, since the concentration of the solution and the dosage of the biomass is directly proportional to each other, so the optimized RES dosage was set at 2 g/L, while the aluminum initial concentration up to 3 mmol/L reveals to favor the process. pH showed to be a very influent parameter in the aluminum biosorption by RES and, better removal results were obtained at pH 4. The kinetic study revealed that the process equilibrium time (60 min) was not influenced by the increase in the initial concentration. Mathematical modeling indicated the occurrence of more than one removal mechanism, being associated with physical and chemical interactions such as ion exchange. In addition, the equilibrium model adjustments revealed that the residue has an energetically heterogeneous surface. The maximum removal capacity obtained was 1.431 mmol/g at 25 ºC. Thermodynamic study revealed that the process is exothermic and spontaneous. The simplified batch design showed that a small amount of waste (140 g) is needed to treat 10L of solution, removing 90% of aluminum at 1 mmol/L. The biosorbent was characterized before and after Al adsorption and the analyses indicated that the biomaterial is basically composed of macropores, in addition to having considerable thermal resistance at temperatures up to 150 ºC. In the efficiency comparison, the biomaterial stands out in relation to other biosorbents derived from algae previously studied for the removal of aluminum. The evaluation of ion exchange along with SEM-EDX analysis showed that sodium ions are the main exchangeable cations involved in the bio-absorption mechanism of the Al-RES system, followed by calcium, magnesium and a small share of potassium ions. The FTIR analysis and the functional group esterification test showed that mainly carboxylic groups, amine and sulfonate are involved in the studied biosorption system. The fixed bed study showed that the optimized parameters of continuous operation were a feed flow rate of 0.5 mL/min and an initial aluminum concentration of 1 mmol/L. Under these conditions the breakthrough time was about 200 minutes with a satisfactory percentage of aluminum removal (93%). The eluent tested most suitable for the regeneration of the biosorbent was the acid solution of 0.1 mol/L of HNO_3. The residue demonstrated viable application, maintaining good performance for up to four continuous cycles of bioadsorption/desorption. The mathematical modeling of the breakthrough curves revealed that the phenomenological model DualSD and the mathematical model Yan et al. were the ones that best described the data in fixed bed. The aluminum bioadsorption system using RES has demonstrated in general to have a viable potential for future applications in real effluents, being effective, reusable and of low cost.

Keywords: Bioadsorption. Aluminum. Brown seaweed. *Sargassum filipendula*. Residue.

LISTA DE ILUSTRAÇÕES

LISTA DE TABELAS

SUMÁRIO

1. Introdução

Os metais tóxicos como alumínio, cádmio, cromo e zinco podem ser encontrados no meio ambiente de forma natural ou oriundos de efluentes industriais. Processos industriais como a mineração, por exemplo, geram grande quantidade de resíduos que são compostos, principalmente, por estes metais [1,2]. Além da mineração, processos metalúrgicos, de galvanização e de pigmentação também geram efluentes contaminados por metais desta classe [3].

O alumínio é um metal não essencial ao ser humano e que está presente em seu cotidiano. Dentre os metais tóxicos, este é encontrado em maior abundância de forma natural na crosta terrestre [4]. Também está presente em diversos produtos de uso rotineiro, principalmente em embalagens e utensílios de cozinha. Em relação aos resíduos de processos industriais, o alumínio é encontrado, por exemplo, na lama vermelha proveniente do processo de refino de bauxita [5] e em efluentes de estações de tratamento de água [6]. Quando em altas concentrações este metal pode contribuir para o desenvolvimento de doenças relacionadas aos sistemas neurológico e ósseo [3]. O limite máximo de alumínio tolerado em corpos hídricos e efluentes industriais é estabelecido por órgãos de fiscalização ambiental, como o Conselho Nacional do Meio Ambiente (CONAMA), o Conselho Estadual do Meio Ambiente (CONSEMA) e o Instituto Estadual do Ambiente (INEA). A Tabela 1.1 apresenta os valores máximos permitidos de alumínio definidos pelo CONAMA. Já a quantidade máxima deste metal presente em água potável é controlada por setores governamentais nacionais, como o Ministério da Saúde, e internacionais, como a Organização Mundial da Saúde (OMS).

Tabela 1.1 Padrões e valores orientadores da presença de alumínio em águas.

Meio	Valor máximo permitido (mg/L)
Águas doces	0,1 – 0,2
Águas salinas	1,5
Águas salobras	0,1

Existem diversas tecnologias que envolvem processos químicos, físicos e biológicos para remover poluentes de soluções aquosas. No caso da remoção de metais tóxicos técnicas como bioadsorção, precipitação química, tratamento eletroquímico e osmose reversa têm se mostrado viáveis [7]. Por ser um processo de menor custo e grande

eficiência quando comparado aos supracitados, a bioadsorção vem sendo amplamente aplicada para a remoção de metais contaminantes em soluções aquosas [8].

Segundo Fourest e Volesky [9], a bioadsorção é o processo em que materiais biológicos concentram espécies orgânicas ou inorgânicas dissolvidas em soluções aquosas. O processo de bioadsorção utiliza mecanismos físico-químicos passivos que funcionam com base na afinidade entre as células da biomassa (adsorvente) com os íons metálicos (adsorbato) a serem removidos e na diferença de concentração entre a fase líquida e sólida [10]. A principal vantagem desse método é conseguir remover de forma satisfatória metais que estão em baixas concentrações, além da baixa geração de subprodutos contaminados [11].

Dentre as biomassas utilizadas como adsorventes, algas marinhas, microrganismos e resíduos agrícolas vêm sendo amplamente estudados para a remoção de metais tóxicos. As algas se destacam por serem fontes de bioadsorventes de alta disponibilidade e com rápido ciclo de crescimento/produção. Devido à grande viabilidade técnica e econômica no uso das algas como bioadsorventes, Davis e colaboradores [12] analisaram o uso da biomassa de algas marrons na remoção de metais tóxicos como chumbo, cádmio e cobre. Ao contrário de algumas espécies, essas algas possuem parede celular, uma característica importante para o processo de bioadsorção devido aos grupos funcionais presentes em sua estrutura.

O alginato é um biopolímero presente na parede celular das algas marrons e é considerado o principal responsável pelo mecanismo de bioadsorção de metais [13]. Devido ao seu expansivo uso, pode ser considerado um produto com alta competitividade industrial, por isso cresce o interesse em estudar a viabilidade da utilização do rejeito resultante de sua extração sólido-líquido [14,15].

Trabalhos anteriores realizados pelo grupo de pesquisa do Laboratório de Engenharia Ambiental/Laboratório de Engenharia e Processos Ambientais (LEA/LEPA) da Faculdade de Engenharia Química da Unicamp avaliaram que o resíduo da extração do alginato possui potencial para o processo de bioadsorção de metais tóxicos, pois ainda apresenta em sua estrutura grupos funcionais, como carboxílicos e sulfônicos, que favorecem esse processo [16,17].

A busca por tratamentos de efluentes que sejam econômicos, sustentáveis e ainda assim eficientes é uma tendência mundial. A bioadsorção de metais tóxicos utilizando algas marrons e seus derivados abrange todas as vantagens procuradas nestes tratamentos

alternativos como menor geração de resíduo contaminado, possibilidade de reutilização do bioadsorvente e baixo custo. Diversas pesquisas obtiveram resultados promissores utilizando o resíduo proveniente da extração sólido-líquido de alginato da alga *Sargassum filipendula* como material adsorvente para a bioadsorção de diferentes metais tóxicos como cromo, cádmio, cobre, níquel e zinco [18,19]. No entanto, não foram encontrados na literatura estudos aprofundados que investigassem a bioadsorção de alumínio utilizando essa biomassa. Neste contexto, neste trabalho se propôs a avaliação do processo de bioadsorção de íons Al (III) utilizando o resíduo da extração do alginato em sistemas estático e dinâmico de leito fixo, elucidando os mecanismos envolvidos no processo e otimizando o desempenho deste material para a remoção destes íons de soluções aquosas.

1.1 Objetivos

O objetivo geral desta dissertação foi avaliar a remoção de íons alumínio através do processo de bioadsorção utilizando o resíduo proveniente do processo de extração de alginato da alga marrom *Sargassum filipendula* como material adsorvente não convencional e de baixo custo. Para tanto, os seguintes objetivos específicos foram propostos:

a) Obtenção do bioadsorvente a partir da extração sólido-líquido de alginato da alga *Sargassum filipendula*;
b) Avaliar a influência da variação do pH no sistema bioadsortivo;
c) Realizar o planejamento experimental do tipo Delineamento Composto Central Rotacional (DCCR) para a definição das condições ótimas de agitação, quantidade de bioadsorvente e concentração inicial da solução metálica;
d) Investigar a bioadsorção de íons de alumínio em batelada e em sistema dinâmico de coluna de leito fixo;
e) Avaliar o potencial de regeneração/reutilização do bioadsorvente por eluição;
f) Aplicar os modelos matemáticos cinéticos, de equilíbrio e dinâmicos aos dados experimentais e;
g) Caracterizar o bioadsorvente antes e após os ensaios de bioadsorção, visando elucidar os mecanismos envolvidos no processo de remoção.

1.2 Estrutura dos capítulos da dissertação

Esta dissertação é composta por capítulos que são artigos elaborados e submetidos para publicação em periódicos internacionais, os quais se encontram aceito para publicação ou em fase de revisão.

No Capítulo 2 apresenta-se o artigo de revisão intitulado *Biosorption of aluminum ions from aqueous solutions using non-conventional low-cost materials*: *A Review* publicado na revista *Journal of Water Process Engineering*. Este manuscrito traz o levantamento e a discussão de diversos artigos sobre a bioadsorção de alumínio utilizando materiais adsorventes não convencionais, com baixo custo e derivados de matéria prima biológica como microrganismos e algas. Os artigos desta revisão foram criticamente analisados e comparados em relação à cinética, equilíbrio e termodinâmica. Além disso, compilou-se resultados referentes ao tratamento de efluentes reais e apresentou-se as perspectivas futuras de estudo na área.

O Capítulo 3 se refere ao planejamento fatorial realizado com o objetivo de avaliar a influência de determinadas condições operacionais do processo de bioadsorção em relação à capacidade adsortiva e percentual de remoção. Para isto, a agitação, a concentração inicial da solução e a dosagem de RES foram as variáveis selecionadas.

O Capítulo 4 contém o artigo *Application of alginate extraction residue for Al(III) ions biosorption: A complete batch system evaluation*, publicado no periódico *Environmental Science and Pollution Research*. Este artigo teve como objetivo principal estudar a bioadsorção de alumínio em RES em sistema de banho finito avaliando aspectos cinético, de equilíbrio e termodinâmico do processo, além da caracterização da estrutura do bioadsorvente antes e após a remoção de Al. Os resultados foram discutidos buscando principalmente elucidar os possíveis mecanismos envolvidos na remoção.

No Capítulo 5 a troca iônica e o sistema de bioadsorção de íons Al por RES em sistema contínuo de leito fixo foram reportados no artigo *Fixed bed biosorption and ionic exchange of aluminum by brown algae residual biomass*, publicado no periódico *Journal of Water Process Engineering*. Neste manuscrito a bioadsorção de alumínio utilizando o resíduo é discutida em primeiro momento em banho finito, avaliando os possíveis mecanismos de troca iônica e os grupos funcionais chave envolvidos no processo e, com relação ao sistema de leito fixo, apresentou-se um estudo de otimização das condições operacionais e da capacidade de regeneração/reutilização do bioadsorvente. A modelagem matemática das curvas de ruptura visou selecionar o modelo que melhor

prediz o comportamento do sistema. Neste artigo as caracterizações foram realizadas em relação à composição química e à estrutura do resíduo.

Por fim, os Capítulos 6 e 7 apresentam, respectivamente, a discussão geral dos principais resultados obtidos nesta Dissertação, e as conclusões e perspectivas futuras para esta pesquisa.

2. Revisão bibliográfica

Biosorption of aluminum ions from aqueous solutions using non-conventional low-cost materials: A review*

Heloisa Pereira de Sá Costa[1], Meuris Gurgel Carlos da Silva[1], Melissa Gurgel Adeodato Vieira[1]

[1]Department of Processes and Products Design, School of Chemical Engineering, University of Campinas, Albert Einstein Av., 500, Campinas, São Paulo, 13083-852, Brazil

Abstract

Aluminum is one of the most common pollutant found in wastewaters from processes like mining, galvanizing and metal alloy casting. The release of aluminum-contaminated effluents into water bodies may cause several harmful effects on the environment and living beings due to its capacity for gradual bioaccumulation. Biosorption is a process that has gained prominence in water/wastewater treatment for its satisfactory results in removing metal pollutants. This technology has many advantages, like being low-cost and eco-friendly, making it one of the main alternatives to conventional approaches. This review features an overview of studies on biosorption of Al^{3+} ions, highlighting the performance of biosorbents derived from bacterial, fungal and algal biomasses, and agro-industrial wastes. For this purpose, the main mechanisms involved in this process are investigated and discussed regarding its kinetic, equilibrium and thermodynamic behavior. The application of biosorption for treating real effluents and regeneration/reuse of the biosorbents are also presented. Finally, the prospects for future research on Al^{3+} biosorption are outlined.

Keywords: Biosorption; metals; aluminum; wastewater treatment; low-cost biosorbents; biomass.

* Manuscript published in *Journal of Water Process Engineering* 40 (2021) 101925. DOI: 10.1016/j.jwpe.2021.101925. Reprinted with permission from *Journal of Water Process Engineering.*

2.1 Introduction

Water pollution increases exponentially with the intensification of industrial activities. The release of effluents contaminated by toxic metals without proper treatment causes great damage to the environment. Industrial processes such as mining, galvanizing and pigmentation generate significant amounts of waste mainly composed of toxic metals like chromium, lead, arsenic, cadmium and aluminum [1,2].

There are several technologies available that involve chemical, physical and biological processes to remove metals from aqueous solutions. Different methods are studied for the removal of toxic metals from aqueous media, such as biosorption, chemical precipitation, electrochemical treatment and reverse osmosis [3]. Among current treatment processes, biosorption has been widely studied for the removal of polluting metals from aqueous solutions [4]. Promising results have been obtained for the biosorption of toxic metals ranging from zinc, copper, chromium, nickel and cadmium [5–10] to metals with high added value such as silver, gold, platinum and rare earth metals (REMs) [11–13].

Biosorption is a process in which biological materials concentrate organic or inorganic species dissolved in aqueous solutions, e.g., metals, dyes and emerging pollutants [14–16]. This process uses passive physicochemical mechanisms based on the affinity between biomass cells (adsorbent) and the metal ions (adsorbate) to be removed and the difference in concentration between the liquid and solid phase [17]. Its main advantages include low cost, efficiency in removing metals in low concentrations, good selectivity and the ability to regenerate/reuse the adsorbent biomaterial [18]. Among the biomasses used as adsorbents, seaweed, microorganisms and agricultural waste have proved to be efficient in removing toxic metals [19–21].

Aluminum is found in large quantities in its natural form in the earth's crust [22]. Approximately 63 million tons of aluminum were produced worldwide in 2019 [23]. Its widespread use in different industrial sectors that involve aluminum processing, from its mining through finishing procedures such as rolling, machining and casting to its final application as a chemical, produces high amounts of effluents contaminated by this metal. Inadequate disposal of these effluents in bodies of water causes several environmental problems, affecting aquatic systems, soils, plants and living beings [24]. The maximum amount of aluminum tolerated in bodies of water and industrial effluents is determined

by environmental inspection bodies, with small variations between countries. In particular, the maximum amount of this metal tolerated in drinking water is controlled by national and international government sectors linked to the area of health, like the World Health Organization (WHO).

An in-depth literature search, using Scopus database, indicated that over the last 25 years, the biosorption of aluminum has been the subject of several papers. The search was performed using the keywords “biosorption,” “aluminum” and similar. As displayed in Figure 1, the number of publications varies from year to year. However, it is observed that recently in 2016 and 2019, publications on aluminum biosorption were more numerous.

Figure 2.1 Number of articles addressing aluminum biosorption published per year from 1995 to 2020. Data retrieved through in-depth search on Scopus database, selecting publications that involved the terms “biosorption,” “aluminum” and similar.

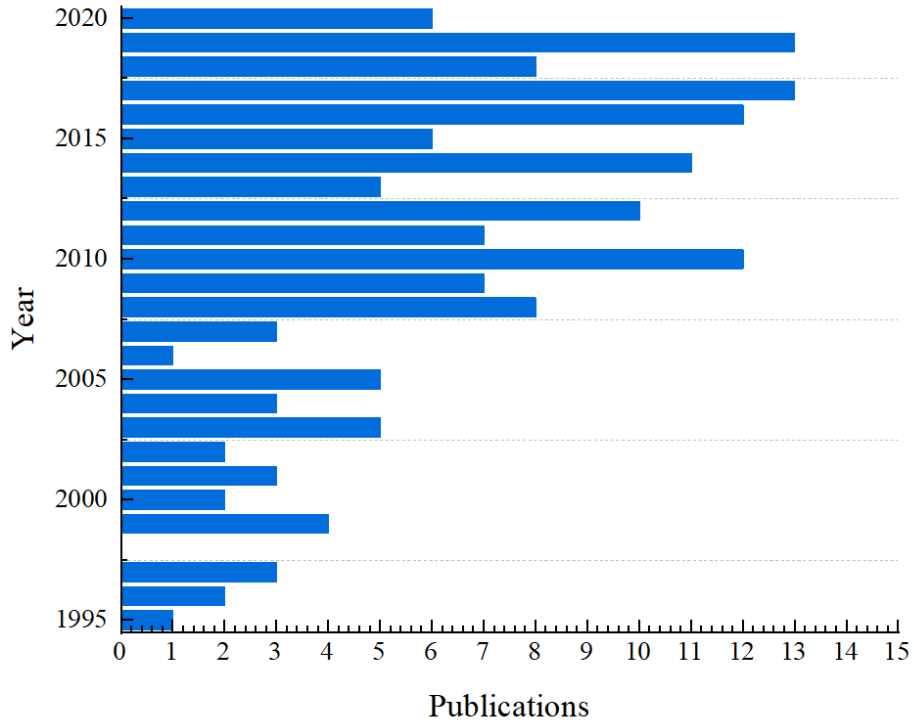

Considering the environmental context, this work features a review of surveys that specifically address the removal of aluminum by biosorption processes that use unconventional and low-cost materials as biosorbents. Therefore, the main topics addressed in this review are: (i) overview of aluminum applications, toxicological effects and legislation; (ii) brief introduction to processes for aluminum removal; (iii) theoretical aspects of biosorption processes – biosorbents, mechanisms, kinetics, equilibrium,

thermodynamics, fixed-bed applications; (iv) performance evaluation of non-conventional biosorbents for aluminum removal (bacteria, fungus, algae and agro-industrial wastes); (v) future prospects for biosorption of aluminum ions.

2.2 Chemical speciation, applications and environmental toxicological effects of aluminum

Classified in group 13-th of the periodic table, aluminum is one of the most common and reactive metals in nature. The form in which it occurs in the environment depends directly on the pH, as this is the main factor governing its solubility in aqueous media. Figure 2 shows the direct dependence between the pH of the medium and the percentage of formation of species derived from the metal. The speciation diagram was simulated using Visual MINTEQ 3.1 software [25] with the initial aluminum concentration of 3 mmol/L. At pH values below 5 the Al^{3+} ion, which is the most toxic form of the metal in the environment, is more easily formed. As the pH increases, the formation of precipitated species ($Al(OH)_3$) is favored, a condition associated with their strong affinity with hydroxide-forming ions, responsible for the phenomenon of precipitation [26,27].

Figure 2.2 Metal speciation of aluminum species obtained using Visual MINTEQ software at initial aluminum solution concentration of 3 mM.

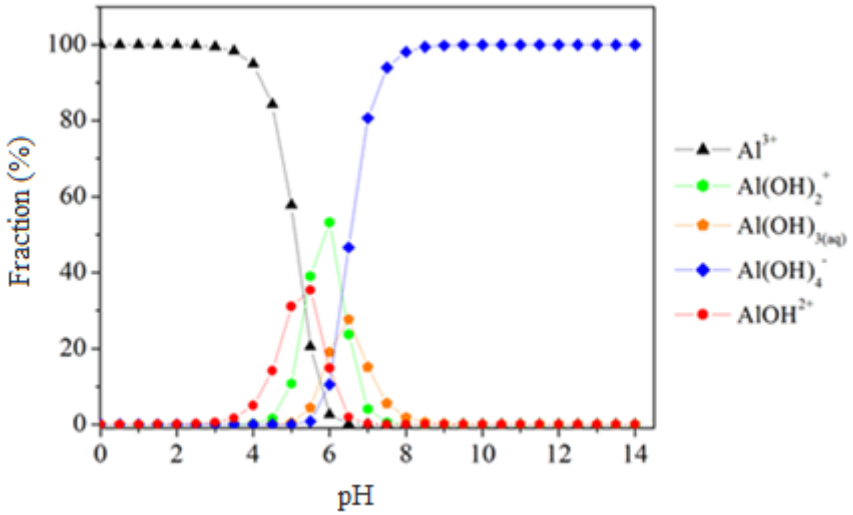

Some toxic metals such as zinc and iron are considered essential to living organisms and have been recommended as daily intakes [1]. However, there is no evidence of the biological relevance of aluminum for humans, which may be linked to its characteristic of low solubility in neutral pH ranges (between 6.5 and 7.5), such as that of

the blood flow. In evolutionarily terms, therefore, aluminum ion-dependent metabolisms would be unviable [22].

Due to its physical and chemical characteristics such as high conductivity, malleability and corrosion resistance, aluminum is extensively used in several industrial sectors. In the machine and construction industries, aluminum is used mainly to compose metal alloys. In the pharmaceutical industry, in turn, its use is focused on packaging, antacids and vaccines. Aluminum is also used in the textile industry as a tanning agent for leather. In addition, aluminum sulfate and polyaluminum chloride (PAC) are the main coagulating agents used in water treatment plants [22,28]. In literature, effluents with aluminum levels vary greatly on dependence of the region of collect and the effluent origin, e. g., Comber et al. found Al (III) total concentration around 0.05 – 0.45 mg/L for effluents from water treatment plant in UK [29], while Maleki et al. [30] observed an aluminum concentration of 2 mg/L on the final discharge from a water treatment plant in Iran. Shaaban et al. performed a vast analysis of real effluents from industrial district of Borg El-Arab, Egypt, and observed relatively high concentrations of aluminum, for example, in food sector the aluminum concentration reached 39.03 mg/L and in metal processing Al (III) levels around 4.38 mg/L were found.

Intensive use therefore generates a large amount of effluent contaminated by the metal, which is sometimes discarded into bodies of water without proper treatment, triggering several damages to the environment and human health. Another form of contamination may occur in water treatment systems where the use of aluminum derivatives may leave residue even in treated water [31].

Besides exposure in contaminated environments, humans are also exposed to aluminum ions through the daily use of products such as deodorants and antacids, which contain significant amounts of this metal ion [27]. Food additives containing aluminum are also commonly used, especially in the baking industry. However, since 2019 the World Health Organization (WHO) expert committee on chemical additives has discouraged its use in several food categories. Normally, the main routes of metal contamination are oral and respiratory and more than 95% of the aluminum consumed daily is rapidly eliminated by the urinary system, except in the case of individuals suffering from some kind of kidney failure or children under one year old and adults over 60 years old, in this case, oral intake of aluminum can be highly harmful, with the metal absorbed into the bloodstream tending to accumulate mainly in the bones [32].

According to the toxicological opinion issued by the Agency for Toxic Substances and Disease Registry (ATSDR) [33], aluminum levels present in products consumed daily are considered safe for humans, but several studies suggest the need for further investigation. Stephens and Jolliff [28] observed that when the metal is absorbed into the bloodstream, around 40% binds to bones and muscles and may even reach the brain. Aluminum may negatively affect bone mineralization and inhibit bone cell growth and activity [34]. Other researchers have investigated the relationship between aluminum and neurological diseases, such as Alzheimer's disease, but studies with more conclusive results are still needed [35–37].

In plants, toxic effects caused by the accumulation of aluminum include deficiency in nutrient absorption and transport, genotype changes and biomass reduction, with roots being the most affected area. Excessive aluminum also considerably decreases cell respiration and the transport of water and other macronutrients, such as calcium, phosphorus and magnesium, a condition that may be linked to competition between those metals and aluminum for active sites [32]. Soil acidification is a factor strictly linked to aluminum phytotoxicity. Initially the metal exists in the nature in a harmless form such as aluminosilicates or aluminum oxides in clays, but when the pH of the soil reaches values below 5.0 this metal is solubilized in forms potentially toxic to plants, such as Al^{+3} [38].

Organisms living in aquatic environments are also affected by the presence of aluminum in the form of Al^{3+}, the effects on fish being the most widely addressed in the literature. Researchers report that concentrations of this ion form above 0.5 mg/L may cause a high mortality rate in several species, mainly affecting osmoregulation and the respiratory system [26,39,40].

Consequently, worldwide, local legislations standardize the maximum levels of aluminum in drinking water and effluents discharged in water bodies. WHO, for example, sets its maximum level at 0.2 mg/L in water for human consumption [41].

2.3 Water and wastewater treatment approaches for aluminum removal

Aiming to comply with the limits imposed by national and international legislation, several treatment alternatives have been studied for the removal of aluminum present in aqueous systems. Processes such as precipitation, ion exchange with resins,

membrane separation and adsorption have shown satisfactory results for the removal of this metal in the environmental sector [42].

Precipitation is still the simplest and most used process. It consists of the precipitation of Al^{3+} ions, recovering them in the form of hydroxides. Basic substances are used for this such as sodium hydroxide, which raises the pH of the solution to an average range between 5 - 8. The precipitate is separated from the solution by filtration or sedimentation [43]. However, this process is not suitable for large volumes of effluents that contain toxic metals in low concentrations and, moreover, it produces large amounts of contaminated residual sludge [44].

Ion exchange is commonly applied for the uptake of toxic metals. Its mechanism use as basis the electrostatic interaction between the ion of the solution and the surface of the solid (resin), which consists of a polymeric matrix with functional groups linked to ion exchange resin that can be cationic or anionic [45]. Satisfactory results have been obtained using cationic resins that present the following order of selectivity [46]:

$$Al^{3+} > Pb^{2+} > Sr^{2+} > Ca^{2+} > Cu^{2+} > Zn^{2+} > Mg^{2+} > K^{+} > Na^{+} > H^{+}$$

Although these resins can be reused in several regenerative cycles, their regeneration after each process requires large amounts of chemical reagents, such as highly concentrated acids, which generates polluting waste [47].

Membrane separation processes for the removal of toxic metals involve techniques such as electrodialysis, ultrafiltration, nanofiltration and reverse osmosis. The process depends on the type of membrane used and the classification is based on the pore diameter of the material. Metal removal occurs through the percolation of the solution containing the metal ion, which can be of the conventional type or parallel (crossflow) to the surface of the membrane. The driving force of this process stems from applying greater pressure than the system's osmotic pressure [48]. In the case of electrodialysis, the membrane is electrically charged, and the driving force is an electric field applied to the system. Membrane separation shows good results in removing Al^{3+} ions, but there are disadvantages such as the high cost and complexity of the process [49,50]. In addition, aluminum tends to form encrustation layers on these types of membranes [51,52].

Removal of aluminum and toxic metals in general by adsorption has proved to be quite promising [53]. Adsorption is based on the process of diffusion and transfer of mass,

in which the adsorbate in an aqueous solution is transported to the surface of an adsorbent solid. The main driving force behind this phenomenon is the difference in concentration between the two phases. Adhesion of the adsorbate to the solid surface can be governed by physical (physisorption) or chemical (chemisorption) interactions [17,54–56].

A variety of different materials have been investigated as adsorbents for the uptake of aluminum, ranging from the most commonly used ones such as activated carbon and zeolites, to low-cost alternative materials like wood charcoal, clays and biomaterials like polymers and starch [57–60].

2.4 Biosorption: general approaches

2.4.1 Biosorbent materials

Biosorption can be defined as a type of adsorption in which the adsorbent is a material of biological origin, either natural or waste from an agro-industrial process. According to Vieira and Volesky [61], biosorbents should preferably be industrial waste with no added value, high bioavailability and a fast production/growth cycle. The combination of these factors reduces the cost of the biosorption process, which is the main advantage of this approach. High biosorption capacity, rapid removal and resistance to friction are highly desirable features for the material to be considered as a potential biosorbent. In general, the most commonly used biosorbents for the uptake of toxic metals can be divided into three groups: microorganisms, algae and agro-industrial waste [50]. It is important to highlight that only research papers that uses biomass of deactivated microorganisms were discussed in this review, since the definition of biosorption adopted here is that this is a metabolic-independent process with passive removal of toxic metals [62].

Among the most used microorganisms biomasses are bacteria, including *Streptomyces rimosus, Rhodococcus opacus, Pseudomonas luteola, Brochothrix thermosphacta* and *Vibrio alginolyticus* [63–66]. However, fungal biosorbents, such as *Aspergillus niger*, are also very interesting due to their high contents of cell-wall material, which boost the assortment of functionalities available for metal binding [67]. Algae have high affinity with a wide variety of metals, which is an advantage in their use as biosorbents. The seaweeds are divided into three major groups: red algae, green algae and brown algae [68–71]. Brown algae stand out for having high rates of alginate in their

composition, a compound described as being mainly responsible by the uptake of metal ions. In the biosorption of Al^{3+}, algae such as *Padina pavonica*, *Sargassum fluitans* and *Laminaria japonica* presented satisfactory metal removal results [72–74]. Lee [75] also investigated the influence of chemical and physical pretreatments to modify the algae *Sargassum fluitans* and improve aluminum removal. Waste materials produced by industrial or agro-industrial processes have also been studied for the removal of Al^{3+}. Biomass such as sludge from wastewater treatment ponds [76], coconut husks [77], powdered eucalyptus bark [78], tea residue [79] and beach-cast seaweed [80] have been investigated as promising biosorbents. The main advantages are their low cost, high availability and environmental sustainability [81].

Other biosorbent materials such as nanomaterials derived from alternative sources, mainly from agro-industrial waste and bacterial biomass, have been increasingly investigated for the removal of toxic metals [82]. These biosorbents are known to have a large surface area and high porosity, which substantially improves the adsorptive capacity of these materials [83]. Studies on the use of nano-adsorbents for the removal of toxic metals are recent and still in their early development, but promising results have been reported for the uptake of metals such as copper, cadmium, chromium and lead [84–86]. However, specifically for the removal of aluminum, there is still a lack of research that delves into the topic.

2.4.2 Biosorption mechanisms

In the biosorption process, contaminants are removed through adsorption onto the cell wall or active sites that exist on the surface of the biomaterial. Both the biosorbent material and the adsorbate must be evaluated. In the case of metal contaminants, biosorbent-metal affinity should be the first factor to be investigated to assess the potential application of the process. The effluent aspects to be evaluated are treated volume, metal concentration, pH, temperature, and presence of other contaminants that may compete for active sites. For the biosorbent, in turn, one must analyze the features which directly influence the viability of the process, such as its origin, selectivity, physical, chemical and biological properties, and reuse capacity [16,20,87]. This process differs from bioaccumulation process in which metals are removed by the metabolic action of living cells [4].

In this process, metal ions are removed from the aqueous solution due to the affinity/bond of the metal at the active sites and functional groups of the biomaterial structure. Studying the mechanisms that govern the biosorption of toxic metals can help elucidate the interaction between biosorbent and adsorbate. As reported by Robalds and collaborators [88], biosorption process may involve several mechanisms, such as physisorption, chemisorption, which may include covalent bonds and complexation, ion exchange and microprecipitation. Figure 3 depicts the main mechanisms involved in biosorption processes.

Figure 2.3 Main mechanisms potentially involved in a biosorption process.

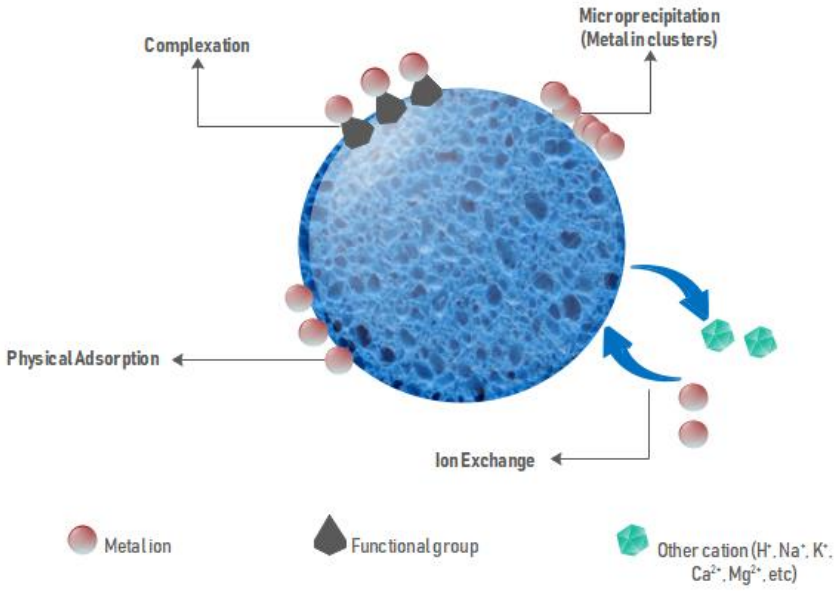

Hydroxyl, carboxyl, sulfonate and amine functional groups have been identified in literature as those that can most favor the removal of metals from aqueous solutions [68,89,90]. The Hard and Soft Acids and Bases (HSAB) concept can help to understand the binding preferences between metals and certain functional groups. In this theory, metals are divided into groups. Those classified as Type A (Al^{3+}, Mg^{2+}, Ca^{2+}, Na^{+}, among others) have a strong tendency to bond with compounds containing oxygen such as OH^{-}, HPO_4^{2-}, =C=O, while metals classified as Type B (Ag^{+}, Hg^{2+}, Pb^{2+}, Zn^{2+} and others) form strong bonds with groups containing N or S such as CN^{-}, NH_2^{-}, $-SH^{-}$. Moreover, bonds containing type A metals tend to be ionic, while for type B they tend to be covalent. However, this cannot be considered a determinant definition, since many other factors, such as metal concentration and biomass type, may affect the system's behavior [91,92].

Studies reported in the literature suggest that the main mechanisms participating in the biosorption of Al^{+3} ions are largely related to chemisorption but may also have several additional mechanisms like complexation and ion exchange. Understanding the biosorption of toxic metals, especially aluminum, requires studying the kinetics, equilibrium and thermodynamics of the process.

2.4.3 Biosorption kinetics

Analysis of biosorption kinetics provides information regarding the uptake rate, and the time required to reach equilibrium, as well as insights about the controlling mechanisms of the overall process. Kinetic paremeters can be used to develop predictive modeling for continuous biosorption in fixed-bed dynamic systems [93].

The application of kinetic models is important to identify the rate-limiting phase of the biosorption process. The most commonly applied models to describe the kinetic rate of adsorption in biosorption studies of toxic metals, including aluminum, are pseudo-first order (PFO) [94] and pseudo-second order (PSO) [95] models, being both based on the adsorptive capacity of the solid phase. Besides these models, others can be used to evaluate mass transfer behavior, such as intraparticle diffusion [96], Boyd's [97] Elovich's [98]. These models are based on the system's internal or external diffusion mechanism. Internal diffusion, also called intraparticle, describes the transport rate of ions via pores or on the adsorbent surface, whereas external diffusion relates to the transport rate of the solution adsorbate across the outer film of the biomaterial [99].

Adsorption kinetics modeling is considered an important step to understand the phenomenon of mass transfer in biosorption and the dynamics of the adsorbate binding mechanism on the biosorbent surface [100]. Table 2.1 features the results of various works in the literature for kinetic modeling of Al^{3+} biosorption using different biosorbents. In most studies the PSO model best describes Al^{3+} removal, indicating that the main mechanism involved in this process is the chemisorption, since the derivation of this model was based on the classic equation of the Langmuir equilibrium model, in which adsorption is assumed to be governed by chemical reactions occurring on a energetically homogenous surface [101, 102].

Although several authors supports this assumption, Tran et al. [89] and other researchers [103–105] emphasize that the biosorption mechanism cannot be defined by

kinetic analysis only. For them, it requires complementary analytical information determined by characterization techniques, such as Fourier-Transform Infrared spectroscopy (FTIR), Scanning Electron Microscopy (SEM), Thermogravimetric/ Differential Thermal Analysis (TGA/DTA), and the examination of isotherm and thermodynamic data. In addition, the knowledge about the nature of the biosorbent is crucial to understand the process mechanism.

Table 2.1 Kinetic modeling of Al^{3+} removal by different low-cost biosorbents.

Source	Biosorbent	Kinetic model	Experimental conditions	Kinetic parameters	R^2	Reference
Bacterial biomass	*Rhodococcus opacus*	PSO	C_0: 50 mg/L; D: 2 g/L; pH: 5; 175 rpm; 298 K	k_2 = 1.828; q_e = N/A	0.999	[64]
	Streptomyces rimosus	PSO	C_0: 30 mg/L; D: 2 g/L; pH: 3.98; 250 rpm; 353 K	k_2 = 7.462; q_e = 1.18	1	[63]
Fungal biomass	*Cortinarius armillatus*	PSO	C_0: 10 mg/L; D: 8 g/L; pH: 5; 1 h; 120 rpm; 293 K	$k_2 = 4.2 \times 10^{-2}$; q_e = 2.10	0.995	[106]
Algal biomass	*Turbinaria conoides*	PFO	C_0: 987.5 mg/L; D: 2 g/L; pH: 4; 4 h; 160 rpm; 295 K	k_1 = 0.048; q_e = 1.97	0.989	[100]
	Padina pavonica	PSO	C_0: 10 mg/L; D: 8 g/L; pH: 4.5; 60 min; 120 rpm; 323 K	$k_2 = 23.9 \times 10^{-2}$; q_e = 2.36	0.996	[72]
Agro-industrial waste	*Eucalyptus camaldulensis* bark	PSO	C_0: 50 mg/L; D: 12 g/L; pH: 5; 90 min; 400 rpm; 303 K	k_2 = 6.80; q_e = 17.40	0.995	[78]
	Humin	PSO	C_0: 10 mg/L; D: 2 g/L; pH: 5;	k_2 = 0.032; q_e = 1.93	0.945	[107]
	Humin ash	PFO	C_0: 10 mg/L; D: 2 g/L; pH: 5;	k_1 = 0.038; q_e = 0.68	0.964	[107]

Pond sludge	PSO	C_0: 50 mg/L; D: 1 g/L; pH: 4; 1 h; 298 K	-	0.999	[76]
Typha domingensis	PSO	C_0: 7 mg/L; D: 10 g/L; pH: 2.5; 100 rpm; 298 K	k_2 = 0.0622; q_e = 0.677	1	[108]
Pongamia pinnata leaf powder	PSO	C_0: 5 mg/L; D: 3 g/L; pH: 6; 120 min; 323 K	k_2= 0.0573; q_e= 0.5179	0.999	[109]
Pongamia pinnata leaf ash	PSO	C_0: 5 mg/L; D: 3 g/L; pH: 6; 120 min; 323 K	k_2= 0.0489; q_e= 0.2071	1	[109]
Pongamia pinnata stem powder	PSO	C_0: 5 mg/L; D: 3 g/L; pH: 6; 120 min; 323 K	k_2= 0.0489; q_e= 0.1804	0.999	[109]
Pongamia pinnata stem ash	PSO	C_0: 5 mg/L; D: 3 g/L; pH: 6; 120 min; 323 K	k_2= 0.0394; q_e= 0.1373	0.999	[109]
Curcuma longa	PSO	D: 6 g/L; pH: 5; 200 rpm; 150 min;	k_2 = 0.040; q_e = 24.57	0.999	[110]
Rice husk	PSO	C_0: 30 mg/L; D: 5 g/L; pH: 5; 11 h; 160 rpm; 298 K	k_2 = 0.004; q_e = 4.74	0.996	[111]
Immobilized Sewage-Sludge	PFO	C_0: 50 mg/L; D: 2 g/L; pH: 5; 3 h; 200 rpm; 298 K	k_1 = 0.022	0.9869	[112]

D = adsorbent dosage; q_e = adsorbed metal in equilibrium predicted by the model (mg/g); k_1 = kinetic constant of the PFO model (min-1); k_2 = kinetic constant of the PSO model (g/(mg.min)); N/A = not available

2.4.4 Biosorption equilibrium

Biosorption equilibrium described by the isotherms represents the dynamic equilibrium between the metal concentration present in the liquid phase and the adsorbate concentration in the biosorbent, at constant temperature and pH. The application of isotherm modeling provides important information regarding the affinity level of the biosorbent-adsorbate system, the properties of the biomaterial surface and the nature of the process. Therefore, equilibrium parameters are essential for the design of a biosorption system [113,114].

The isotherm models most commonly applied to analyze biosorption systems are Langmuir [115] and Freundlich [116], besides a few classic models such as Dubinin-Radushkevich (D-R) [117], Langmuir-Freundlich [118] and Temkin [119].

The Langmuir model assumes that biosorption is reversible and occurs in monolayers, the biosorbent surface is homogeneous and has a fixed number of active sites and there is no interaction between the ions once they are bound to the surface [115]. This model does not clarify aspects about the removal mechanism, although it provides information about maximum removal capacity (q_{max}), which is useful to contrast the performance of distinct biosorbent materials. [120,121]. The Freundlich model is recommended for systems with medium to low ion concentrations. The main consideration is that it represents multilayer biosorption on a non-homogeneous surface. The D-R model can be applied to investigate the nature of adsorption, which may be chemical or physical [46].

Table 2.2 features the results of the fit of the models to the equilibrium experimental data of several studies of Al^{3+} biosorption with different biosorbents. Most systems are largely described by the Langmuir model, which may indicate that, in general, aluminum biosorption occurs with monolayer formation.

Table 2.2 Isotherm adsorption models of Al^{3+} removal by different biosorbents.

Source	Biosorbent	Experimental conditions	Isotherm model	q_{max} (mg/g)	Other information	Reference
Bacterial biomass	*Chryseomonas luteola*	C_0 = 0-100; D = 1; T = 298; pH 5	F	55.3	K_F= 20.5; n= 0.3	[65]
	Rhodococcus opacus	C_0 = 50; D = 2; T = 298; pH 5	Temkin	41.59	b = 7.705; K_T= 287.13	[64]
	Streptomyces rimosus	C_0 = 30-960; D = 25; T = 298; pH 4	L	11.76	K_L= 0.06	[63]
	Pseudomonas putida	C_0 = 0-8.09; D = 6; T = 298; pH 4.3	L/Boeris	0.55	K_L = 11.36/M = 36; K_{eq} = 1.24	[122]
Fungal biomass	*Aspergillus oryzae*	C_0 = 10-50; D = 20; T = 303; pH 6	F	0.071	K_f = 0.0949; n = 1.46	[123]
	Cortinarius armillatus	C_0 = 10-400; D = 8; T = 293; pH 5	L	161.23	$K_L = 1.3x10^{-2}$	[106]
Algal biomass	Beach-cast seaweed	C_0 = 5-500; D = 2.5; T = 298; pH 4	L/L-F	22.5	K_L = 0.28±0.05	[80]
	Turbinaria conoides	C_0 = 493.76-987.52; D = 2; T = 295; pH 4	Toth/L	63.94	b_t = 0.165; n_T = 0.968 K_L = 0.168	[100]
	Gelidium latifolium	C_0 = 0.5-1000; D = 1; T = 298; pH 4	L	55.6	K_L= 0.139	[124]
	Ulva lactuca	C_0 = 0.5-1000; D = 1; T = 298; pH 4	L	56.2	K_L = 0.14	[124]

	Colpomenia sinuosa	C_0 = 0.5-1000; D = 1; T = 298; pH 4	L	57.1	K_L = 0.144	[124]
	Padina pavonica	C_0 = 10-400; D = 8; T = 323; pH 4.5	L/D-R	77.3	K_L = 0.02	[72]
Agro-industrial waste	Coconut shell	C_0 = 10-200; D = 1; T = 293; pH 7	F	120.48	K_F = 0.0118; n = 1.83	[77]
	Humin	C_0 = 1-50; D = 1; T = not informed; pH 5	L	1.91	K_L = 1.03±0.1	[107]
	Humin ash	C_0 = 1-50; D = 1; T = not informed; pH 5	F	0.87	K_F = 0.31±0.02; n = 3.44±0.24	[107]
	Eucalyptus camaldulensis bark	C_0 = 0-200; D = 5; T = 308; pH 5	L	52.63	K_L = 0.116	[78]
	Pond sludge	C_0 = 30-500; D = 1; T = 328; pH 4	L	142	K_L = 0.0795	[76]
	Typha domingensis	C_0 = 7-56; D = 10; T = 298; pH 2.5	L	0.348	K_L = 0.2876	[108]
	Pongamia pinnata leaf powder	C_0 = 30-500; D = 1; T = 328; pH 4	L	-	R_L= 0.01594	[109]
	Pongamia pinnata leaf ash	C_0 = 30-500; D = 1; T = 328; pH 4	L	-	R_L = 0.0142	[109]
	Pongamia pinnata stem powder	C_0 = 30-500; D = 1; T = 328; pH 4	L	-	R_L = 0.0212	[109]
	Pongamia pinnata stem ash	C_0 = 30-500; D = 1; T = 328; pH 4	L	-	R_L = 0.1174	[109]
	Curcuma longa (Turmeric)	C_0 = 30-500; D = 1; T = 328; pH 4	F	7.68	K_F = 0.2519; n = 0.309	[110]

Cassia occidentalis stem powder	C_0 = 30-500; D = 1; T = 328; pH 4	L	-	R_L = 0.0212	[125]
Chitosan	C_0 = 5-40; D = 0.2; T = 303; pH 4	L	45.45	K_L = 7.829	[126]
Immobilized Sewage-Sludge	C_0 = 0-500; D = 2; T = 298; pH 5	L	27.00	K_L = 0.0022	[112]

C_0 = Initial concentration (mg/L); D = biosorbent dosage (g/L); T = temperature (K); L = Langmuir; F = Freundlich; K_F = Freundlich biosorption equilibrium constant (L/g); b = constant associated to the heat of adsorption; K_T = Temkin isotherm constant (g/mol); b_T = Toth model constant (L/mmol); n_T = Toth model exponent; K_L = Langmuir biosorption equilibrium constant (L/mg); M = maximum number of adsorption sites per microorganism; K_{eq} = the affinity of adsorbate for the adsorbent surface sites (L/mol); R_L = Dimensionless separation factor.

2.4.5 Thermodynamic aspects of biosorption

Thermodynamics of a biosorption process can be examined using the following parameters: variation of Gibbs energy (ΔG^o), variation of enthalpy (ΔH^o) and variation of entropy (ΔS^o). Analysis of ΔH^o values indicates whether the process is endothermic ($\Delta H^o > 0$) or exothermic ($\Delta H^o < 0$). Process spontaneity is verified by ΔG^o and may be spontaneous ($\Delta G^o < 0$) or not ($\Delta G^o > 0$). ΔS^o values, in turn, are related to the affinity of the metal by the biosorbent material, which can be high ($\Delta S^o > 0$) or low ($\Delta S^o < 0$). Some authors also associate this variable with the degree of disorder in the system's interface [15,127]. The study of the value of enthalpy variation can also help in defining if the process is governed mostly by chemical or physical interactions. Values below 80 kJ/mol generally indicate that the adsorption mechanism is physical and reversible, mostly governed by weak interactions as Van der Waals forces. In irreversible chemical processes, enthalpy variation values usually vary between 80 and 400 kJ/mol, and for electrostatic interactions this values vary from 30 to 70 kJ/mol [128,129].

Table 2.3 features the thermodynamic data of several studies on Al^{3+} biosorption with different biosorbents. The results show that the biosorption processes of Al^{3+} ions are largely spontaneous and endothermic, as they present positive values for Gibbs energy and enthalpy variation, respectively. Entropy variation ranged from -164.4 J/mol.K to 207.6 J/mol.K, depending on the system. Most studies presented positive values for ΔS^o, indicating increased disorder in the system's biosorbent-adsorbate interface and high affinity of Al^{3+} ions for most of the biosorbents used. However, this cannot be fully confirmed, since each type of biomass has its particularities, such as different types of active sites, which are strongly affected by temperature.

In some of the studies selected in this review, although the thermodynamic quantities of the process were not determined, considerable enhancement in aluminum uptake was noticed when the temperature was raised, indicating that the adsorption is essentially endothermic [76,78]. The main explanation for this behavior is that increased temperature leads the boundary layer to become less thick, thus facilitating the transfer of metal ions to the biosorbent [130]. In other works, however, the authors observed an opposite behavior, a reduced metal uptake with increasing temperature, indicating an exothermic process [64].

Table 2.3 Thermodynamic parameters of Al^{3+} biosorption using different biosorbents.

Source	Biosorbent	T (K)	ΔGº (kJ/mol)	ΔHº (kJ/mol)	ΔSº (J/mol.K)	Reference
Bacterial biomass	*Streptomyces rimosus*	283	1.07	20.76	0.0685	[63]
		298	0.69			
		323	-1.26			
		353	-3.62			
Fungal biomass	*Cortinarius armillatus*	293	18.93	37.72	64.54	[106]
		303	17.99			
		313	16.95			
Algal biomass	*Gelidium latifolium*	298	8.25	644.05	-25.54	[124]
		313	8.55		-25.27	
		333	8.99		-25.08	
	Ulva lactuca	298	7.69	455.74	-24.29	[124]
		313	8.00		-24.1	
		333	8.43		-23.97	
	Colpomenia sinuosa	298	7.50	402.23	-23.82	[124]
		313	7.80		-23.63	
		333	8.24		-23.53	
	Padina pavonica	293	-15.43	45.96	0.21	[72]
		303	-17.23			
		313	-19.44			
		323	-21.70			
	Chitosan	303	103.5	53.7	-164.4	[126]
		318	106.0			

		333	108.5			
Agro-industrial waste	*Pongamia pinnata* leaf powder	303 313 323	-3.72 -4.85 -7.87	59.18	207.6	[109]
	Pongamia pinnata leaf ash	303 313 323	-0.60 -1.02 -1.44	12.16	42.13	[109]
	Pongamia pinnata stem powder	303 313 323	-3.16 -4.63 -6.10	41.29	146.75	[109]
	Pongamia pinnata stem ash	303 313 323	-0.36 -0.78 -1.20	12.35	41.96	[109]

2.5 Biosorption of aluminum using biomaterials

2.5.1 Using bacterial biomass as biosorbent of aluminum

Bacteria are ubiquitous, able to spread under controlled conditions, and highly resistant to variations in the medium. Therefore, bacterium biomass is an advantageous biosorbent [122]. The cell walls of bacteria present macromolecules, such as enzymes, (lipo-) polysaccharides, peptidoglycan and (lipo-) proteins, which are rich in functionalities like carboxyl, sulfate, phosphate and amino groups. The coexistence of cationic and anionic groups grants the bacterial cell wall with an amphoteric behavior. Nevertheless, Van Der Wal et al. [131] verified that the anionic groups prevail over cationic groups, and so the isoelectric point of most bacterial biomasses does not exceed pH 4. Consequently, electrostatic interactions between bacteria and positively charged contaminants, such as Al^{3+}, may favor the biosorption process [64].

The biomass of *Rhodococcus opacus* strain (gram-positive) was selected by Cayllahua and Torem [64] for removing aluminum from water. First, zeta potential measurements indicated an isoelectric point at pH 3.26 for *R. opacus*, which is consonant with the literature. Accordingly, at pH conditions above 3.26 the net charge of *R. opacus* bacterium is negative, which can directly impact biosorption through electrostatic forces. In fact, the authors reported an increase in Al^{3+} removal efficiency from 11% to 92% by increasing the solution pH from 3 to 5, respectively. Hence, pH 5 was selected as the optimum condition for Al^{3+} biosorption onto *R. opacus*. The key role of electrostatic attractions in the process was confirmed by ionic strength tests, in which Al^{3+} uptake capacity augmented by decreasing electrolyte NaCl concentration. This last finding agrees with that observed in the study by Tassit et al. [63], who, by calculating the activation energy of the process, reached the same conclusion. The kinetic study of Al^{3+} biosorption onto *R. opacus* demonstrated that the system reached equilibrium after approximately 20 minutes with 100% removal efficiency. PFO, PSO, intraparticle diffusion and Boyd's were the kinetic models applied to the results, which were best represented by the PSO model. In the equilibrium study, the authors observed a significant decrease in q_{max} with increasing temperature, an indication that the system is exothermic. Comparatively to Langmuir, Freundlich and Dubinin-Radushkevich models, Temkin model provided the best fit to the equilibrium data. Temkin isotherm, by definition, indicates that the adsorption heat reduces linearly with the raise of biosorbent surface

coverage [132]. FTIR spectra showed that the biomass of *R. opacus* bacterium is rich in hydroxyl, amino, carbonyl, carboxyl and phosphate functional groups. The shifts in their vibrational bands reveal the complexation/coordination of Al^{3+} onto the biomass during the process. More clear insights on Al^{3+} uptake mechanism depends on further characterizations and analysis.

Tassist et al. [63] proposed *Streptomyces rimosus*, which is a mycelial gram-positive bacterium, as biosorbent of Al^{3+}. This bacterium is extensively used for the biosynthesis of oxytetracycline antibiotic. The authors received *S. rimosus* biomass from a local Algerian pharmaceutical industry and, after cleaning and grinding, the material was sieved to obtain samples of different particle sizes. FTIR characterization of *S. rimosus* biomass showed the presence of methyl, carboxyl, hydroxyl, amino, thiol and phosphate groups. Such functionalities agree with the chemistry of the wall and cellular membrane of the selected bacterium. The Al^{3+} biosorption onto of *S. rimosus* biomass was studied for the effects of particle size, biosorbent dosage, agitation speed, temperature and pH. Remarkably, there was a significant increase in Al^{3+} removal capacity with increasing temperature, indicating an endothermic process. Moreover, the increase in pH from 2 to 4 favored Al^{3+} biosorption onto *S. rimosus.* Kinetics was better represented by PSO model than PFO model. The activation energy in the Arrhenius equation was estimated as 52.18 kJ/mol. According to Aksu [133], activation energy in 8.4–83.7 kJ/mol range indicates an activated chemisorption process. The authors also considered the involvement of ion exchange mechanisms, in which the chemical biding between the metal and the biosorbent might be mainly of electrostatic nature. Equilibrium was better represented by Langmuir model than Freundlich or D-R isotherms.

Nevertheless, the magnitude of mean free adsorption energy of D-R isotherm (12.91 kJ/mol) reinforced the fact that chemical ion exchange mechanisms governed Al^{3+} biosorption. The thermodynamic parameters listed in Table 2.3 indicates that the process is feasible, endothermic and spontaneous at 10–80 °C. In the study of isotherms, the authors also evaluated the influence of controlled pH. They obtained q_{max}=11.76 mg/g at fixed pH 4 and q_{max}=6.62 mg/g at free pH. The lower biosorption capacity at free pH was related to the fact that the solution pH diminished to 3.24 at equilibrium. The number of anionic sites, especially carboxyl groups, available to bind Al^{3+} cations is lower at pH 3.24 than pH 4. On one hand, Al^{3+} biosorption onto *S. rimosus* presented the highest value

of maximum biosorption capacity among the bacterial biomasses of Table 2.2, but on the other hand, it took a relatively long time of 150 min to reach equilibrium.

Ozdemir and Bayasal [65] innovated using *Chryseomonas luteola* strain, which is habitually found in activated sludge, as metal biosorbent. *C. luteola* is a floc-forming bacterium, so it can form a polysaccharide capsule that binds and accumulates the contaminants. Al^{3+} uptake by *C. luteola* was examined in 1.0–7.0 pH range, and the highest biosorption yield was verified at pH 5.0. According to Langmuir isotherm, the maximum biosorption capacity of Al^{3+} was 55.2 mg/g. The cell demonstrated a greater affinity for aluminum than chromium ions, since the maximum Cr^{6+} biosorption capacity at pH 4 did not exceed q_{max}=3 mg/g.

Boeris et al. [122] analyzed the potential of the non-living (non-viable) biomass of the gram-negative bacterium *Pseudomonas putida* A (ATCC 12633) as biosorbent of Al^{3+}. For comparison purposes, they also evaluated the removal capacity using the living (viable) biomass of *P. putida* A (ATCC 12633). The effects of pH (2–12), biosorbent dosage (0–60 g/L) and contact time (1–15 min) on Al^{3+} biosorption were evaluated. For both types of biomass, pH 4.3 provided the highest biosorption efficiency (around 95%). However, lower quantities of biosorbent were required by the non-viable *P. putida* A (ATCC 12633) system to attain 100% removal of Al^{3+}. Resistance to mass transfer using either viable biomass (40 g/L) or non-viable biomass (8 g/L) was negligible, since only 1 min of contact time was sufficient to completely remove Al^{3+} from solution. Furthermore, Boeris et al. [122] proved that the membrane phosphatidylcholine (PC) present in *P. putida* A (ATCC 12633) plays a key role in the biosorption of Al^{3+}. For that purpose, they developed a mutant bacterium without PC and compared q_{max} values obtained using all kinds of biomass (viable, non-viable and non-viable without PC). The biomass without PC showed the worst performance, with fast saturation and low Al^{3+} removal capacity (q_{max}=0.27 mg/g). Conversely, the non-viable *P. putida* A (ATCC 12633) showed the best results (q_{max}=0.55 mg/g). This indicates that biosorbent performance may be associated with pre-treatment by autoclaving, which causes the destruction of cells and may promote enhanced surface area and greater availability of binding sites in the non-living biomass. Thus, efficiency could be mostly linked to quantitative characteristics of the biosorbent, that is, the number of active sites, and qualitative factors, such as metal-biosorbent affinity, had a secondary role [18,134]. The exact interactions of aluminum ions onto non-viable biomass could not be completely

elucidated; however, the changes in FTIR spectra before and after biosorption indicated the involvement of functional groups of the cells in the process, including aluminum complexation with phosphate ester groups. The biosorption isotherms were adjusted not only by the traditional Langmuir model, but also by the model proposed by Bueno et al. [135], which applies to systems that use microorganism-derived biosorbents. The parameters from the fitting of Bueno et al. [135] model confirmed the non-viable *P. putida* A (ATCC 12633) biomass as the most efficient biosorbent for Al^{3+} removal, especially because it presents the highest amount of binding sites on the surface (M=36 x 10^5 sites/microorganism).

From Table 2.2, it is noticeable that gram-positive bacteria (*R. opaccus* and *S. rimosus*) show better removal results than gram-negative bacteria (*P. putida*), which some authors associate with the fact that the cell wall of gram-positive bacteria presents a thicker peptidoglycan layer, which favors the removal of metals [136].

2.5.2 Using fungal biomass as biosorbent of aluminum

Fungal biomass has also attracted great interest as a biosorbent because it offers several advantages. First, fungus can have up to 30% of its dry weight in the form of cell wall. The high cell wall content elevates the variety of functional groups available for metal binding. Moreover, fungus can be easily produced and has a fast life cycle with high yields of biomass. To top that, fungal biosorbents are mostly non-pathogenic and can be safely applied. Many types of fungal biomass can be obtained from industrial wastes, such as *Saccharomyces cerevisiae* from brewery production and *Aspergillus niger* from citric acid production [67]. On the other hand, research shows that the efficiencies of metal biosorption using fungal biomasses vary substantially. This triggered by several reasons, including differences in the chemical composition of the cell wall of fungal species.

Boriová et al. [137] examined four distinct wild-type strains of *A. niger* for Al^{3+} removal, using living and non-living microorganisms. The results obtained by using non-living *A. niger* biomass were unsatisfactory, since the biosorption efficiency did not exceed 9%. In turn, the Al^{3+} removal efficiency reached 53% using a strain of living *A. niger*. The living fungal biomass acts in passive biosorption and active uptake (bioaccumulation) of Al^{3+}. The difference in effectiveness between the processes may be

associated with several factors, from the pre-treatment method to obtain the biosorbent to the system's operating conditions [138,139].

Omeike et al. [123] investigated Al^{3+} removal using *Aspergillus oryzae* biomass obtained from an aluminum industry waste site in Nigeria. In comparison to other *Aspergillus* ssp and *Trichoderma* spp, *A. oryzae* strain showed the highest metal tolerance considering the inhibition zone around the colonies and so was selected for Al^{3+} biosorption. The pH influence testing indicated that the biosorption process reaches 45% maximum removal at pH 6. Moreover, 24 hours was determined as the optimum equilibrium time for Al^{3+} biosorption onto *A. oryzae* biomass. Langmuir isotherm and Freundlich isotherm were linearly adjusted to the experimental data but the adjustments had R^2 values lower than 0.85. Of the works listed in Table 2.2, this study presented the lowest values for q_{max} (0.071 mg/g), which shows the need to optimize the operating conditions of the biosorption process in order to achieve more satisfactory removal capacity values. On the other hand, Naeemullah et al. [106] achieved the greatest adsorption capacity (161.23 mg/g) among the fungal biomasses here presented, demonstrating that this microorganism may have a higher affinity to Al^{3+} ions, which can be associated to an improved metal bond capacity by the optimized batch conditions, highlighting the importance of this step to obtain reasonable results in the biosorption process.

2.5.3 Using algal biomass as biosorbent of aluminum

Algae are among the most popular biosorbents because of their abundance all over the world and the ability to undergo pre-treatment compared to microorganisms [140]. Another advantage is that algae have several potential metal-binding groups in their cell wall, such as carboxyl, sulfate and hydroxyl, which favors the uptake of toxic metals. Considering factors such as operating conditions, for example, one observes that metal biosorption onto algae shows favorable results for a wide range of concentrations, using low amounts of biomass and at mild temperatures [141]. Brown algae are found to be excellent biosorbents for removing metal contaminants, including Al^{3+} ions. The cell wall of brown algae contains fucoidan and alginate. Alginate can make up 40% of the algae dry weight and holds almost three quarters of the total amount of functional groups [68].

Vijayaraghavan et al. [100] explored the capacity of the brown algae *Turbinaria conoides* to remove aluminum and cadmium ions from in mono- and multicomponent

systems. First the pH effect was evaluated, with Al^{3+} removal favored at pH 4 and Cd^{2+} removal at pH 5. The authors observed that *T. conoides* has greater affinity for Al^{3+} ions than Cd^{2+} ions, since at pH 4 the q_{max} value on a molar basis was around 3 times higher for aluminum. In the binary-solute system containing Al^{3+} and Cd^{2+}, both ions compete strongly for the sites on the biosorbent surface. The maximum biosorption capacities of Al^{3+} and Cd^{2+} reduced by approximately 56% and 27%, respectively. This verified that the presence of cadmium significantly affects the removal of aluminum by *T. conoides* biomass. Regarding kinetic study, Vijayaraghavan et al. [100] found that both PFO and PSO models fitted well the experimental data with high R^2 values, but the values of equilibrium removal capacity estimated by PFO model were closer to those collected experimentally. The authors discussed the fact that PSO model tends to overestimate the q_e value, while the PFO model tends to underestimate it. The biosorption isotherms of Al^{3+} and Cd^{2+} onto *T. conoides* algae were evaluated by two-parameter models (Langmuir and Freundlich) and three-parameter models (Toth and Redlich-Peterson). Langmuir and Toth models were the ones that best described the equilibrium data, although the latter assumes that the biosorption system is heterogeneous, going against what is suggested as a hypothesis in the Langmuir model. This contradictory result may be explained by the occurrence of multiple stages and mechanisms on the metal-biosorbent binding, still in-depth analysis, such as micrographs of the biomaterial surface or isosteric heat calculation, may be necessary to support this hypothesis.

Sari and Tuzen [72] evaluated the efficiency of aluminum ion removal in aqueous solution by the brown algae *Padina pavonica*, which abundant in Atlantic Ocean and Mediterranean Sea and is customarily known as Peacocks tail. The authors obtained q_{max} = 77.3 mg/g at pH 4.5 with 60 minutes of contact time. The equilibrium was well represented by the Langmuir model, indicating that Al^{3+} biosorption on the surface of *P. pavonica* occurs with a monolayer formation. In addition, the D-R model indicated that metal removal in this system may be occurring by chemical ion exchange. The PSO model fit well with the kinetic data, showing that the possible controlling step of biosorption is chemisorption. Thermodynamic analysis revealed that Al^{3+} biosorption onto *P. pavonica* is favorable, viable and endothermic, and there was also an increase in the disorder of the adsorbate-biosorbent interface. FTIR characterization of the biosorbent before and after the process indicated that the ion exchange between Al^{3+} and H^+ ions possibly occurred mainly in the carboxyl, hydroxyl and amide groups. This observation corroborates the

analyses by Davis et al. [68], who found that brown algae's carboxyl groups are majorly involved in the removal of metals.

Lodeiro et al. [80] examined the use of beach cast seaweed from Galician Coast in Spain as biosorbent of aluminum. The main component of the biomass was identified as the brown seaweed *Cystoseira baccata*. The study was developed not only in batch, but also in fixed-bed systems. The latter is discussed in Section 5.6. In the finite bath assays, synthetic aluminum solutions were used at initial concentrations of 10 and 100 mg/L. The authors verified that the biosorption onto beach cast seaweed was reasonably fast and reached equilibrium after about 60 min at the highest concentration. Biosorption isotherms were obtained at three acidic conditions, pH 1, 2.5 and 4. There was strong pH influence on the maximum removal capacity of aluminum. At pH 4, the q_{max} value of 22.5 mg/g was about twice as high as that obtained at pH 2.5 (q_{max} = 11.1 mg/g). Langmuir isotherm model and Langmuir-Freundlich three-parameter model provided good fittings to the experimental data, indicating monolayer formation on the surface of the seaweed. From potentiometric titration assays in deionized water, total amount of weak acid groups in the beach cast seaweed was estimated as 2.61 mmol/g. Considering the much lower value of q_{max} (22.5 mg/g ~ 0.83 mmol/g), it was speculated that some of the weak acid groups were not ionized at pH 4 and that some of these groups were unavailable for binding aluminum because they were already occupied with cations such as Na, K and Mg, which are abundant in seawater.

Shaaban et al. [124] evaluated the performance of three different marine algae as biosorbents for the uptake of aluminum, zinc and iron present in synthetic aqueous solutions and in real effluents. The selected algae were: *Gelidium latifolium* (red algae), *Ulva lactuca* (green algae) and *Colpomenia sinuosa* (brown algae). The authors concluded that the brown algae *C. sinuosa* showed better results in removing all the metals evaluated. Next in Al^{3+} biosorption efficiency came the red algae *G. latifolium*, followed by the green algae *U. lactuca*. This order is in agreement with that reached by Romera et al. [142] when comparing the performance of green, red and brown algae in biosorption of different toxic metals. Noteworthy, the excellence of brown algae as biosorbent for a wide variety of metals may be associated with the alginate present in the composition of their cell wall. Shaaban et al. [124] also investigated the interaction between the marine algae and aluminum, zinc and iron. It was verified that Al^{3+} ions had the lowest biosorption affinity to the three algae, which may be associated with the fact

that Zn^{2+} and Fe^{3+} are heavier ions and so can bind more easily to the cell wall. In addition, other intrinsic factors of the metals, for example ionic radius and electronegativity, may also affect the bonding with the active sites of the biosorbent [143,144]. However, despite this result, the three algae in question showed satisfactory capabilities of Al^{3+} removal in both low (0.5 mg/L) and high (1000 mg/L) concentrations, varying on average between 0.437 and 60.2 mg/g, respectively. By analyzing the thermodynamic parameters and equilibrium data, the researchers concluded that the Al^{3+} biosorption process in all algae was endothermic ($\Delta H° > 0$) and that it occurred in an orderly manner at the interface with high affinity between the metal and the biosorbent ($\Delta S° > 0$). The satisfactory fit of the Langmuir model to the experimental indicates a monolayer disposition on the biosorbent surface. Analyzing the biosorbent surfaces by scanning electron microscopy, they observed that the brown algae *C. sinuosa* had a stratified and extensively papillary surface, thus having a greater contact surface, corroborating the fact that this biomass had good removal results. Participation of the C-N-S group in the Al removal mechanism was analyzed by FTIR, especially in *C. sinuosa*, where the band change was more pronounced; the C-O group (alcoholic group) participated in Al biosorption only in the red algae *G. latifolium*; groups C-O, C= O and NH were present in all algae; the OH group contributed to the removal of the metal in all algae, except *U. lactuca*.

Overall, one may conclude that biosorption processes of Al^{3+} ions using microorganisms: (i) tend to be fast; some authors claim that this may be linked to the fact that the cells are very small, so resistance to mass transfer may be negligible [145]; (ii) agitation generally does not directly affect the removal results, only the time to reach equilibrium; (iii) the cell walls contain functional groups, such as hydroxyl, carboxyl, amino and phosphoric, which are mainly involved in Al^{3+} removal by microorganisms; (iii) the solution pH plays a pivotal role in Al^{3+} biosorption onto bacterial, fungal and algal biomasses. Regarding this last point, it is noteworthy that at low pH conditions, phosphate and carboxyl groups are negatively charged, due to pKa between 3 and 5. This favors the binding of cations, such as Al^{3+}. Conversely, aluminum chemical speciation and solubility are function of pH. High pH values are prohibitive for Al biosorption, because there is the formation of insoluble hydroxide species [122].

2.5.4 Using agro-industrial waste as biosorbent of aluminum

In the segment of biosorbents derived from agro/industrial waste, Yurtsever and Nalçak [77] evaluated the feasibility of using coconut shells to remove Al^{3+} in aqueous solutions. The biosorbent was submitted to acid pre-treatment with HNO_3, HCl and H_2SO_4. This type of treatment is often used in biomass to remove impurities and assist in the exposure of active sites, increasing the ability to remove metal ions. However, acid treatment tends to increase the amount of protons on the surface of the biomaterial, potentially making it positive, which could, in theory, hinder cation removal [146]. However, fairly satisfactory values of maximum removal capacity of Al^{3+} (q_{max}) were achieved using the acid-treated coconut shells when compared to other biosorbents, as shown in Table 2.2. Yurtsever and Nalçak [77] observed that the biosorption kinetics of Al^{3+} onto acid treated coconut shell was initially fast and well defined by PSO model. System equilibrium was best expressed by Freundlich isotherm. It was noticed that the biosorbent surface showed several imperfections (heterogeneous). Thermodynamic analysis (Table 2.3) verified that the process was endothermic. Remarkably, the authors performed the experiments at pH 7 and claimed that aluminum is still in transition to its precipitated form at this pH value. However, according to the speciation diagram of Figure 2 and several works in the literature, above pH 6 aluminum forms the precipitated species $Al(OH)_3$. Metal precipitation can affect both the definition and the understanding of biosorption mechanisms [65,126,147,148].

Rosa et al. [107] investigated the biosorption of aluminum using humin and ashes from its calcination. In the kinetic study, the authors observed that PSO model fitted better to the biosorption using humin, while the process using ashes was better represented by the PFO model (Table 2.1). From FTIR spectra, it was observed that groups, such as OH, C=C and C=O, were possibly involved in Al^{3+} removal using both biosorbents. However, small differences in the structure of the ashes compared to humin were identified, such as bands indicating the presence of carbonates, aliphatic ethers and polysaccharides or silicates. These particularities may explain the fit of distinct models to the kinetic biosorption data using humin and its ashes, considering that removal capacity may be influenced by the presence of certain components on the structure of the biomaterial and by the way they interact in the biosorption process, which can occur through van der Waals forces, hydrogen bonds or electrostatic interactions. Zeta potential analysis indicated that, at pH below 7.2 the surface of both biosorbents are positively charged, a

fact that can hinder the biosorption of aluminum cations. As with kinetic modeling, the biosorbents also differed in isotherm modeling. The equilibrium of aluminum/humin system was better represented by the Langmuir model, while the Freundlich model showed an enhanced fit for aluminum/ash system. The satisfactory fit of Freundlich isotherm using the ashes can be associated to the greater heterogeneity of their surface, which is motivated by the fact that the calcination process of humin to obtain ashes cannot indeed be controlled. The q_{max} values also reveal that the removal capacity of humin is about twice as high as that of its respective ashes. The authors relate this to the presence of a greater number of complexing groups on the surface of humin.

Rajamohan et al. [78] analyzed the biosorbent applicability of powder made from the bark of *Eucalyptus camaldulensis*, a tree species widely used in pulp and paper industry. *E. camaldulensis* bark is mostly composed of cellulose (37.4%), lignin (28%) and hemicellulose (19.2%). The biomaterial underwent acid treatment with $C_4H_6O_6$ to remove impurities and improve the number of available sites on its surface. The study analyzed the influence of the variation of important operating parameters such as amount of biosorbent, pH, and initial concentration of the metal solution, temperature and agitation for the aluminum biosorption from aqueous solutions. Removal of metal ions was favored at pH 5, decreasing below 4 and above 6. The PSO model was observed as the to be that which best fitted the kinetic data at all studied concentrations and temperature, while the intraparticle diffusion model did not fit satisfactorily under any experimental condition. System equilibrium was explained by Langmuir isotherm, indicating that aluminum adsorption occurs through the formation of monolayers and that the biosorbent surface is homogeneous. The increase in q_{max} and K_L values with temperature indicated an endothermic process. Evaluation of the system's activation energy (E_a) provided insights about the type of adsorption. In this case, E_a=43.23 kJ/mol, a value considered high, indicated that aluminum biosorption using *E. camaldulensis* residue is intrinsically a chemical process.

El Houda Larbi et al. [76] researched the removal of aluminum and cadmium ions using sludge from treatment ponds as biosorption material. As this is a complex organic material, characterization was a key step. It was found that the sludge was basically composed of a large fraction of organic matter (high values of chemical e biological oxygen demand) and also low percentages of phosphorus and metal elements, such as zinc, copper, manganese, nickel and iron. FTIR analysis showed the presence of OH, C-

H (aliphatic), COOH and aromatic groups (C=C). In kinetic and equilibrium studies, the most favorable pH for aluminum removal was 4. The system reached equilibrium after 1 hour, obtaining a removal of 76% for Al^{3+} and only 18% for Cd^{3+} for monocomposite solutions with initial concentration of 50 mg/L. The kinetics of both systems was adequately described by the PSO model, while the equilibrium data of these processes were represented by the Langmuir model. Moreover, the q_{max} value of aluminum using the sludge was the highest among the works featured in Table 2.2. However, the preparation of this biosorbent, as described by the authors, is extremely time-consuming, since the sludge must undergo the humification process, which takes about 180 days. In this study, a greater affinity of the biosorbent with aluminum than cadmium can be observed. The opposite behavior was observed by Seo et al. [112], whom studied a similar biosorbent, a biomass derived from sludge from a wastewater treatment plant, for the removal of heavy metals. In this study, the authors evaluated the affinity and kinetic and equilibrium parameters for several cations, among them aluminum was the metal with worst results of maximum removal capacity, while cadmium presented one of the highest values for this variable.

Abdel-Ghani et al. [108] used *Typha domingensis* leaves as biosorption material in a multi-metal solution containing aluminum, iron, zinc and lead. Characterization of the material revealed that its composition contains mainly cellulose, hemicellulose and other components such as carbon, hydrogen and nitrogen. By analyzing the FTIR spectrum before and after biosorption, functional groups such as OH, N-H and -CH proved to be the main agents of metal removal. All processes were carried out at the natural pH of the mixture (2.5), without any adjustment or control. System equilibrium was reached after 120 minutes. Kinetics was described using the PSO model, while isotherms were described using the Langmuir model. Analysis of q_{max} values showed that Al removal was not favored. This may be associated with the experimental conditions adopted, such as very low pH and the presence of other more competitive ions in the solution.

To sum up, like algae, agro-industrial waste is abundant and rapidly produced. The main positive point of using such waste is the sustainability of the process, since the biosorbents can be used in the same process plant where they are generated. In general, this waste has functional groups like OH, C=O, NH and CH, which favor the removal of aluminum. Table 2.2 presents the highest adsorption capacity (q_{max}) of Al^{3+} ions given by residual sludge from treatment ponds, which has no added value and often requires simple

pre-treatment to be used as a biosorbent. However, its use would be recommended to treat effluents rather than drinking water due to the total levels of organic carbon and the chemical and biological oxygen demand of the treated water, which may result in the generation of compounds such as lignin, tannin, pectin, etc. thus resulting in secondary pollutants [89].

2.5.5 Biosorbent regeneration

The capacity for regeneration and reuse is an important characteristic in selecting biosorbents, given its substantial contribution to the economic and environmental viability of the biosorption process. Regeneration of saturated biomass and recovery of metals can be carried out using acidic or basic eluents, chelating agents and even deionized water [149,150]. Approximately 90% of the works listed in Table 2.2 did not perform biosorbent regeneration studies, revealing a gap in this investigation.

Table 2.4 features a summary of studies on the regeneration of different saturated biosorbents after Al^{3+} uptake. Two to ten adsorption-desorption cycles were performed in these studies, with biosorbents showing an average of 88% desorption efficiency in the first cycle and 58.5% in the last. Average aluminum removal efficiency in processes using regenerated biosorbents was 84% in the first cycle and 66% in the last. The most commonly used eluent was HCl, but some studies used reagents such as ethylenediamine tetraacetic acid (EDTA) and NaOH. The most promising results were obtained with HCl, which may be associated with the reduced pH of the medium that favors metal desorption, besides increasing competition between Al^{3+} and H^{+} ions for active sites on the biosorbent surface [151]. However, the use of acid solutions must be controlled, as they can permanently damage the structure of the biomaterial [81].

Table 2.4 Recovery of Al^{3+} and reuse of different biosorbents.

Biosorbent	Eluent	Desorption efficiency	Removal efficiency	Reference
Pseudomonas putida	HCl	90 – 100% in 4 cycles	> 90% in 4 cycles	[122]
Cortinarius armillatus	HNO_3	95 – 61 % in 7 cycles	96 – 65 % in 7 cycles	[106]
Beach-cast seaweed	HCl	99 – 116 % in 2 cycles	-	[80]
Turbinaria conoides	HCl	> 95% in 3 cycles	-	[100]
Gelidium latifolium	Na_2EDTA	91.3 – 62.1 % in 4 cycles	73.9 – 45.16 % in 4 cycles	[124]
Ulva lactuca	Na_2EDTA	91.1 – 65.3 % in 4 cycles	76.1 – 49.1 % in 4 cycles	[124]
Colpomenia sinuosa	Na_2EDTA	90.6 – 65.2 % in 4 cycles	77.4 – 51.2 % in 4 cycles	[124]
Padina pavonica	HCl	90 – 75 % in 10 cycles	99 – 90 % in 10 cycles	[72]
Cassia occidentalis	NaOH	-	100 – 50.5 % in 8 cycles	[125]

2.5.6 Aluminum biosorption in fixed-bed dynamic system

Aiming at large scale industrial applications, continuous applications are more indicated to treat large volumes. In this sense, fixed-bed configurations have to be inspected in laboratory and pilot scales to obtain information about the biosorbent saturation in the column and resistance to mass transfer, which are important factors in analyzing the efficiency of the process in treating contaminated waters [152].

Despite the importance of the subject, there are few studies in the literature addressing aluminum biosorption in fixed-bed systems or using real wastewaters. This review shows that the works addressing aluminum biosorption are largely restricted to discontinuous batch experiments and use synthetic solutions. Although these trials are the first step to understanding the process and defining the optimal operating conditions of biosorption, assays using real effluents and fixed-bed columns are necessary aiming at practical large-scale applications of the technology. In this section, we will discuss some works available in literature that explores aluminum biosorption using real effluents and/or fixed-bed columns.

Lodeiro et al. [80] performed dynamic tests of Al^{3+} biosorption using beach cast seaweed, rich in *C. baccata*. The authors worked with real effluent from a water treatment plant in which aluminum was the main constituent, with a concentration of approximately 481 mg/L. With the goal of obtaining sufficient "empty bed contact time" to reach process equilibrium (26 min), a system was developed using a column of 80 cm in length and 12 cm in diameter filled with 1100 g of seaweed and with an average flow rate of 250 mL/min. The maximum removal capacity was 14 mg/g. The authors carried out the same process using commercial activated charcoal as adsorbent and the maximum removal value achieved was only 1.6 mg/g. It was also observed that under the same conditions, the system with activated charcoal reached the rupture point more quickly than with the beach cast seaweed.

2.5.7 Practical applications

Costa and coworkers [153] applied the alginate extraction waste from the brown algae *Sargassum filipendula* for the treatment of real effluents. Four types of effluents were examined: one from the wastewater from a tannery industry (A1), one from the exit

of the wastewater treatment facility of a leather industry (A2) and two from the entrance and exit of a French urban water treatment station (A3 and A4, respectively) in Strasbourg. These effluents contain several metals, including aluminum, chromium, lead and zinc, but in different concentrations. Aluminum levels in A1 (1.62 mg/L) and A2 (0.31 mg/L) were above the recommended levels. The biosorption process was initially carried out in discontinuous systems using the effluents at natural pH and also with pH controlled at 3.5. Unlike what has been frequently observed for synthetic effluents, in most cases Al^{3+} removal was hardly affected by the solution pH. The removal percentages were mostly similar in the systems with or without pH control (around 43%, 81% and 44% for A1, A2 and A3, respectively). In A4, aluminum concentration was already very low (<0.02 mg/L) and showed no variation whatsoever. It is known that aluminum uptake may be inhibited in the presence of other metals [100,154,155]; however, aluminum removal percentages obtained by Costa et al. [153] were quite significant, despite the coexistence of other metals in A1, A2, and A3 effluents. It is important to mention that A2 effluent had natural pH around 7.85. It is known that at this value aluminum is in its precipitated form, so the highest removal efficiency obtained for A2 can be also associated to chemical precipitation.

Shaaban et al. [124] analyzed the efficiency of three different types of algae for the Al^{3+} biosorption. The best removal results in synthetic effluents were obtained by the brown algae *C. sinuosa*, which was selected to study the viability of biosorption using 21 types of wastewater from different industries in the city of Borg El-Arab. High concentrations of aluminum were found in effluents from food, paper, soap and metal processing industries, where the levels were reduced from 39.03 mg/L, 3.13 mg/L, 9.09 mg/L and 4.38 mg/L to 12.67 mg/L, 0.964 mg/L, 3.21 mg/L and 0.93 mg/L, respectively, after biosorption onto brown algae *C. sinuosa*. Remarkably, aluminum concentrations in effluents from paper and metal processing industries were reduced to values below that required by Egyptian legislation (3 mg/L). However, the levels reached are still higher than WHO recommendation (0.2 mg/L). Overall, the biosorption process using brown algae *C. sinuosa* was considered promising, since it reached an average of 80.8% aluminum removal in all effluents, despite not reaching the maximum concentration parameter defined by international bodies. Based on these results, pretreatment is still recommended to reduce the initial concentration of aluminum before the biosorption process.

Kumari and Ravindhranath [109] evaluated the performance of biosorbents derived from the plant *Pongamia pinnata* in removing aluminum from wastewater of alumina manufacturing industries. The stems and leaves of *P. pinnata* were evaluated in the form of powder and ash, summing four types of biosorbents. The initial concentration of aluminum in the samples varied between 10 and 16 mg/L. Good aluminum removal percentages were obtained, varying from 90.5 to 93.5% for the effluent with the lowest aluminum concentration and 91.5 to 96.5% for that with the highest concentration. Similar results were obtained under the same operating conditions using a biosorbent derived from the plant *Cassia occidentalis*, indicating that it can also be a viable biomaterial for the removal of aluminum present in real effluents [125].

Loiacono et al. [156] investigated the removal of aluminum and other metals present in the wastewater of a metal-finishing factory, using hemp felt as biosorbent. The samples were collected from exit of the precipitation process of the factory wastewater treatment plant. Aluminum concentration in samples varied between 1.1 and 9.6 mg/L and removal efficiency was between 43 and 49%. The authors suggested that factors such as ionic radius, electronegativity and molar mass may affect the system's affinity and selectivity. Among the metals present in the effluent, aluminum has the smallest ionic radius and molar mass, which would explain its lower removal percentage. As in the work by Costa [153], removal percentages did not exceed 50%, yet may be considered promising in view of the system's competitiveness.

2.6 Conclusion and prospects

This work presented a review of studies on metal ion biosorption, more specifically the removal of aluminum ions. Although the toxicity of this metal ion is not highlighted in a significant way in the literature compared to other toxic metals, aluminum can cause significant damage to the environment and human health, as well as water resources. Among the many processes used to remove aluminum in aqueous media, biosorption stands out as one of the most viable in terms of cost-benefit and efficiency. The studies reviewed involved non-conventional and low-cost biosorbents for Al^{3+} uptake. The performance of biosorbents based on bacteria, fungus, algae and agro-industrial wastes was evaluated based on q_{max} values. This article presented the mechanisms involved in the processes using different biosorbents, addressing kinetics, equilibrium and thermodynamics. Modeling revealed that most studies have kinetic data

described by the PSO model, while the Langmuir model best represents most equilibrium data. Biosorption of aluminum are in general spontaneous and endothermic processes. Factors such as temperature, pH and initial metal concentration are those that most directly affect the processes. The main functional groups involved in the removal of Al^{3+} by most of the investigated biosorbents, regardless of their source, are the carboxyl, hydroxyl and amine groups. Although fixed-bed dynamic tests are essential to scale up the process, few articles approached this system. Future studies related to aluminum biosorption from aqueous media could address other topics such as:

(i) Process and product life cycle assessment of aluminum biosorption, evaluating the impacts on humans, fauna and flora;
(ii) Studies involving other biosorbents and functionalization, especially biomass derived from microorganisms;
(iii) Application of bionanomaterials from alternative sources for Al (III) biosorption;
(iv) Aluminum biosorption studies using real wastewaters in fixed-bed dynamic systems;
(v) Evaluation of biosorbent reuse, with adsorption-desorption cycles aimed at commercial/industrial application;
(vi) Evaluation of the costs involved in a potential large-scale system aimed at industrial application.

Acknowledgments

The authors are grateful to *Coordenação de Aperfeiçoamento de Pessoal de Nível Superior* - CAPES [Coordination Office for the Improvement of Higher Education Personnel], *Conselho Nacional de Desenvolvimento Científico e Tecnológico* – CNPq [Brazilian Council for Scientific and Technological Development] (Proc 308046/2019-6) and *Fundação de Amparo à Pesquisa do Estado de São Paulo* – FAPESP [São Paulo Research Foundation] (Proc. 2017/18236-1 and 2019/11353-8) for the funding provided.

References

[1] J.O. Duruibe, M.O.C. Ogwuegbu, J.N. Egwurugwu, Int. J. Phys. Sci. 2(5) (2007) 112–8.

[2] F.R. Segura, E.A. Nunes, F.P. Paniz, A.C.C. Paulelli, G.B. Rodrigues, G.Ú.L. Braga, W. dos Reis Pedreira Filho, F. Barbosa, G. Cerchiaro, F.F. Silva, B.L. Batista, Environ.

Pollut. 218 (2016) 813–25. 10.1016/j.envpol.2016.08.005.

[3] M.N. Othman, M.P. Abdullah, Y.F.A. Aziz, Sains Malaysiana 39(1) (2010) 51–5.

[4] M. Tsezos, in: A. Schippers, F. Glombitza, W. Sand (Eds.), Geobiotechnology I, Springer, 2013, pp. 173–209.

[5] T.L. da Silva, A.C. da Silva, M.G.A. Vieira, M.L. Gimenes, M.G.C. da Silva, J. Clean. Prod. 137 (2016) 1470–8. 10.1016/j.jclepro.2015.05.067.

[6] M.G.A. Vieira, R.M. Oisiovici, M.L. Gimenes, M.G.C. Silva, Bioresour. Technol. 99(8) (2008) 3094–9. 10.1016/j.biortech.2007.05.071.

[7] E. Nishikawa, M.G.C. da Silva, M.G.A. Vieira, J. Clean. Prod. 178 (2018) 166–75. 10.1016/j.jclepro.2018.01.025.

[8] E. Nishikawa, S.L. Cardoso, C.S.D. Costa, M.G.C. da Silva, M.G.A. Vieira, J. Water Process Eng. 36 (2020) 101322. 10.1016/j.jwpe.2020.101322.

[9] B.P. Moino, C.S.D. Costa, M.G. Carlos da Silva, M.G.A. Vieira, Chem. Eng. Commun. 207(1) (2020) 17–30. 10.1080/00986445.2018.1564909.

[10] B.P. Moino, C.S.D. Costa, M.G.C. da Silva, M.G.A. Vieira, Can. J. Chem. Eng. 95(11) (2017) 2120–8. 10.1002/cjce.22859.

[11] N.T. das G. Santos, M.G.C. da Silva, M.G.A. Vieira, Environ. Sci. Pollut. Res. 26(28) (2019) 28455–69. 10.1007/s11356-018-3378-z.

[12] T.B. da Costa, M.G.C. da Silva, M.G.A. Vieira, J. Rare Earths 38(4) (2020) 339–55. 10.1016/j.jre.2019.06.001.

[13] S. Rangabhashiyam, K. Vijayaraghavan, J. Ind. Eng. Chem. 80 (2019) 318–24. 10.1016/j.jiec.2019.08.010.

[14] A. Srinivasan, T. Viraraghavan, J. Environ. Manage. 91(10) (2010) 1915–29. 10.1016/j.jenvman.2010.05.003.

[15] Z. Aksu, Process Biochem. 40(3–4) (2005) 997–1026. 10.1016/j.procbio.2004.04.008.

[16] G.R. Freitas, M.G.C. Silva, M.G.A. Vieira, Environ. Sci. Pollut. Res. 26(19) (2019) 19097–118. 10.1007/s11356-019-05330-8.

[17] D.M. Ruthven, Principles of Adsorption and Adsorption Processes, Wiley, 1984.

[18] J. Wang, C. Chen, Biotechnol. Adv. 27(2) (2009) 195–226. 10.1016/j.biotechadv.2008.11.002.

[19] L.K.S. Lima, B.T. Pelosi, M.G.C. Silva, M.G.A. Vieira, Chem. Eng. Trans. 32 (2013) 1045–50.

[20] S.L. Cardoso, C.S.D. Costa, E. Nishikawa, M.G.C. da Silva,, M.G.A. Vieira, J. Clean. Prod. 165 (2017) 491–9. 10.1016/j.jclepro.2017.07.114.

[21] J.R. de Andrade, M.G.C. da Silva, M.L. Gimenes, M.G.A. Vieira, Environ. Sci.

Pollut. Res. 25(26) (2018) 25967–82. 10.1007/s11356-018-2651-5.

[22] E. Merian, M. Anke,, M. Ihnat, M. Stoeppler, Elements and Their Compounds in the Environment Edited by Related Titles Joachim Nölte Bernhard Welz , Michael Sperling Handbook of Elemental Speciation Markus Stoeppler , Wayne R . Wolf , Peter J . Jenks (eds) Reference Materials for Chemical Analysis, 2004.

[23] International Aluminium Institute, Primary Aluminium Production. Available at: http://www.world-aluminium.org/statistics/primary-aluminium-production/. Accessed April 20, 2020.

[24] E. Lydersen, S. Löfgren, R.T. Arnesen, Crit. Rev. Environ. Sci. Technol. 32(2–3) (2002) 73–295. 10.1080/10643380290813453.

[25] J.P. Gustafsson, Visual MINTEQ 3.1 user guide. Available at: https://vminteq.lwr.kth.se/download/. Accessed December 22, 2020.

[26] J.R. Walton, Encyclopedia of Environmental Health, Elsevier, 2011, pp. 343–52.

[27] D. Krewski, R. a Yokel, E. Nieboer, D. Borchelt, J. Cohen, S. Kacew, J. Lindsay, A.M. Mahfouz, V. Rondeau, KREWSKI, D. et al. Human Health Risk Assessment For Aluminium, Aluminium Oxide, and Aluminium Hydroxide. [s.l: s.n.]. v. 10Human Health Risk Assessment For Aluminium, Aluminium Oxide, and Aluminium Hydroxide, Vol. 10, 2007.

[28] B.R. Stephens, J.S. Jolliff, Aluminum and Alzheimer's Disease, Elsevier Inc., 2015.

[29] S.D.W. Comber, M.J. Gardner, J. Churchley, Chem. Speciat. Bioavailab. 17(3) (2005) 117–28. 10.3184/095422905782774874.

[30] A. Maleki, B. Roshani, F. Karakani, J. Appl. Sci. Environ. Manag. 9(2) (2005). 10.4314/jasem.v9i2.17291.

[31] S. Nasseh, N. Mehranbod, R. Eslamloueyan, J. Environ. Chem. Eng. 7(6) (2019) 103513. 10.1016/j.jece.2019.103513.

[32] E. Skibniewska, M. Skibniewski, Mammals and Birds as Bioindicators of Trace Element Contaminations in Terrestrial Environments, Springer International Publishing, Cham, 2019, pp. 413–62.

[33] Agency for Toxic Substances and Disease Registry, ATSDR's Toxicological Profiles, CRC Press, 2008, p. .

[34] M. Dermience, G. Lognay, F. Mathieu, P. Goyens, J. Trace Elem. Med. Biol. 32 (2015) 86–106. 10.1016/j.jtemb.2015.06.005.

[35] C.A. Shaw, L. Tomljenovic, Immunol. Res. 56(2–3) (2013) 304–16. 10.1007/s12026-013-8403-1.

[36] L. Tomljenovic, J. Alzheimer's Dis. 23(4) (2011) 567–98. 10.3233/JAD-2010-101494.

[37] C. Exley, Environ. Sci. Process. Impacts 15(10) (2013) 1807–16. 10.1039/C3EM00374D.

[38] S. Singh, D.K. Tripathi, S. Singh, S. Sharma, N.K. Dubey, D.K. Chauhan, M. Vaculík, Environ. Exp. Bot. 137 (2017) 177–93. 10.1016/j.envexpbot.2017.01.005.

[39] J. Freda, Environ. Pollut. 71(2–4) (1991) 305–28. 10.1016/0269-7491(91)90035-U.

[40] R.W. Gensemer, R.C. Playle, Crit. Rev. Environ. Sci. Technol. 29(4) (1999) 315–450. 10.1080/10643389991259245.

[41] M.J.K. Fawell, J. Guidel. Drink. Qual. (1998) 8–23.

[42] F.W. Pontius, S.W. Clark, in: R. D. Letterman (Ed.), Water Quality and Treatment: A Handbook of Community Water Supplies, 5th ed., McGraw-Hill, Inc., 1999, pp. 1.1-1.41.

[43] X. Wei, R.C. Viadero, K.M. Buzby, Environ. Eng. Sci. 22(6) (2005) 745–55. 10.1089/ees.2005.22.745.

[44] A. Dąbrowski, Z. Hubicki, P. Podkościelny, E. Robens, Chemosphere 56(2) (2004) 91–106. 10.1016/j.chemosphere.2004.03.006.

[45] Z. Hubicki, D. Koodynsk, in: A. Kilislioğlu (Ed.), Ion Exchange Technologies, InTech, 2012, pp. 193–240.

[46] F.G. Helfferich, Ion exchange, McGraw-Hill, Inc., 1962.

[47] Z. Liu, S. Zhu, Y. Li, Front. Environ. Sci. Eng. China 6(1) (2012) 45–50. 10.1007/s11783-010-0262-6.

[48] F.S.E. Monteagudo, M.J.D. Cassidy, P.I. Folb, Med. Toxicol. Adverse Drug Exp. 4(1) (1989) 1–16. 10.1007/BF03259899.

[49] H. Al-Zoubi, A. Rieger, P. Steinberger, W. Pelz, R. Haseneder, G. Härtel, Sep. Sci. Technol. 45(14) (2010) 2004–16. 10.1080/01496395.2010.480963.

[50] F. Fu, Q. Wang, J. Environ. Manage. 92(3) (2011) 407–18. 10.1016/j.jenvman.2010.11.011.

[51] T. Tran, B. Bolto, S. Gray, M. Hoang, E. Ostarcevic, Water Res. 41(17) (2007) 3915–23. 10.1016/j.watres.2007.06.008.

[52] K. Ohno, Y. Matsui, M. Itoh, Y. Oguchi, T. Kondo, Y. Konno, T. Matsushita, Y. Magara, Desalination 254(1–3) (2010) 17–22. 10.1016/j.desal.2009.12.020.

[53] M. Hua, S. Zhang, B. Pan, W. Zhang, L. Lv, Q. Zhang, J. Hazard. Mater. 211–212 (2012) 317–31. 10.1016/j.jhazmat.2011.10.016.

[54] S. De Gisi, G. Lofrano, M. Grassi, M. Notarnicola, Sustain. Mater. Technol. 9 (2016) 10–40. 10.1016/j.susmat.2016.06.002.

[55] E. Eskandari, M. Kosari, M.H. Davood Abadi Farahani,, N.D. Khiavi, M. Saeedikhani, R. Katal, M. Zarinejad, Sep. Purif. Technol. 231 (2020) 115901. 10.1016/j.seppur.2019.115901.

[56] A. Tripathi, M. Rawat Ranjan, J. Bioremediation Biodegrad. 06(06) (2015). 10.4172/2155-6199.1000315.

[57] P.G. Pour, M.A. Takassi, T. Hamoule, Orient. J. Chem. 30(3) (2014) 1365–9. 10.13005/ojc/300356.

[58] A.M. Abdullah, J. Pollut. Eff. Control 02(02) (2014) 2–5. 10.4172/2375-4397.1000120.

[59] P.M. Choksi, V.Y. Joshi, Desalination 208(1–3) (2007) 216–31. 10.1016/j.desal.2006.04.081.

[60] Z. Aly, A. Graulet, N. Scales, T. Hanley, Environ. Sci. Pollut. Res. 21(5) (2014) 3972–86. 10.1007/s11356-013-2305-6.

[61] R.H. Vieira, B. Volesky, Int. Microbiol. 3(1) (2000) 17–24.

[62] M. Bilal, T. Rasheed, J.E. Sosa-Hernández, A. Raza, F. Nabeel, H.M.N. Iqbal, Mar. Drugs 16(2) (2018) 1–16. 10.3390/md16020065.

[63] A. Tassist, H. Lounici, N. Abdi, N. Mameri, J. Hazard. Mater. 183(1–3) (2010) 35–43. 10.1016/j.jhazmat.2010.06.078.

[64] J.E.B. Cayllahua, M.L. Torem, Chem. Eng. J. 161(1–2) (2010) 1–8. 10.1016/j.cej.2010.03.025.

[65] G. Ozdemir, S.H. Baysal, Appl. Microbiol. Biotechnol. 64(4) (2004) 599–603. 10.1007/s00253-003-1479-0.

[66] H.S. Titah, I.F. Purwanti, B.V. Tangahu, S.B. Kurniawan, M.F. Imron, S.R.S. Abdullah, N. ‘Izzati Ismail, J. Environ. Manage. 238 (2019) 194–200. 10.1016/j.jenvman.2019.03.011.

[67] R. Dhankhar, A. Hooda, Environ. Technol. 32(5) (2011) 467–91. 10.1080/09593330.2011.572922.

[68] T.A. Davis, B. Volesky, A. Mucci, Water Res. 37(18) (2003) 4311–30. 10.1016/S0043-1354(03)00293-8.

[69] C.S.D. Costa, M.G.C. da Silva, M.G.A. Vieira, J. Clean. Prod. 200 (2018) 890–9. 10.1016/j.jclepro.2018.07.314.

[70] W.J. do Nascimento Júnior, M.G.C. da Silva, M.G.A. Vieira, Environ. Sci. Pollut. Res. 26(23) (2019) 23416–28. 10.1007/s11356-019-05471-w.

[71] W.J. Nascimento Júnior, M.G.C. Silva, M.G.A. Vieira, J. Water Process Eng. 36 (2020) 101294. 10.1016/j.jwpe.2020.101294.

[72] A. Sari, M. Tuzen, J. Hazard. Mater. 171(1–3) (2009) 973–9. 10.1016/j.jhazmat.2009.06.101.

[73] H.S. Lee, J.H. Suh, Korean J. Chem. Eng. 18(5) (2001) 692–7. 10.1007/BF02706388.

[74] H.S. Lee, J.H. Suh, I.B. Kim, T. Yoon, Miner. Eng. 17(4) (2004) 487–93. 10.1016/j.mineng.2004.01.002.

[75] H.S. Lee, Biotechnol. Bioprocess Eng. 2(2) (1997) 126–31. 10.1007/BF02932340.

[76] N. El Houda Larbi, D.R. Merouani, H. Aguedal, A. Iddou, A. Khelifa, Key Eng. Mater. 800 KEM (2019) 181–6. 10.4028/www.scientific.net/KEM.800.181.

[77] M. Yurtsever, M. Nalçak, Glob. Nest J. 21(4) (2019) 477–83. 10.30955/gnj.002566.

[78] N. Rajamohan, M. Rajasimman, R. Rajeshkannan, V. Saravanan, Alexandria Eng. J. 53(2) (2014) 409–15. 10.1016/j.aej.2014.01.007.

[79] K.S. Rani, Int. J. Sci. Res. 4(2) (2015) 1701–4.

[80] P. Lodeiro, Á. Gudiña, L. Herrero, R. Herrero, M.E. Sastre de Vicente, J. Hazard. Mater. 178(1–3) (2010) 861–6. 10.1016/j.jhazmat.2010.02.017.

[81] K. Vijayaraghavan, R. Balasubramanian, J. Environ. Manage. 160 (2015) 283–96. 10.1016/j.jenvman.2015.06.030.

[82] A. Masoumi, K. Hemmati, M. Ghaemy, Chemosphere 146 (2016) 253–62. 10.1016/j.chemosphere.2015.12.017.

[83] A. Mehdinia, H. Mehrabi, Industrial Applications of Nanomaterials, Elsevier, 2019, pp. 365–402.

[84] T. Hasanin, S. Ahmed, T. Barakat, Egypt. J. Chem. (2019) 0–0. 10.21608/ejchem.2019.5921.1504.

[85] G. López-Téllez, C.E. Barrera-Díaz, P. Balderas-Hernández, G. Roa-Morales, B. Bilyeu, Chem. Eng. J. 173(2) (2011) 480–5. 10.1016/j.cej.2011.08.018.

[86] S. Wadhawan, A. Jain,, J. Nayyar, S.K. Mehta, J. Water Process Eng. 33 (2020) 101038. 10.1016/j.jwpe.2019.101038.

[87] B.W. Atkinson, F. Bux,, H.C. Kasan, Water SA 24(2) (1998).

[88] A. Robalds, G.M. Naja, M. Klavins, J. Hazard. Mater. 304 (2016) 553–6. 10.1016/j.jhazmat.2015.10.042.

[89] H.N. Tran, S.J. You, A. Hosseini-Bandegharaei, H.P. Chao, Water Res. 120 (2017) 88–116. 10.1016/j.watres.2017.04.014.

[90] A.A. Beni, A. Esmaeili, Environ. Technol. Innov. 17 (2020) 100503. 10.1016/j.eti.2019.100503.

[91] G.M. Gadd, FEMS Microbiol. Lett. 100(1–3) (1992) 197–203. 10.1016/0378-1097(92)90209-7.

[92] S. V. Avery, G.A. Codd, G.M. Gadd, Appl. Microbiol. Biotechnol. 39(6) (1993) 812–7. 10.1007/BF00164471.

[93] N.K. Lazaridis, D.D. Asouhidou, Water Res. 37(12) (2003) 2875–82. 10.1016/S0043-1354(03)00119-2.

[94] S. Lagergren, Handlingar 24 (1898) 1–39. 10.1007/BF01501332.

[95] Y.. Ho, G. McKay, Process Biochem. 34(5) (1999) 451–65. 10.1016/S0032-9592(98)00112-5.

[96] W.J. Weber, C.J. Morris, J. Sanit. Eng. Div. 89(2) (1963) 31–60.

[97] G.E. Boyd, A.W. Adamson, L.S. Myers, J. Am. Chem. Soc. 69(11) (1947) 2836–48. 10.1021/ja01203a066.

[98] S.Y. Elovich, O.G. Larinov, Izv. Akad. Nauk. SSSR, Otd. Khim. Nauk 2(2) (1962) 209–16.

[99] H. Qiu,, L. Lv, B. Pan, Q. Zhang, W. Zhang, Q. Zhang, J. Zhejiang Univ. A 10(5) (2009) 716–24. 10.1631/jzus.A0820524.

[100] K. Vijayaraghavan, S. Gupta, U.M. Joshi, Water. Air. Soil Pollut. 223(6) (2012) 2923–31. 10.1007/s11270-012-1075-y.

[101] W. Plazinski, W. Rudzinski, A. Plazinska, Adv. Colloid Interface Sci. 152(1–2) (2009) 2–13. 10.1016/j.cis.2009.07.009.

[102] S. Azizian, J. Colloid Interface Sci. 276(1) (2004) 47–52. 10.1016/j.jcis.2004.03.048.

[103] K.V. Kumar, J. Hazard. Mater. 137(1) (2006) 638–9. 10.1016/j.jhazmat.2006.03.056.

[104] É.C. Lima, M.A. Adebayo, F.M. Machado, 2015, pp. 33–69.

[105] E.C. Lima, A.R. Cestari, M.A. Adebayo, Desalin. Water Treat. 57(41) (2016) 19566–71. 10.1080/19443994.2015.1095129.

[106] N. Naeemullah, M. Tuzen, A. Sari, D. Mendil, At. Spectrosc. 38(5) (2017) 149–57. 10.46770/as.2017.05.005.

[107] L.M.T. Rosa, W.G. Botero, J.C.C. Santos, T.A. Cacuro, W.R. Waldman, J.B. do Carmo, L.C. de Oliveira, J. Environ. Manage. 215 (2018) 91–9. 10.1016/j.jenvman.2018.03.048.

[108] N.T. Abdel-Ghani, A.K. Hegazy, G.A. El-Chaghaby, Int. J. Environ. Sci. Technol. 6(2) (2009) 243–8. 10.1007/BF03327628.

[109] A.A. Kumari, K. Ravindhranath, J. Chem. Pharm. Sci. 10(1) (2017) 398–409.

[110] A.A. Halim, E. Ezani, M.S. Othman, N. Awang, M.I. Wahab, A. Ithnin, Nat. Environ. Pollut. Technol. 11(2) (2012) 193–7.

[111] A.M.S. Mimura, T.V. de A. Vieira, P.B. Martelli, H. de F. Gorgulho, Quim. Nova 33(6) (2010) 1279–84. 10.1590/S0100-40422010000600012.

[112] J.H. Seo, N. Kim, M. Park, S. Lee, S. Yeon, D. Park, Environ. Eng. Res. 25(5) (2020) 700–6. 10.4491/eer.2019.201.

[113] K.Y. Foo, B.H. Hameed, Chem. Eng. J. 156(1) (2010) 2–10. 10.1016/j.cej.2009.09.013.

[114] M.C. Ncibi, J. Hazard. Mater. 153(1–2) (2008) 207–12. 10.1016/j.jhazmat.2007.08.038.

[115] I. Langmuir, J. Am. Chem. Soc. 40(9) (1918) 1361–403. 10.1021/ja02242a004.

[116] H. Freundlich, Zeitschrift Für Phys. Chemie 57U(1) (1907). 10.1515/zpch-1907-5723.

[117] M.M. Dubinin, L. V Radushkevitch, Proc. Acad. Sci. USSR 55 (1947).

[118] R. Sips, J. Chem. Phys. 16(5) (1948) 490–5. 10.1063/1.1746922.

[119] M.I. Temkin, Acta Physiochim. URSS 12 (1940) 327–56.

[120] U. Farooq, J.A. Kozinski, M.A. Khan, M. Athar, Bioresour. Technol. 101(14) (2010) 5043–53. 10.1016/j.biortech.2010.02.030.

[121] Y. Liu, Y.J. Liu, Sep. Purif. Technol. 61(3) (2008) 229–42. 10.1016/j.seppur.2007.10.002.

[122] P.S. Boeris, M. del R. Agustín,, D.F. Acevedo, G.I. Lucchesi, J. Biotechnol. 236 (2016) 57–63. 10.1016/j.jbiotec.2016.07.026.

[123] S.O. Omeike, S.O. Kareem, S. Adewuyi, S.A. Balogun, Ife J. Sci. 15(1) (2013).

[124] A.E.S.M. Shaaban, R.K. Badawy, H.A. Mansour, M.E. Abdel-Rahman, Y.I.E. Aboulsoud, J. Appl. Phycol. 29(6) (2017) 3221–34. 10.1007/s10811-017-1185-4.

[125] P.K. Meghana, A.A. Kumari, K.V. Pravalika, P.J. Sriram, K. Ravindhranath, Rasayan J. Chem. 12(1) (2019) 338–46. 10.31788/RJC.2019.1215064.

[126] C. Septhum, S. Rattanaphani, J.B. Bremner, V. Rattanaphani, J. Hazard. Mater. 148(1–2) (2007) 185–91. 10.1016/j.jhazmat.2007.02.024.

[127] S.K. Srivastava, R. Tyagi, N. Pant, Water Res. 23(9) (1989) 1161–5. 10.1016/0043-1354(89)90160-7.

[128] P. Saha, S. Chowdhury, in: M. Tadashi (Ed.), Thermodynamics, InTech, 2011, pp. 349–64.

[129] I. Anastopoulos, A. Bhatnagar, E.C. Lima, J. Mol. Liq. 221 (2016) 954–62. 10.1016/j.molliq.2016.06.076.

[130] A.K. Meena, G.K. Mishra, P.K. Rai, C. Rajagopal, P.N. Nagar, J. Hazard. Mater. 122(1–2) (2005) 161–70. 10.1016/j.jhazmat.2005.03.024.

[131] A. van der Wal, W. Norde, A.J.B. Zehnder, J. Lyklema, Colloids Surfaces B Biointerfaces 9(1–2) (1997) 81–100. 10.1016/S0927-7765(96)01340-9.

[132] C. Aharoni, M. Ungarish, J. Chem. Soc. Faraday Trans. 1 Phys. Chem. Condens. Phases 73 (1977) 456. 10.1039/f19777300456.

[133] Z. Aksu, Process Biochem. 38(1) (2002) 89–99. 10.1016/S0032-9592(02)00051-1.

[134] E. López Errasquín,, C. Vázquez, Chemosphere 50(1) (2003) 137–43. 10.1016/S0045-6535(02)00485-X.

[135] D.J. Bueno, C.H. Casale, R.P. Pizzolitto, M.A. Salvano, G. Oliver, J. Food Prot.

70(9) (2007) 2148–54. 10.4315/0362-028X-70.9.2148.

[136] G. Naja, B. Volesky, Microbial Biosorption of Metals, Springer Netherlands, Dordrecht, 2011, pp. 19–58.

[137] K. Boriová, S. Čerňanský, P. Matúš, M. Bujdoš, A. Šimonovičová, M. Urík, Bioprocess Biosyst. Eng. 42(2) (2019) 291–6. 10.1007/s00449-018-2033-x.

[138] A. Hansda, V. Kumar, Anshumali, World J. Microbiol. Biotechnol. 32(10) (2016) 1–14. 10.1007/s11274-016-2117-1.

[139] T. Viraraghavan, A. Srinivasan, Microbial Biosorption of Metals, Springer Netherlands, Dordrecht, 2011, pp. 143–58.

[140] M. Bilal, T. Rasheed, J.E. Sosa-Hernández, A. Raza, F. Nabeel, H.M.N. Iqbal, Mar. Drugs 16(2) (2018) 1–16. 10.3390/md16020065.

[141] F. González, E. Romera, A. Ballester, M.L. Blázquez, J.Á. Muñoz, C. García-Balboa, Microbial Biosorption of Metals, Springer Netherlands, Dordrecht, 2011, pp. 159–78.

[142] E. Romera, F. González, A. Ballester, M.L. Blázquez, J.A. Muñoz, Bioresour. Technol. 98(17) (2007) 3344–53. 10.1016/j.biortech.2006.09.026.

[143] M.M. Figueira, B. Volesky, V.S.T. Ciminelli, F.A. Roddick, Water Res. 34(1) (2000) 196–204. 10.1016/S0043-1354(99)00120-7.

[144] K.H. Chong, B. Volesky, Biotechnol. Bioeng. 49(6) (1996) 629–38. 10.1002/(SICI)1097-0290(19960320)49:6<629::AID-BIT4>3.0.CO;2-Q.

[145] K. Vijayaraghavan, Y.S. Yun, Biotechnol. Adv. 26(3) (2008) 266–91. 10.1016/j.biotechadv.2008.02.002.

[146] H. Qin, T. Hu, Y. Zhai, N. Lu, J. Aliyeva, Environ. Pollut. 258 (2020) 113777. 10.1016/j.envpol.2019.113777.

[147] S. Regmi, K.N. Ghimire, M.R. Pokhrel, D.B. Khadka, J. Inst. Sci. Technol. 20(2) (2015) 145–52. 10.3126/jist.v20i2.13969.

[148] A.A. Kumari,, K. Ravindhranath, Int. J. ChemTech Res. 4(4) (2012) 1733–45. 10.5829/idosi.ijwres.2012.1.1.1101.

[149] M. Fomina, G.M. Gadd, Bioresour. Technol. 160 (2014) 3–14. 10.1016/j.biortech.2013.12.102.

[150] S. Lata, P.K. Singh, S.R. Samadder, Int. J. Environ. Sci. Technol. 12(4) (2015) 1461–78. 10.1007/s13762-014-0714-9.

[151] Y.F. Zhou, R.J. Haynes, Water. Air. Soil Pollut. 218(1–4) (2011) 457–70. 10.1007/s11270-010-0659-7.

[152] K.H. Chu, Chem. Eng. J. 97(2–3) (2004) 233–9. 10.1016/S1385-8947(03)00214-6.

[153] C.S.D. Costa, C. Bertagnolli, A. Boos, M.G.C. da Silva, M.G.A. Vieira, J. Water

Process Eng. 37 (2020) 101546. 10.1016/j.jwpe.2020.101546.

[154] A. Bakir, P. Mcloughlin, S.A.M. Tofail, E. Fitzgerald, Clean - Soil, Air, Water (2009) 712–9. 10.1002/clen.200900164.

[155] N.T. Abdel-Ghani, G.A. El-Chaghaby, F.S. Helal, Desalin. Water Treat. 51(16–18) (2013) 3558–75. 10.1080/19443994.2012.750806.

[156] S. Loiacono, G. Crini,, G. Chanet, M. Raschetti, V. Placet, N. Morin-Crini, J. Chem. Technol. Biotechnol. 93(9) (2018) 2592–601. 10.1002/jctb.5612.

3. Planejamento fatorial

3.1 Introdução

No Capítulo 2 foi apresentada a problemática da contaminação de corpos hídricos por íons de Al(III) bem como o uso de processos bioadsortivos utilizando materiais alternativos para o tratamento de meios aquosos contaminados por este metal. No geral, nota-se que as condições operacionais são de grande importância para o processo. Fatores como pH, concentração da solução, temperatura, tempo de contato, agitação, dosagem da biomassa e diâmetro das partículas adsorventes são frequentemente apontados como grandes influentes no processo de bioadsorção [1-3]. Diversos autores relatam que o efeito e a otimização destas variáveis que afetam sobremaneira o processo de bioadsorção de alumínio [4-6].

Entretanto, a avaliação do efeito de tantas variáveis normalmente requer a realização de muitos experimentos. Por isso, o planejamento de experimentos tem o intuito de verificar o impacto destas variáveis no sistema por meio de análise estatística, dessa forma reduzindo o número de ensaios a serem conduzidos. O tipo de planejamento depende diretamente do objetivo específico e da quantidade de variáveis analisadas. Neste trabalho o experimento fatorial definido foi o Delineamento Composto Central Rotacional (DCCR) associado à metodologia de superfície de resposta (MSR).

O planejamento DCCR consiste em um modelo fatorial 2k, onde k representa o número de fatores analisados, com 2^k pontos adicionais, chamados de ponto axial, e n repetições no ponto central. Nesse planejamento, o conceito de rotabilidade está associado a variância dos valores, que deve ser constante e em pontos igualmente distantes dos valores centrais do sistema [7]. Já a metodologia de superfície de resposta é aplicada de forma a reduzir o número de experimentos realizados, uma vez que combina o *design* do experimento com a análise de regressão, encontrando, assim, a otimização dos valores das variáveis operacionais do processo [8].

Adicionalmente, o DCCR apresenta uma série de vantagens como uma ferramenta flexível, podendo ser aplicada em diversas regiões experimentais, além da possibilidade de estimar efeitos de interações lineares e de curvatura [9]. Diversos estudos de adsorção de metais tóxicos reportados na literatura empregam este tipo de planejamento para a otimização de condições operacionais [10-13].

Nesse sentido, esta etapa do trabalho teve por objetivo avaliar e otimizar os principais parâmetros envolvidos no processo de bioadsorção de alumínio pelo resíduo

da alga *S. filipendula*, sendo estes: agitação, concentração inicial da solução metálica e dosagem do bioadsorvente. O efeito do pH claramente não pode ser desconsiderado, mas a análise deste fator foi realizada de forma separada e está apresentada na Figura 4.1, do Capítulo 4.

3.2 Materiais e métodos

As variáveis independentes analisadas pelo planejamento DCCR com superfície de resposta foram a velocidade de agitação (X_1), a concentração inicial da solução de alumínio (X_2) e a massa do resíduo adsorvente por volume de solução (X_3). As análises foram realizadas utilizando o *software Statistica* 13.05. O nível de confiança estudado foi de 95% e as variáveis de resposta foram o percentual de remoção (%R) e a capacidade de adsorção (q). Ao todo foram realizados 17 ensaios em pH definido pelo estudo anterior, temperatura ambiente (25 ºC) por 2 horas e 30 minutos, com o volume de cada ensaio fixado em 50 mL. A Tabela 3.1 apresenta os níveis dos fatores deste planejamento.

Tabela 3.1 Níveis dos fatores aplicados ao planejamento experimental.

Fator	**Níveis**				
	-1,68	**-1**	**0**	**1**	**1,68**
X_1	100	200	225	250	275
X_2	0,5	1	3	5	5,50
X_3	0,032	0,1	0,2	0,3	0,368

X_1 – Agitação (rpm), X_2 – Concentração inicial da solução (mmol/L), X_3 – Dosagem de adsorvente (g/50 mL)

O modelo empírico quadrático proposto para ambas as variáveis resposta é representado pela equação 3.1.

$$\%R/q = b_0 + b_1.X_1 + b_2.X_2 + b_3.X_3 + b_4.X_1^2 + b_5.X_2^2 + b_6.X_3^2 + b_7.X_1X_2 + b_8.X_1X_3 + b_9.X_2X_3 \quad (3.1)$$

A validade do modelo obtido pelo planejamento foi analisada por diversas ferramentas como, teste de curvatura, ANOVA e Teste F, sendo este último calculado pela Equação 3.2 [14].

$$F_{\frac{regressão}{resíduos}} = \frac{MQ_{regressão}}{MQ_{resíduos}} \quad (3.2)$$

Em que, $MQ_{regressão}$ e $MQ_{resíduos}$ representam a média quadrática da regressão e dos resíduos, respectivamente.

3.3 Resultados e discussão

Na Tabela 3.2 são apresentados os resultados das variáveis de resposta (capacidade de adsorção e porcentagem de remoção) para cada ensaio realizado em diferentes configurações experimentais.

Tabela 3.2 Resultados de %Rem e q da bioadsorção de Al (III).

Ensaio	X_1	X_2	X_3	%R	q (mmol/mg)
1	200	1,0	0,100	88,20	0,45
2	200	1,0	0,300	75,33	0,13
3	200	5,0	0,100	34,50	0,84
4	200	5,0	0,300	87,68	0,71
5	250	1,0	0,100	90,14	0,46
6	250	1,0	0,300	80,07	0,14
7	250	5,0	0,100	33,99	0,82
8	250	5,0	0,300	86,57	0,70
9	175	3,0	0,200	90,85	0,65
10	275	3,0	0,200	90,22	0,65
11	225	0,5	0,200	61,00	0,12
12	225	5,5	0,200	68,62	0,89
13	225	3,0	0,032	51,96	2,32
14	225	3,0	0,368	94,72	0,37
15	225	3,0	0,200	86,78	0,62
16	225	3,0	0,200	88,54	0,63
17	225	3,0	0,200	89,17	0,64

Nota-se que a concentração inicial da solução (X_2) e a dosagem do adsorvente (X_3) são as variáveis de maior impacto no processo, sendo que os valores mais baixos de remoção foram encontrados em condições experimentais onde a concentração da solução era alta e a dosagem baixa, por isso, pode-se concluir que estas duas variáveis são proporcionais e dependentes entre si. Por outro lado, a velocidade de agitação (X_1) não pareceu influenciar diretamente os resultados analisados, essa observação é confirmada na Tabela 3.3, onde estão apresentados os efeitos dos fatores analisados e suas interações entre si sobre o percentual de remoção.

Tabela 3.3 Efeitos das variáveis independentes e suas interações para %R.

Fator	Efeito	Desvio padrão	t (7)	p
Média	**87,5196**	**4,8666**	**17,9837**	**0,0000**
X_1	0,4743	4,3124	0,1100	0,9155
X_1^2	2,0028	3,7029	0,5409	0,6054
X_2	**-14,6450**	**5,1717**	**-2,8318**	**0,0253**
X_2^2	**-25,8377**	**7,5696**	**-3,4133**	**0,0112**
X_3	**22,6663**	**4,6698**	**4,8538**	**0,0018**
X_3^2	-9,0580	5,0496	-1,7938	0,1159
X_1X_2	-2,0773	6,0987	-0,3406	0,7434
X_1X_3	0,5503	6,0987	0,0902	0,9306
X_2X_3	**32,1754**	**6,0987**	**5,2758**	**0,0012**

Os valores destacados são os que apresentam significância para o processo. Por definição, o p-valor representa a probabilidade de erro envolvida ao aceitarmos o valor observado como válido [14]. Para o intervalo de 95% de confiança adotado, o limite de p-valor é 0,05, significando que existe uma probabilidade de 5% de que a relação entre variáveis observadas seja devido ao acaso. Portanto, foram considerados significativos efeitos cujo valor de p seja menor que o p-valor (0,05) do intervalo utilizado. O diagrama de Pareto apresentado na Figura 3.1 também auxilia na visualização desse resultado, nele as variáveis estão ordenadas das mais para as menos significativas.

Figure 3.1 Diagrama de Pareto para %R.

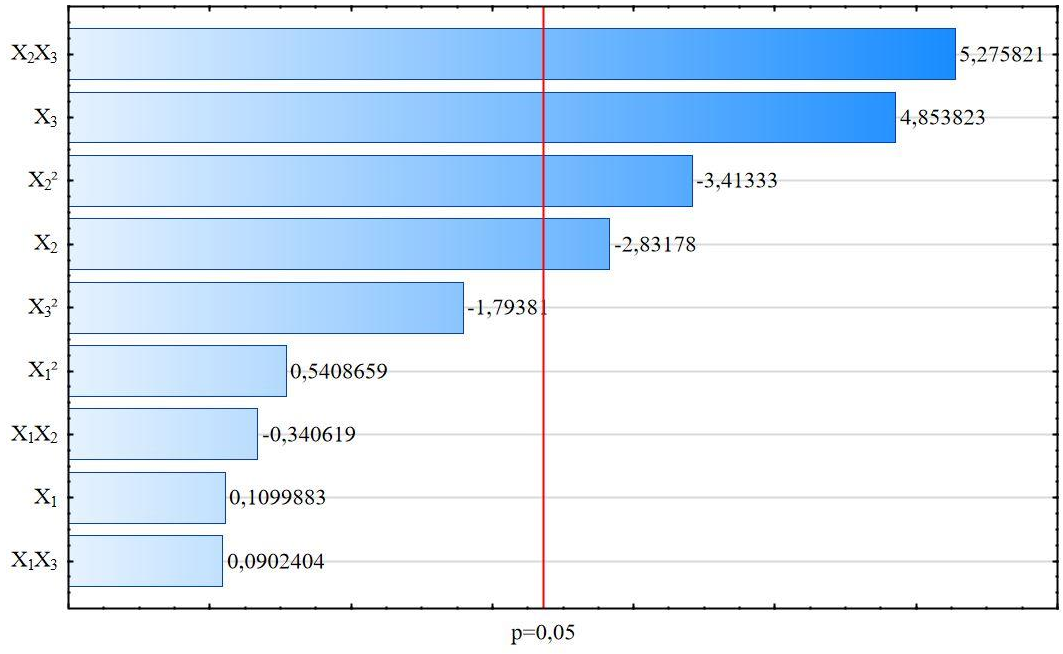

Como mencionado anteriormente, a agitação é confirmada como a única variável não significativa para o percentual de remoção, isso provavelmente signifique que na faixa de agitação analisada a resistência à transferência de massa no filme já era minimizada, de forma que qualquer variação não influenciaria mais no processo. No entanto, isso não significa que a agitação não seja uma variável importante na bioadsorção de metais tóxicos. Stirk e Staden [15] avaliaram que é necessário agitação para que sejam atingidos valores máximos de adsorção e que, além disso, esse fator pode influenciar diretamente na capacidade de remoção no início do processo. Já a concentração inicial da solução é significativa tanto pela avaliação linear quanto pela quadrática. Esse fator apresenta um efeito negativo, uma vez que quanto maior a concentração inicial de alumínio, maior a dificuldade para atingir altos percentuais de remoção. A dosagem da biomassa é um fator significativo e de efeito positivo. Esse resultado já era esperado uma vez que quanto maior a massa de adsorvente, maior o número de sítios ativos e, por consequência, maior o percentual de remoção. A interação entre a concentração e a dosagem também tem influência significativa sobre a variável resposta. Na Tabela 3.2 pode-se observar que altos valores de remoção são diretamente dependentes da proporcionalidade entre estas duas variáveis.

A Equação 3.3 representa o modelo final do sistema, obtido utilizando a metodologia *backward elimination*, considerando apenas os fatores significativos, com coeficiente de correlação (R^2) igual à 0,8598.

$$\%R = 84{,}62 - 7{,}32.X_2 - 12{,}60.X_2^2 + 11{,}33.X_3 + 16{,}87.X_2X_3 \qquad (3.3)$$

Com o auxílio da tabela ANOVA (Tabela 3.4) do modelo é possível verificar se esse modelo é estatisticamente significativo no intervalo de confiança escolhido através do teste F. Esse valor é calculado pela Equação 3.1 e para este modelo é igual a F_{calc} = 18,406. Para que o modelo seja significativo, este valor deve ser maior do que o valor de F tabelado [14]. Nesse caso, F_{tab} = 3,26, demonstrando, assim, que a regressão é significativa.

Tabela 3.4 Análise de variância (ANOVA) do modelo proposto para a variável-resposta %R.

Fonte de variação	**Soma quadrática**	**G.L.**	**Média quadrática**
Regressão	5509,276	4	1377,319
Resíduos	1624,021	12	135,335
Total	7133,297	16	

Outra forma de avaliar se o modelo se ajustou bem aos dados é através do gráfico dos valores preditos versus os valores experimentais obtidos (Figura 3.2). Nele os dados são comparados através de uma reta traçada y=x.

Figure 3.2 Valores preditos versus valores experimentais (%R).

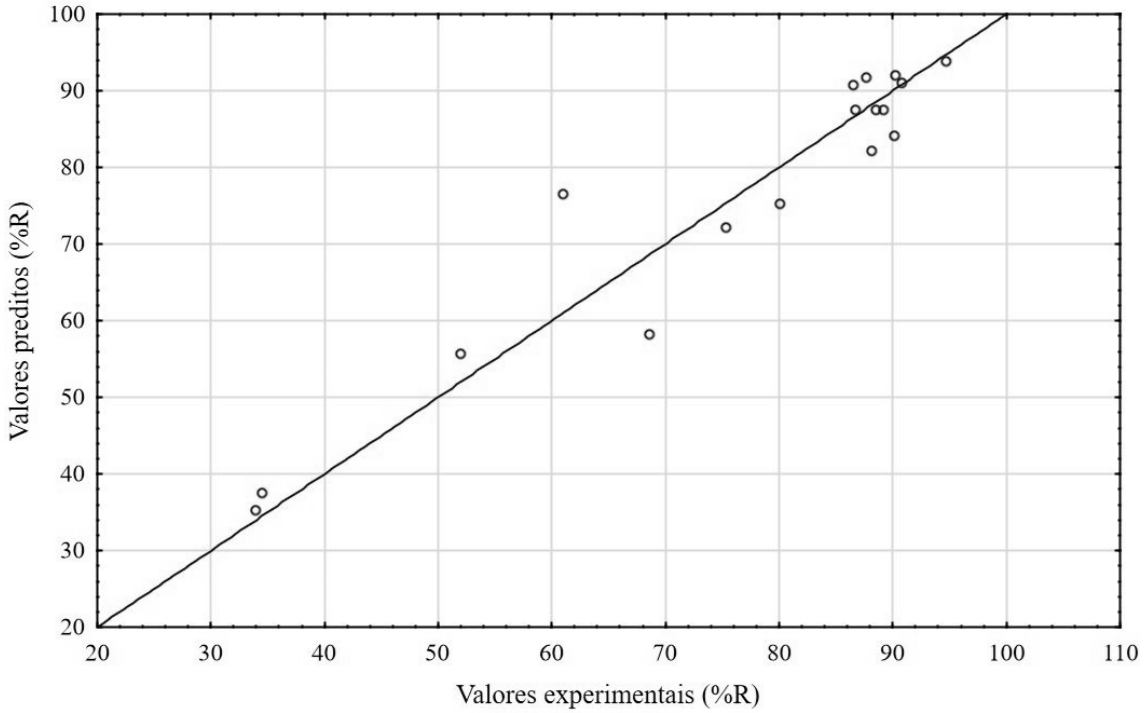

Observa-se que os valores estão próximos à reta e que se distribuem aleatoriamente em torno dela, isso indica que o modelo aplicado descreve os dados de maneira satisfatória, corroborando com o resultado do teste F da ANOVA.

Sendo o modelo bem ajustado aos dados, a próxima etapa foi avaliar o comportamento da interação entre as variáveis significativas através da representação gráfica da superfície de resposta do percentual de remoção do sistema (Figura 3.3).

Figure 3.3 Superfícies de Resposta (A) e de Contorno (B) para o percentual de remoção de Al em função da concentração inicial da solução e dosagem de material adsorvente.

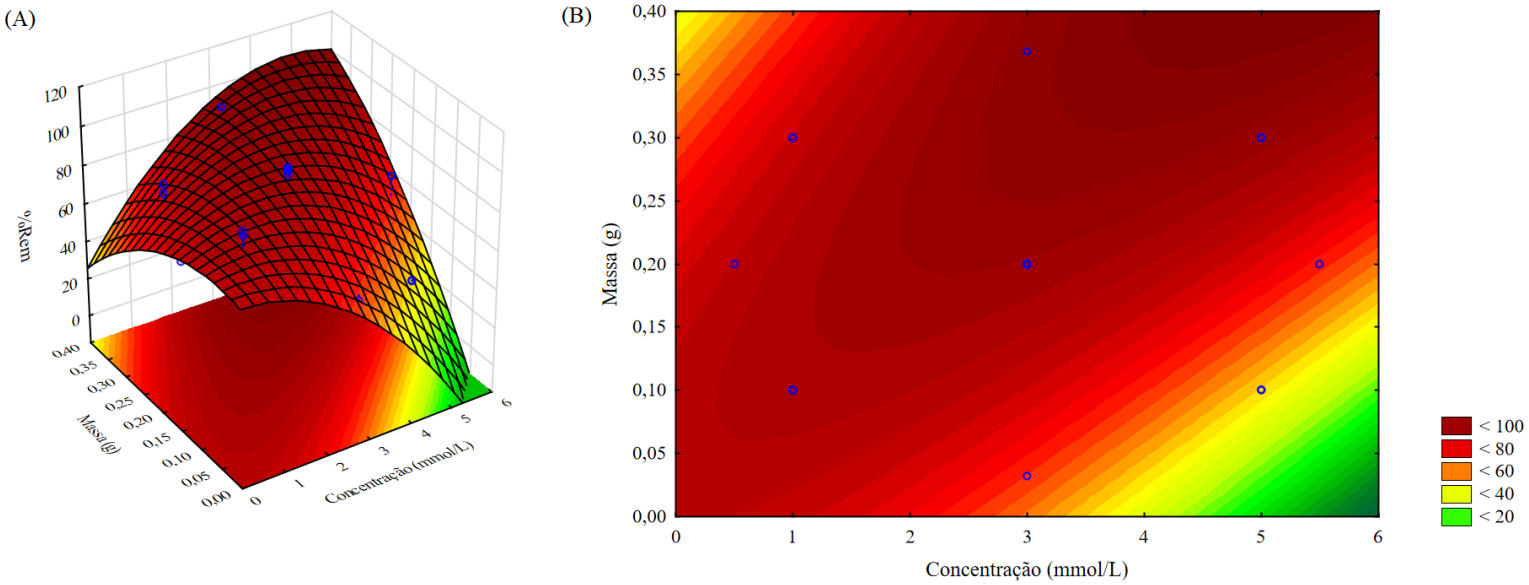

Pela análise das superfícies nota-se a grande interferência da concentração inicial da solução. Pode-se observar que para a concentração inicial de 1 mmol/L os valores das porcentagens de remoção ficaram em torno de 85%, independente da dosagem de biomassa. Outro padrão que pode ser constatado é a relação entre a dosagem e a concentração, verificando-se um aumento significativo na porcentagem de remoção conforme as duas variáveis aumentam proporcionalmente entre si.

O mesmo procedimento foi realizado para a análise da variável resposta q (capacidade de adsorção, mmol/g). Na Tabela 3.5 são apresentados os efeitos de todos os fatores analisados, aqueles que estão destacados são os que apresentam significância, com base no p-valor, para o processo.

Tabela 3.5 Efeitos das variáveis independentes e suas interações para q.

Fator	Efeito	Desvio padrão	t (7)	p
Média	**0,682674**	**0,204789**	**3,33354**	**0,012530**
X_1	-0,001579	0,181468	-0,00870	0,993298
X_1^2	-0,056814	0,155818	-0,36462	0,726164
X_2	**0,515204**	**0,217625**	**2,36739**	**0,049797**
X_2^2	-0,483373	0,318534	-1,51749	0,172930
X_3	**-0,612582**	**0,196506**	**-3,11737**	**0,016906**
X_3^2	0,391082	0,212487	1,84050	0,108266
X_1X_2	-0,009807	0,256634	-0,03821	0,970584
X_1X_3	0,000401	0,256634	0,00156	0,998797
X_2X_3	0,096993	0,256634	0,37794	0,716672

O diagrama de Pareto (Figura 3.4) também indica quais são as variáveis significativas para capacidade de adsorção.

Figure 3.4 Diagrama de Pareto para q.

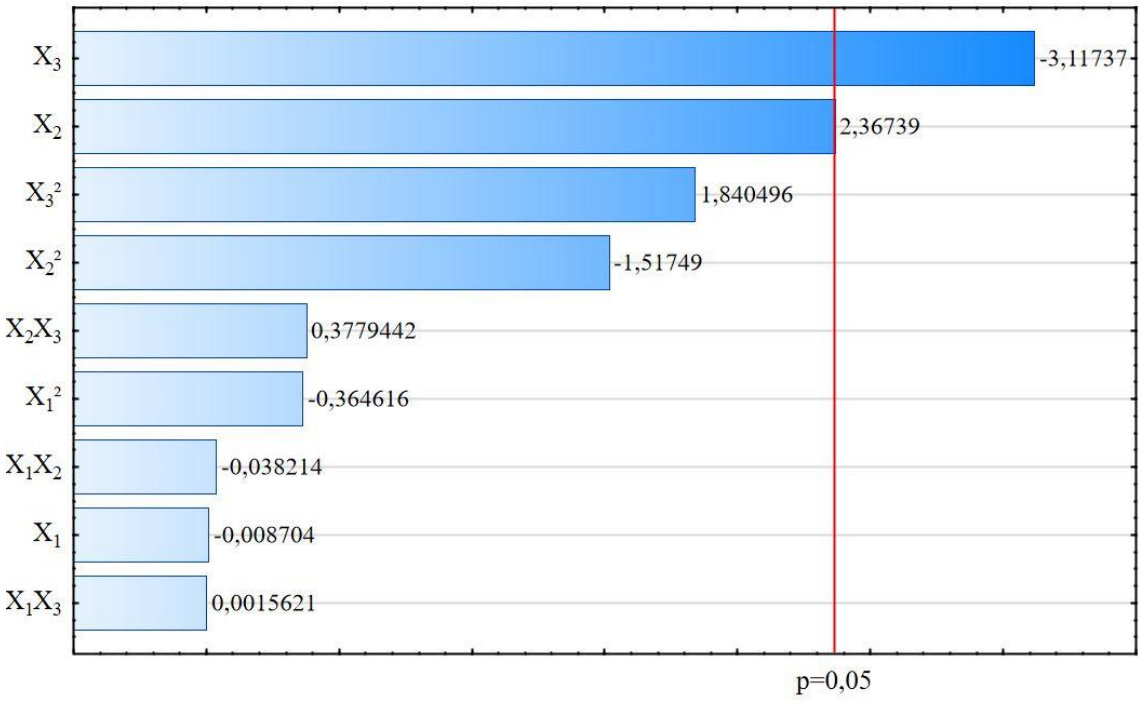

Observa-se pelo diagrama de Pareto que a dosagem da biomassa é o fator de maior impacto para esta variável de resposta. Além disso, seu efeito é negativo, o que pode ser diretamente relacionado à equação utilizada para o cálculo da capacidade de adsorção, em que a massa está no denominador. Logo, quanto menor o seu valor, maior será a capacidade. A concentração da solução (X_2) também é significativa e tem efeito positivo na capacidade de remoção. Pode-se concluir a partir destes resultados que altas concentrações de metal em baixas dosagens de adsorvente favorecem o aumento do valor desta variável resposta, ao contrário do observado nos resultados para a porcentagem de remoção.

Para a elaboração do modelo (Equação 3.4) e para a elaboração da tabela ANOVA (Tabela 3.6) foram desconsiderados os fatores não significativos no intervalo de confiança de 95%. No entanto, a partir da técnica *backward elimination*, constatou-se que as variáveis X_2^2 e X_3^2, apesar de inicialmente serem apontadas como não significativas, devem ser incluídas na equação do modelo final. O coeficiente de correlação deste modelo é de 0,7548.

$$q = 0{,}637 + 0{,}2576.X_2 - 0{,}227.X_2^2 - 0{,}306.X_3 + 0{,}207.X_3^2 \qquad (3.4)$$

Tabela 3.6 Análise de variância (ANOVA) do modelo proposto para a variável-resposta q.

Fonte de variação	Soma quadrática	G.L.	Média quadrática
Regressão	2,952	2	1,476101
Resíduos	0,958584	12	0,079882
Total	3,910786	16	

Pelo teste F observa-se que F_{calc} = 18,478 e, para este modelo, o F_{tab} = 3,89, sugerindo que o modelo é significativo. Entretanto, devido ao baixo R^2 obtido outros testes são necessários para confirmar o ajuste do modelo aos dados. Pelo gráfico dos valores preditos *versus* observados (Figura 3.5), nota-se que há uma distribuição regular dos dados no eixo y=x, assim é possível concluir que o modelo não seria o mais adequado para descrever o sistema, como para a variável %R. Contudo, ainda sim, pode ser representativo.

Figure 3.5 Valores preditos versus valores observados experimentalmente para q.

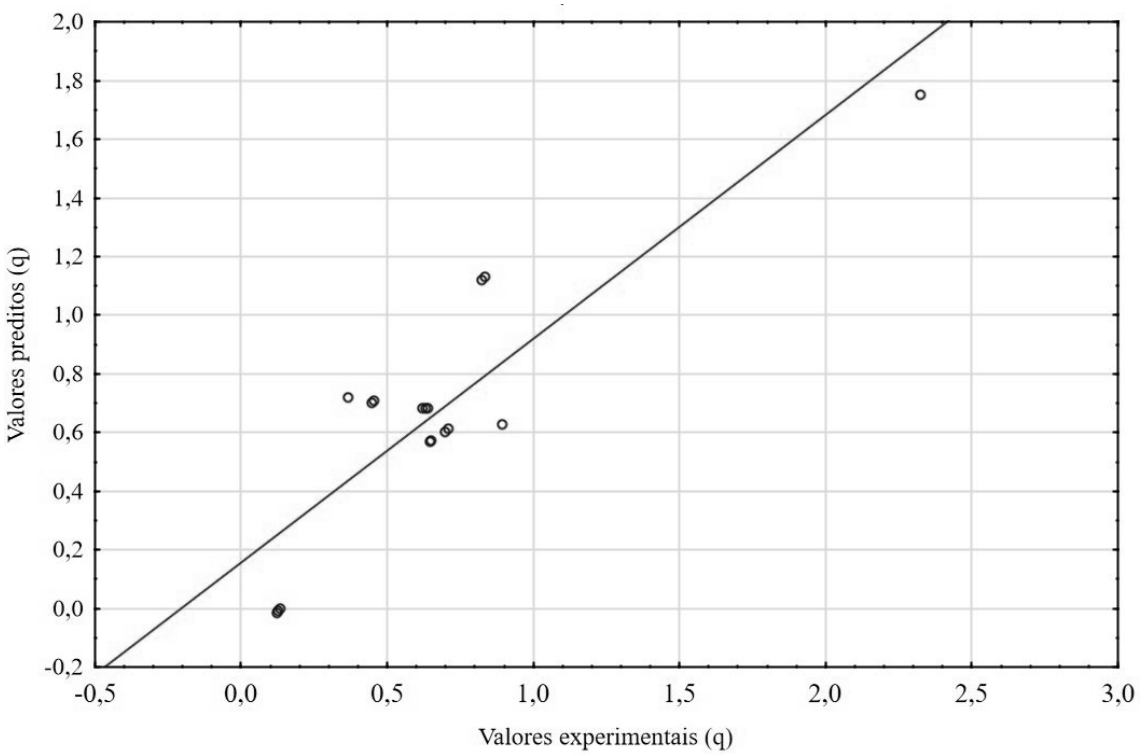

A Figura 3.6 apresenta os gráficos da superfície de resposta e de contorno para o modelo proposto em função da concentração inicial da solução de alumínio e da dosagem do resíduo adsorvente.

Figure 3.6 Superfícies de Resposta (A) e de Contorno (B) para a capacidade de adsorção em função da concentração inicial da solução e dosagem de material adsorvente.

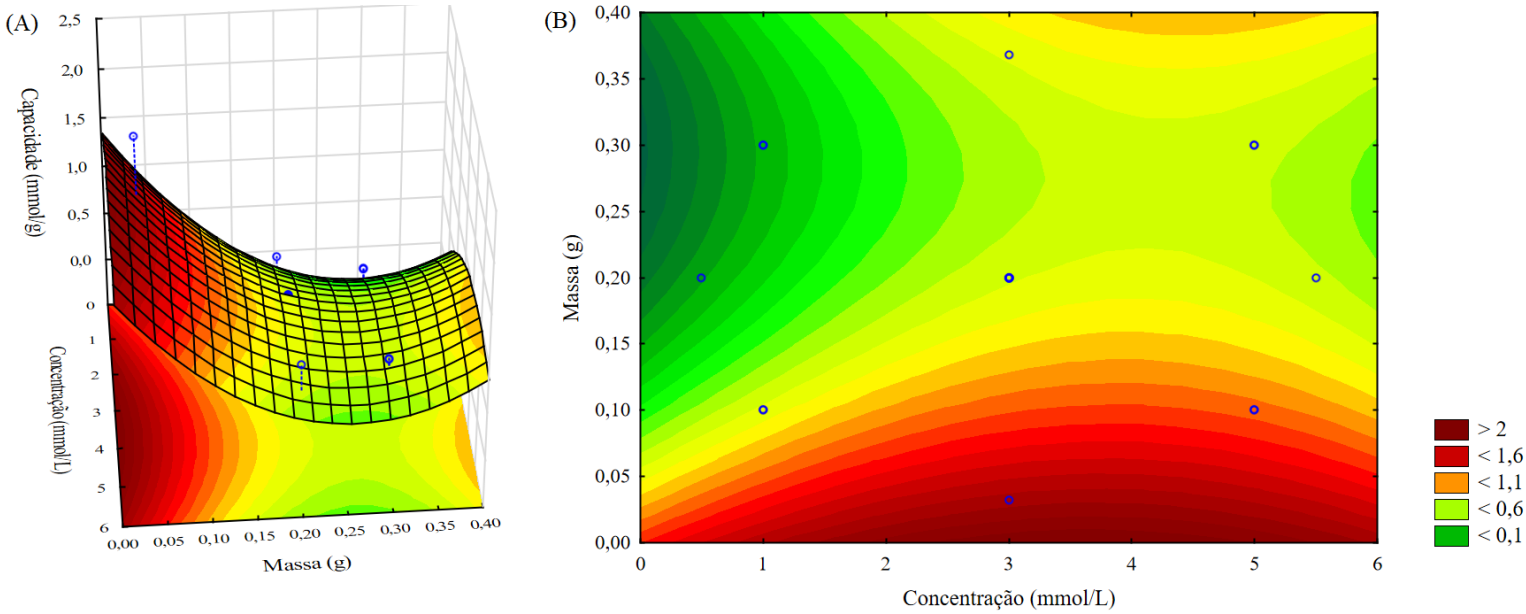

Conforme observado nos testes anteriores, maiores valores de concentração inicial e menores de dosagem da biomassa fornecem maior capacidade de remoção. Desta forma, concentração inicial de 3 a 5 mmol/L e dosagem da biomassa entre 0,1 e 0,3 g/50 mL fornecem resultados satisfatórios de remoção. Nota-se que quando apenas a dosagem ou a concentração são aumentadas não há favorecimento da capacidade de adsorção, reforçando, assim, a forte influência no sistema da dependência entre estas duas variáveis.

Para maximizar a porcentagem de remoção uma maior dosagem de biomassa deve ser utilizada uma massa de 0,368 g para um *range* de concentração entre 3 e 5,5 mmol/L. Entretanto, maiores valores de massa podem prejudicar a viabilidade do processo por acarretarem uma menor capacidade de adsorção e maior consumo de adsorvente. Buscando otimizar o processo, X_3 = 0,2 g/50 mL seria a dosagem mais viável, pois tem menor impacto negativo nos valores de capacidade de adsorção e ao mesmo tempo mantém os percentuais de remoção altos para a faixa de concentração estudada.

3.4 Conclusão

No planejamento fatorial realizado nesta etapa variáveis importantes do processo de bioadsorção de Al(III) em resíduo da alga *Sargassum filipendula* foram analisadas e otimizadas por meio do delineamento central composto rotacional associado à superfície de resposta. Os efeitos estudados foram a velocidade de agitação, concentração inicial da solução e dosagem de adsorvente. Observou-se que apenas os efeitos individuais dos dois últimos e de sua interação são significativos no sistema avaliado para a faixa de estudo e

intervalo de confiança de 95%. A velocidade de agitação, por sua vez, não apresentou influência em nenhuma das variáveis resposta (capacidade adsortiva ou percentual de remoção). Além disso, a dosagem e a concentração inicial de asdorbato apresentaram um comportamento de relação diretamente proporcional entre si. O modelo obtido se mostrou representativo, ajustando-se satisfatoriamente aos dados de percentual de remoção. Na análise da superfície de resposta, os maiores percentuais de remoção foram obtidos nas condições otimizadas de 3 mmol/L e 0,2 g/50 mL, ou seja, 4g/L de adsorvente. Já para a capacidade de adsorção, somente a dosagem de adsorvente apresentou efeito significativo. O modelo empírico para esta resposta não se mostrou adequado para predição dos dados. Desta forma, não foi possível definir os valores otimizados para as condições avaliadas. Todavia, é possível assumir que estes valores estejam próximos aos analisados, ou seja, concentração inicial de 3 a 5 mmol/L e dosagem da biomassa entre 0,1 e 0,3 g/50 mL.

Referências

[1] G.M. Gadd, Biosorption: Critical review of scientific rationale, environmental importance and significance for pollution treatment, J. Chem. Technol. Biotechnol. 84 (2009) 13–28. https://doi.org/10.1002/jctb.1999.

[2] K. Vijayaraghavan, Y.S. Yun, Bacterial biosorbents and biosorption, Biotechnol. Adv. 26 (2008) 266–291. https://doi.org/10.1016/j.biotechadv.2008.02.002.

[3] L.P. Mazur, M.A.P. Cechinel, S.M.A.G.U. de Souza, R.A.R. Boaventura, V.J.P. Vilar, Brown marine macroalgae as natural cation exchangers for toxic metal removal from industrial wastewaters: A review, J. Environ. Manage. 223 (2018) 215–253. https://doi.org/10.1016/j.jenvman.2018.05.086.

[4] A. Sari, M. Tuzen, Equilibrium, thermodynamic and kinetic studies on aluminum biosorption from aqueous solution by brown algae (Padina pavonica) biomass, J. Hazard. Mater. 171 (2009) 973–979. https://doi.org/10.1016/j.jhazmat.2009.06.101.

[5] A.A. Halim, E. Ezani, M.S. Othman, N. Awang, M.I. Wahab, A. Ithnin, Adsorption study of aluminium onto Curcuma longa, Nat. Environ. Pollut. Technol. 11 (2012) 193–197.

[6] N.T. Abdel-Ghani, G.A. El-Chaghaby, F.S. Helal, Simultaneous removal of aluminum, iron, copper, zinc, and lead from aqueous solution using raw and chemically treated African beech wood sawdust, Desalin. Water Treat. 51 (2013) 3558–3575. https://doi.org/10.1080/19443994.2012.750806.

[7] K. Açıkalın, F. Karaca, E. Bolat, Central composite rotatable design for

liquefaction of pine barks, Fuel Process. Technol. 87 (2005) 17–24. https://doi.org/10.1016/j.fuproc.2005.04.005.

[8] R.H. Myers, A.I. Khuri, W.H. Carter, Response Surface Methodology: 1966–l988, Technometrics. 31 (1989) 137–157. https://doi.org/10.1080/00401706.1989.10488509.

[9] R. Verseput, Digging Into DOE, Qual. Dig. (2001) 1–5. https://www.qualitydigest.com/june01/html/doe.html.

[10] M. Tukaram Bai, P. Venkateswarlu, Optimization studies for lead biosorption on Sargassum tenerrimum (Brown Algae) using experimental design: Response Surface Methodology, Mater. Today Proc. 18 (2019) 4290–4298. https://doi.org/10.1016/j.matpr.2019.07.387.

[11] V. Afraz, H. Younesi, M. Bolandi, M.R. Hadiani, Optimization of lead and cadmium biosorption by Lactobacillus acidophilus using response surface methodology, Biocatal. Agric. Biotechnol. 29 (2020) 101828. https://doi.org/10.1016/j.bcab.2020.101828.

[12] N.M.S. Kaminari, M.J.J.S. Ponte, H.A. Ponte, A.C. Neto, Study of the operational parameters involved in designing a particle bed reactor for the removal of lead from industrial wastewater — central composite design methodology, Chem. Eng. J. 105 (2005) 111–115. https://doi.org/10.1016/j.cej.2004.07.011.

[13] S. Biswas, M. Bal, S. Behera, T. Sen, B. Meikap, Process Optimization Study of Zn2+ Adsorption on Biochar-Alginate Composite Adsorbent by Response Surface Methodology (RSM), Water. 11 (2019) 325. https://doi.org/10.3390/w11020325.

[14] B. Barros Neto, I.S. Scarminio, R.E. Bruns, Como Fazer Experimentos, 4 ed., Bookman, 2010.

[15] W.A. Stirk, J. van Staden, Some physical factors affecting adsorption of heavy metals from solution by dried brown seaweed material, South African J. Bot. 67 (2001) 615–619. https://doi.org/10.1016/S0254-6299(15)31191-1.

4. Bioadsorção de Alumínio utilizando resíduo da extração de alginato da alga *S. filipendula* em Banho Finito

Application of alginate extraction residue for Al(III) ions biosorption: A complete batch system evaluation**

Heloisa Pereira de Sá Costa[1], Meuris Gurgel Carlos da Silva[1], Melissa Gurgel Adeodato Vieira[1]*

[1]Department of Processes and Products Design, School of Chemical Engineering, University of Campinas, Albert Einstein Av., 500, Campinas, São Paulo, 13083-852, Brazil

Abstract

The residue derived from the alginate extraction from *S. filipendula* was applied for the biosorption of aluminum from aqueous medium. The adsorptive capacity of the residue (RES) was completely evaluated in batch mode. The effect of pH, contact time, initial concentration and temperature was assessed through kinetic, equilibrium and thermodynamic studies. The biosorbent was characterized prior and post-Al biosorption by N_2 physisorption, Hg porosimetry, He picnometry and thermogravimetry analyses. Equilibrium was achieved in 60 minutes. Kinetics obeys pseudo-second order model at aluminum higher concentrations. Isotherms followed Freundlich model at low temperature (293.15 K) and D-R or Langmuir model at higher temperatures (303 and 313 K). Data modeling indicated the occurrence of both chemical and physical interactions in the aluminum adsorption mechanism using RES. The maximum adsorption capacity obtained was of 1.431 mmol/g at 293 K. The biosorption showed a spontaneous, favorable and exotherm character. A simplified batch design was performed, indicating that the residue is a viable biosorbent, achieving high percentages of removal using low biomass dosage.

Keywords: Aluminum; biosorption; residue; brown algae; batch design; water treatment.

** Manuscript published in *Environmental Science and Pollution Research* (2021). DOI: 10.1007/s11356-021-14333-3. Reprinted with permission from *Environmental Science and Pollution Research.*

Author Contributions

Conceptualization: Melissa Gurgel Adeodato Vieira

Literature search and data analysis: Heloisa Pereira de Sá Costa

Writing - original draft preparation: Heloisa Pereira de Sá Costa

Writing - review and editing: Melissa Gurgel Adeodato Vieira, Meuris Gurgel Carlos da Silva, Heloisa Pereira de Sá Costa

Supervision: Melissa Gurgel Adeodato Vieira

Declarations

Funding: São Paulo Research Foundation (FAPESP) (Grants # 2017/18236-1 and # 2019/11353-8), Brazilian Council for Scientific and Technological Development (CNPq) (Grant # 308046/2019-6), and Coordination Office for the Improvement of Higher Education Personnel (CAPES).

Competing interest: The authors declare that they have no competing interests.

Availability of data and material: Not applicable

Code availability: Not applicable.

Ethics approval and consent to participate: Not applicable.

Consent for publication: Not applicable.

4.1 Introduction

Toxic metals can be widely found in effluents derived from several industrial sectors. They are non-degradable chemical species and have a strong tendency to bioaccumulate, which makes these metals potentially dangerous to living organisms. Aluminum is classified as a toxic metal and remarkable concentrations of this metal have been reported in effluents from several industries, e.g., mining, smelting, metallurgy and electroplating (Vijayaraghavan et al. 2012; Boeris et al. 2016). Another significant source of effluents contaminated by aluminum are water treatment plants, due to the use of chemicals composed of aluminum (aluminum sulfate and polyaluminum chloride) in the flocculation process, often high concentrations of the metal are found in effluents from this treatment step (Merian et al. 2004; Stephens and Jolliff 2015).

Several studies report that aluminum contamination can cause harmful effects on different organisms. In plants, excessive Al^{3+} ions in soils mainly affect the roots and can trigger deficiency in the absorption and transport of nutrients, loss of biomass and genotype changes (Skibniewska and Skibniewski 2019). In fishes, it can induce oxidative stress, in addition to cause fatal damages to the nervous and respiratory system (Freda 1991; Gensemer and Playle 1999; Walton 2011). In humans, the bioaccumulation of this metal is mainly associated with the potential development of neurological diseases such as Alzheimer's and the development of bone diseases related to inhibition of bone cell growth and activity and bone mineralization (Dermience et al. 2015). For this reason, the maximum amount of aluminum present in industrial effluents discharged in water bodies is monitored by environmental pollution control authorities in several countries.

Amidst diverse procedures for removing toxic metals in aqueous media, adsorption is an extensively studied technique. Traditionally, the adsorbent utilized is the active carbon. However, aiming to reduce the process cost, several authors investigate the use of alternative adsorbents, like clays and zeolites (Otunola and Ololade 2020; Irannajad and Kamran Haghighi 2021). In biosorption, unconventional materials are used as sorbents, usually wastes. This process presents several advantages mainly for being ecofriendly and having lower cost (Agarwal et al. 2020).

Plenty of materials have been investigated as a biosorbent for Al(III) removal, including biomass derived from fungi, bacteria, algae and agro-industrial residues (Lee et al. 2004; Ozdemir and Baysal 2004; Sari and Tuzen 2009; Tassist et al. 2010;

Rajamohan et al. 2014; El Houda Larbi et al. 2019; Titah et al. 2019). Among them, algae stand out because they are cheap, have high availability in addition to having high affinity with toxic metals, the latter being directly related to the composition of algae cell wall. Alginate is a biopolymer that composes the structure of brown algae and is considered to play a major role on the uptake of metals by biosorption (Davis et al. 2003). This compound has commercial value since it is used extensively in the cosmetics, food and pharmaceutical industry due to characteristics such as its viscosity and its stabilizing properties. The alginate extraction process produces a fibrous residue with no added commercial value.

Costa et al. (2016) found that the process of alginate obtainment using the brown algae *Sargassum filipendula* generates a residue that still preserves several functional groups identical to those found in raw alga and directly linked to the ion exchange mechanism of the biosorption process. Several studies point to this residue as a promising biosorbent in the uptake of toxic and precious metals, in addition to being also efficient in removing emerging pollutants (Freitas et al. 2018; Cardoso et al. 2020; Coelho et al. 2020; Moino et al. 2020). Furthermore, the use of waste as an adsorbent material has less environmental impact compared to traditional adsorbents like activated carbon (Nishikawa et al. 2018). Costa et al. (2020) also examined the application of the residue for removal of metals present in real industrial effluents and found a remarkable removal of aluminum, revealing a great affinity between this metal and the biosorbent. However, in-depth studies investigating aluminum biosorption using this biomass has not been found in the literature.

In view of this, the aim of this work is to investigate the innovative application of the residue from the alginate extraction from the *Sargassum filipendula* algae as a low-cost adsorbent for the biosorption of Al^{3+} ions. This manuscript aimed to elucidate the mechanisms involved in the process through kinetic, equilibrium and thermodynamic assays. Biosorbent characterizations prior and post the biosorption were carried out, offering significant information regarding the biomaterial characteristics. In fact, some authors report a lack of studies regarding aluminum biosorption in general (Costa et al. 2021), so this article also aims to fill this niche, expecting to contribute to the minimization of impacts caused by this hazardous component on the ecosystem.

4.2 Material and Methods

4.2.1 Biosorbent preparation

Sargassum filipendula was obtained at Cigarras' beach, on the northern coast of São Paulo, Brazil. The seaweed was washed with deionized water and dried at 313.15 K for 24 h. After this process, the alga was milled and sieved in particles with size inferior to 1 mm. For the alginate extraction, McHugh's methodology (1987) was employed. This process originates sodium alginate as its main product and a solid alginate free biomass as waste, here termed as residue (RES). Initially 15 g of dried biomass were added to 500 mL of formaldehyde solution (0.4% v/v) for 30 minutes with constant agitation. This step aims to clarify and remove phenolic compounds present in the seaweed. In order to remove the remaining phenolic compounds, the biomass was washed with deionized water and put in agitation within 500 mL of 0.1 mol/L hydrochloric acid solution for 2 hours. Finally, the extraction of alginate was carried out. In this last step, the washed algae biomass was added to 350 mL of sodium carbonate solution (2% w/v) in constant stirring at 333.15 K for 5 h. As a result of this step a viscous mixture was obtained, it was first manually filtered using a polypropylene filter.

Then, the retained (residue) was washed exhaustively and vacuum filtered, in order to ensure that all the alginate was effectively extracted. After this step, the residue obtained was dried at 333.15 K for 24 h. For the biosorption experiments, RES was also milled and sieved into an average diameter of 0.737 mm.

4.2.2 Evaluation of pH effect

In order to evaluate the impact of pH on the biosorption of aluminum ions using the adsorbent residue, tests were conducted in a finite bath system with aluminum initial concentration of 1 mmol/L, biosorbent dosage of 2 g/L, agitation and temperature of 200 rpm and 298.15 K, respectively. The pH values tested were defined based on the metallic speciation of the aluminum, aiming the non-precipitation of the metal. The biosorption capacity (q) and total aluminum removal percentage (%Rem) were calculated using Eq. 4.1 and 4.2, respectively.

$$q(t) = \frac{(C_0 - C(t))V}{w} \tag{4.1}$$

$$\%Rem = \left(\frac{C_0 - C_{eq}}{C_0}\right).100 \quad (4.2)$$

The initial concentration, the metal ions concentration at time t (min) and solute concentration in equilibrium are respectively represented for C_0, C_t and C_{eq} (mmol/L); w represents the RES dry weight (g); and V is the volume of solution (L).

4.2.3 Kinetic study

Kinetic assays were performed at room temperature (298.15 K), in batch mode, with different initial aluminum concentrations (1, 2 and 3 mmol/L). The dosage of 2 g/L of RES was put in contact with the metallic solution, in continuous agitation of 250 rpm. Aliquots were collected at pre-set times and the remaining aluminum concentration was evaluated through atomic absorption spectroscopy, AAS (model AA-7000, Shimadzu, Japan). The system pH was maintained at 4 using a HNO_3 solution (0.1 mol/L). Eq. 4.1 was applied to obtain the adsorbent's adsorption capacity (q).

The mechanisms involved in Al(III) biosorption were investigated through different kinetic models that were adjusted to the experimental data: pseudo-first order (PFO) (Lagergren 1898), pseudo-second order (PSO) (Ho and McKay 1999), intraparticle diffusion (ID) (Weber and Morris 1963), Boyd (Boyd et al. 1947) and external mass transfer resistance (EMTR) (Puranik et al. 1999). Origin 8.0 and Maple® 20 software were employed for data analysis. Table 4.1 presents each model evaluated and its respective equations.

Table 4.5 Mathematical models used to describe kinetic data

Model	Equation
Pseudo-First Order	$q(t) = q_{eq}\left(1 - exp^{-k_1 t}\right)$
Pseudo-Second Order	$q(t) = \frac{q_{eq}^2 k_2 t}{q_{eq} k_2 t + 1}$
Intraparticle Diffusion	$q\,(t) = k_i t^{0.5} + c$

Boyd	$F = \frac{q(t)}{q_{eq}} = 1 - (\frac{6}{\pi^2})\exp(-B_t)$ $B_t = -0.4977 - \ln(1 - F)$ $D_i = \frac{r^2 B}{\pi^2}$
External Mass Transfer Resistance	$\frac{dC_p}{dt} = \frac{k_{MT} V}{w q_{max} K_L} \left(1 + C_p(t)\right)^2 . (C(t) - C_p(t))$

Parameters: q(t) is the amount of metal removed in relation to time t (mg/g); q_{eq} is the quantity of metal adsorbed in the equilibrium (mg/g); k_1 is the constant of the PFO model (min^{-1}); k_2 is the constant of the biosorption rate of the P-SO model (g/mg.min); k_i is the ID model constant ($mmol/g.min^{0.5}$); c is a parameter that is related to the thickness of the boundary layer; F is the fraction biosorbed at *t*; B_t is a mathematical function of F; r (cm) represents the particles radius; D_i (cm/s^2) is the effective diffusion rate; C(t) is the metal solution concentration at *t*; C_p corresponds to the adsorbate concentration in sorbent-solution interface (mmol/L); k_{MT} stands for the model constant (1/min); K_L is the constant obtained from the Langmuir isotherm model (L/mmol) and q_{max} represents the maximum biosorption capacity (mmol/g).

4.2.4 Equilibrium study

The biosorption equilibrium study was performed with 50 mL of Al(III) solutions, with initial concentration values range from 0.2-20 mmol/L, at pH 4, with 0.1 g of RES, in a shaker with temperature control (Jeio Tech, SI-600R, Korea) with continuous agitation (250 rpm). Three temperatures were studied (293.15, 303.15 and 313.15 K). The pH was established at 4 and controlled with HNO_3 solutions (0.1 and 0.5 mol/L). The initial and final Al(III) concentration was measured by AAS. The amount of adsorbed metal was calculated using Eq. 4.1.

Langmuir (Langmuir 1918), Freundlich (Freundlich 1907) and Dubinin-Radushkevich (D-R) (Dubinin and Radushkevitch 1947) models were applied to represent the sorption isotherm data. Table 4.2 summarizes the equations of equilibrium models employed.

Table 4.6 Mathematical models used to describe equilibrium data

Model	Equation
Langmuir	$q_{eq} = \frac{q_{max} K_L C_{eq}}{1 + K_L C_{eq}}$
Freundlich	$q_{eq} = K_F (C_{eq})^{1/n}$
Dubinin-Radushkevich	$q_{eq} = q_{max} \exp\left(-k\left(RTln\left(1 + \frac{1}{C_{eq}}\right)\right)^2\right)$ $E = \frac{1}{\sqrt{2k}}$

Parameters: K_F is the Freundlich model constant (mmol/g); n is a dimensionless number linked to biosorption intensity; k (mol^2/J^2) corresponds to a parameter associated to the sorption energy; E (kJ/mol) represents the systems' sorption energy; R is the constant of the ideal gas law (J/mol.K) and T is the temperature (K).

4.2.5 Thermodynamic and isosteric heat

The thermodynamic parameters are essential to evaluate important information of the biosorption system. Variation of Gibbs energy (ΔG°, kJ/mol) reveals if the biosorption is spontaneous (ΔG° < 0) or not (ΔG° > 0), variation of enthalpy (ΔH°, kJ/mol) helps to identify if the nature of the process is endothermic (ΔH° > 0) or exothermic (ΔH° < 0) (Srivastava et al. 1989). The variation of entropy (ΔS°, J/mol/K) values can be related to randomness in metallic solution-biosorbent interface (Djeribi and Hamdaoui 2008). Such parameters are determined by the combination of Eq. 4.3 and 4.4 (Gibbs 1873), which provides the Van't Hoff equation (Eq. 4.5), where K_c is the thermodynamic equilibrium constant.

$$\Delta G° = -RT \ln K_C \quad (4.3)$$

$$\Delta G° = \Delta H° - T\Delta S° \quad (4.4)$$

$$\ln K_C = \frac{-\Delta H°}{R}\frac{1}{T} + \frac{\Delta S°}{R} \quad (4.5)$$

In this study, K_c was obtained from Henry's constant (K_H, g/L) by multiplying its value by 1000 (Eq. 4.6), in way to consider the dimensionality (Milonjic 2007), therefore:

$$K_c = 1{,}000\, K_H = 1{,}000 \left(\frac{q_e}{C_e}\right) \tag{4.6}$$

The isosteric heat of an adsorption system (ΔH_{is}, J/mol) can be defined as the energy released when a constant amount of adsorbate (q_{eq}) is attached to the solid surface of the adsorbent. This variable is linked to the process temperature, as well as to the equilibrium concentration (C_{eq}). The analysis of this parameter can provide information about the thermodynamic behavior of the adsorbed phase and the heterogeneity of the adsorbent surface (Hartzog and Sircar 1995; Santos et al. 2020). ΔH_{is} can be determined by the Clausius – Clapeyron equation (Eq. 4.9) and its integrated form becomes Eq. 4.10 (Young and Crowell 1962).

$$\Delta H_{is} = R \frac{d \ln C_{eq}}{d(1/T)} \tag{4.9}$$

$$\ln C_e = \frac{\Delta H_{is}}{R} \frac{1}{T} + constant \tag{4.10}$$

The angular coefficient obtained from plot of $\ln C_e$ in function of 1/T, for a fixed q_e, provides the values of ΔH_{is}.

4.2.6 Error analysis

All model adjustments were evaluated according to the correlation coefficients (R^2), Relative Mean Deviations (RMD) (Eq. 4.11) and the corrected Akaike information criteria (AICc) (Eq. 4.12)(Akaike 1998).

$$RMD = \frac{1}{N} \sum_{i=1}^{N} \left| \frac{q_{exp} - q_{pred}}{q_{exp}} \right| x100 \tag{4.11}$$

$$AICc = N.ln\left(\frac{\sum_{i=1}^{N}(q_{exp} - q_{pred})^2}{N}\right) + 2p + \frac{2p(p+1)}{N-p-1} \qquad \text{when } \frac{N}{p} < 40 \tag{4.12}$$

The predicted and experimental points are represented by q_{exp} and q_{pred}, respectively, N is the number of experimental points and p is the number of model parameters. In cases where two or more models present appropriate adjustments to the experimental data, the calculation of Akaike weight (w_a) in Eq. 4.13 may help to select which one is more suitable by its representativity (Wagenmakers and Farrell 2004).

$$w_a = \frac{exp\left(-\frac{1}{2}(AICc_i - AICc_{min})\right)}{\sum_{i=1}^{r} exp\left(-\frac{1}{2}(AICc_i - AICc_{min})\right)} \quad (4.13)$$

In this Equation, r denotes the number of models; $AICc_i$ represents the corrected Akaike information criteria from each model; and $AICc_{min}$ is the lowest value of AICc obtained among all fittings.

4.2.7 Simplified batch design

Simplified batch design methodology is generally applied to predict the amount of biomass necessary to treat a given volume of solution and achieve the desired level of removal of the contaminant (Aravindhan et al. 2007). It is based on the molar balance (Eq. 4.1) at equilibrium conditions. By replacing q_{eq} for Langmuir parameters (q_{max} and K_L), Eq. 4.1 can be rewritten as Eq. 4.14 to obtain the required amount of biosorbent (w) necessary to treat different volumes of Al(III) solutions achieving a desired removal percentage. In this study, the estimations were performed with initial metal concentration of 1 mmol/L, for volumes varying from 1 to 10 L and aiming removal percentages of 40, 60 and 90%. These values were selected based on articles presented in the literature (Moino et al. 2017; Coelho et al. 2020).

$$w = \frac{V(C_0 - C_{eq})}{\frac{K_L q_{max} C_{eq}}{1 + K_L C_{eq}}} \quad (4.14)$$

4.2.8 Biosorbent characterization

The biosorbent was characterized prior (RES) and post (RES-Al) the process aiming to understand the interactions involved in the Al(III) removal. The true density (ρ_t) of raw and contaminated residue was analyzed by He pycnometry (Accupyc II 1340, Micrometrics). The apparent density (ρ_a) and the pore size distribution were determined using an Hg porosimeter (AutoPore IV, Micrometrics), applying a pressure range of 0.5-60000 psi. The biosorbent porosity (ε_p) was then calculated by Eq. 4.15.

$$\varepsilon_p = 1 - \left(\frac{\rho_a}{\rho_t}\right) \quad (4.15)$$

Adsorption and desorption isotherms of N_2 physisorption for RES and RES-Al were obtained using BET (Brunauer, Emmett and Teller) method. The samples were dried

for 24 hours at 333.15 K. Thermogravimetric analysis was performed in a dynamic nitrogen atmosphere (DTG 60, Shimadzu - Japan), with temperature range of 303.15 - 1223.15 K and gas outflow of 50 mL/min.

4.3 Results and Discussion

4.3.1 Effect of pH

Biosorption systems are influenced by several factors. Temperature, pH, adsorbate initial concentration, adsorbent dosage and stirring are the most investigated parameters for biosorption process optimization (Ruthven 1984). At first, the influence of pH on the Al(III) biosorption was assessed. Moino et al. (2020) presented the isoelectric point of RES (pH_{zpc}) surface at 5.3, indicating that above this point the biosorbent surface is negatively charged, favoring cations adsorption (Zhu et al. 2015). Nevertheless, based on the metallic speciation, at pH values below 5 99.9% of aluminum present in aqueous media are in Al^{3+} form. After that point, the formation of precipitated species begins (Krewski et al. 2007; Walton 2011). Therefore, pH evaluation was conducted in pH 2, 3 and 4.

The results presented in Fig. 4.1 demonstrate that pH 2 was the most unfavorable condition, within the pH range evaluated, with values of maximum removal percentage below 10 % and adsorption capacity of 0.127 mmol/g. This effect can be explained by the high concentration of H^+ ions in low pH ranges, since these ions tend to compete with Al^{3+} ions for the sites in the adsorbent (Costa et al. 2021). At pH 4, removal percentages above 80% and biosorption capacity of 0.4255 mmol/g were reached, indicating the favoring of the system. This value agrees with other studies that carried out biosorption of aluminum in different biomasses as shown in Table 4.5 (section 4.3.3). Therefore, pH 4.0 was defined to accomplish Al^{3+} biosorption experiments.

Fig 4.1 Effect of pH on Al^{3+} removal using RES

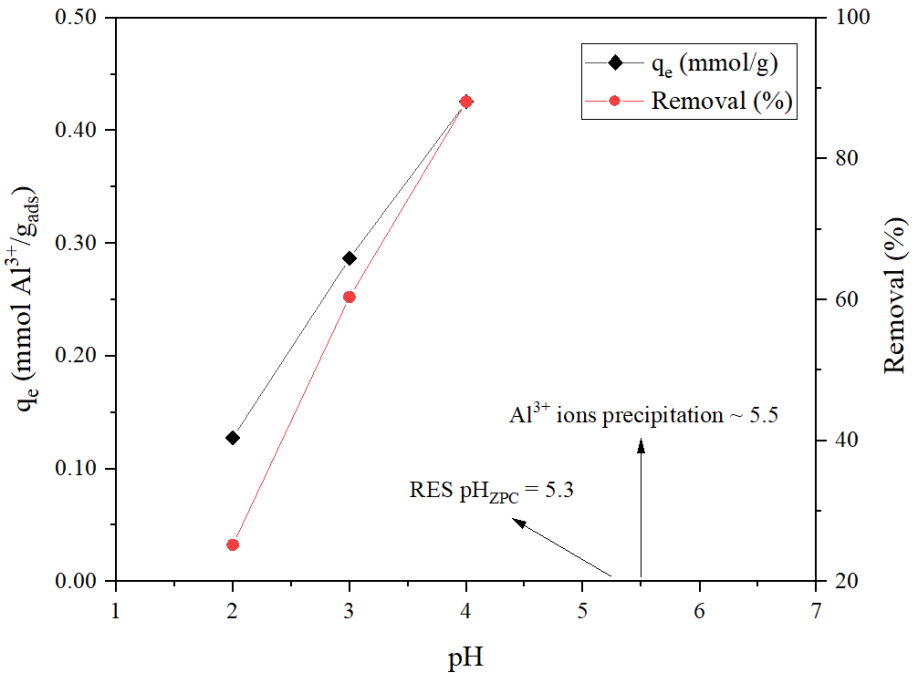

4.3.2 Kinetic study

Figure 4.2 displays biosorption kinetic curves of Al(III) ions onto RES. Analyzing the kinetic profiles, the system achieved the equilibrium in approximately 60 minutes. He and Chen (2014) pointed out that cationic metal biosorption systems using algae-derived biomass tend to be faster, where a remarkable removal occurs between 20 and 60 minutes, followed by a slower stage, reaching equilibrium generally between 2 and 6 hours, a behavior similar to that observed in the system of this work. The capacities of adsorption at equilibrium (q_{eq}) were 0.3825, 0.6152 and 1.0107 mmol/g equivalent to the percentages of 93.96, 61.87 and 72.03 % of removal for concentrations of 1, 2 and 3 mmol/L, respectively. The improvement in the adsorption capacity with the increase of metal concentration is associated to the intensification of the driving force for mass transfer. A similar behavior was observed in former biosorption studies of toxic metals employing the same biosorbent (Freitas et al. 2017; Nishikawa et al. 2018).

Fig 4.2 Biosorption kinetics of Al^{3+} ions by RES for three different aluminum initial concentrations

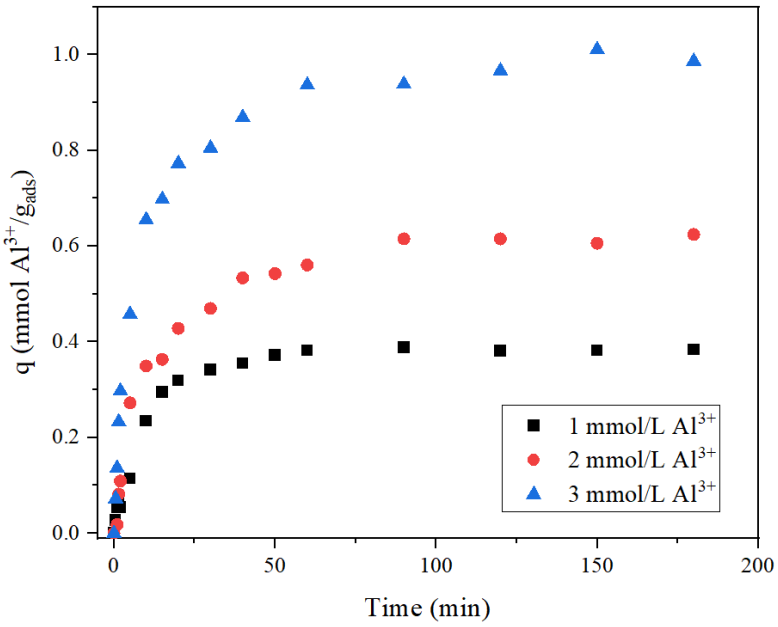

Figures 4.1S to 4.3S (Supplementary Material) show the results of the adjustments of kinetic models (Pseudo-first Order, Pseudo-second Order, Intraparticle Diffusion, Boyd, and External Film Mass Transfer Resistance) to the experimental curves obtained. The variables obtained from the models fitting, along with the adjustment evaluation parameters (R^2, RMD and AICc) are presented in Table 4.3.

It can be noted that, among the phenomenological models, the PFO model demonstrated a better fit in the 1 mmol/L system, while the PSO model better described the 2 and 3 mmol/L kinetics, with higher R^2 values, lower DMR and lower AICc. Since these parameters are very similar for pseudo-first and pseudo-second order models on 1 mmol/L system, it can be said that the PSO model better represented the whole process. In general, it is widely reported that this model tends to better fit the kinetic data of biosorption of Al(III) and other toxic metals (Farooq et al. 2010; Tassist et al. 2010; He and Chen 2014; Naeemullah et al. 2017; El Houda Larbi et al. 2019). Among the reasons that stands out is the fact that the pseudo-first order model better describes the beginning of the process, while the PSO model better describes the system as a whole, so when equilibrium data are used in mathematical modeling applying these two models, k_2 values tends to be favored (Pagnanelli 2011; Daneshvar et al. 2017). It can also be directly related to the interactions occurring between the metal and the functional groups of the biosorbent (Bulgariu et al. 2015). The PSO model indicates that the rate-limiting stage its possibly

related to a chemisorption mechanism, occurring via the electrons sharing between Al(III) ions and the residue in the valence shell (Ho and McKay 1999). It can be observed that the constant k_2 tends to decrease with higher initial concentration, since it is a function of the process conditions (Foo and Hameed 2010).

Table 4.7 Kinetic model adjustments for Al(III) biosorption with different initial concentrations

Model	**Parameters**	**Concentration (mmol/L)**		
		1	**2**	**3**
	q_{exp} (mmol/g)	0.3825	0.6152	1.0107
PFO	q_e (mmol/g)	0.3798	0.5874	0.9254
	k_1 (min^{-1})	0.0905	0.0746	0.1212
	R^2	0.9940	0.9716	0.9720
	RMD (%)	10.7	24.1	12.5
	AICc	-132.413	-91.1839	-83.0646
PSO	q_e (mmol/g)	0.4214	0.6561	1.0103
	k_2 (g/mmol.min)	0.2866	0.1543	0.1693
	R^2	0.9862	0.9902	0.9961
	RMD (%)	10.6	23.8	5.1
	AICc	-118.8427	-104.0165	-104.3081
ID	k_i (mmol/g.$min^{0.5}$)	0.2181	0.1731	0.4715
	c (mmol/g)	0.0216	0.0542	0.0614
	R^2	0.9806	0.9683	0.9787
Boyd	D_i (cm^2/min)	$3.8287.10^{-5}$	$2.2316.10^{-5}$	$1.4268.10^{-5}$
	R^2	0.9799	0.9626	0.8636
EMTR	k_{MT} (m/s)	0.0840	0.04409	0.0799
	R^2	0.9971	0.9867	0.9880
	RMD (%)	7.6	6.4	12.2
	AICc	-135.911	-98.927	-84.102

For the models based on mass transfer resistance, it is possible to note the presence of all the steps described by the intraparticle diffusion model in all studied concentrations:

an initial stage of rapid removal of Al(III) ions, referring to external adsorption; a second gradual stage referring to intraparticle diffusion, which is the controlling-rate step, and the third stage where diffusion is lower due to the low concentration of solute in the solution, representing the equilibrium of system (Chen et al. 2003). The linear adjustment of this model was obtained in the region of the second stage and the high values of R^2, mainly for the 1 mmol/L concentration, indicates the possible relevance of intraparticle diffusion in the process kinetic rate. This result, however, is not in agreement with that observed in the fitting of Boyd model, where the linear coefficient of the line Bt vs. t in all studied concentrations does not cross the origin, indicating that internal diffusion is not the limiting step (Boyd et al. 1947). In addition to this, the D_i values in the order of 10^{-5} suggests that the controlling step is the diffusion in external film (Singh et al. 2005).

Furthermore, it can be observed in Table 4.3 that the effective diffusion coefficients decrease as the concentration is increased, which corroborates with the results obtained in the intraparticle diffusion model. In this model, there is an increase in the effect of the boundary layer (c) along with the initial concentration, implying greater resistance to mass transfer and consequently less effective diffusion. This proportional relationship between the boundary layer and the initial concentration, was also observed by Freitas et al. (2018) in the removal of copper using the same biosorbent, indicating that the increase in aluminum concentration is directly related to the increase in external resistance to mass transfer.

The better adjustment of the EMTR model rather than the DI model to the kinetic data, for all concentrations tested, ratifies that the process is predominantly governed by diffusion in external film. This behavior is consistent with results found in the literature concerning the uptake of other toxic metals onto RES (Cardoso et al. 2017) as well as studies regarding the biosorption of Al(III) employing different biosorbents (Cayllahua and Torem 2010; Halim et al. 2012; Rosa et al. 2018).

4.3.3 Equilibrium study

Figure 4.3 depicts the equilibrium isotherms adjustments employing the Langmuir, Freundlich and Dubinin-Radushkevich (D-R) models at 293.15, 303.15 and 313.5 K. According to Giles et al. (1960) classification, the initial slope of the isotherms obtained is classified as H type, which suggests that the metal has elevated affinity for the biosorbent material. It is also possible to note the decrease in adsorptive capacity with the

increase in temperature, a characteristic behavior of an exothermic system. A similar result was obtained by Freitas et al. (2020) and Nishikawa et al. (2018) for the biosorption of Ag(I) and Cd(II), respectively, using the same biomaterial as adsorbent. Cayllahua and Torem (2010) found the same behavior for aluminum biosorption using a bacterial biomass. This can be confirmed in Table 4.4, where the experimental q_{max} values decreases as the temperature increases. Although an endothermic behavior predominates in most studies concerning the biosorption of Al(III), some authors like Yurtsever and Nalçak (2019) also found an exothermic process for Al(III) biosorption.

Fig 4.3 Langmuir, Freundlich and D-R models adjustment to biosorption isotherms of Al^{3+} removal using RES at a. 293.15 K; b. 303.15 K; c. 313.15 K

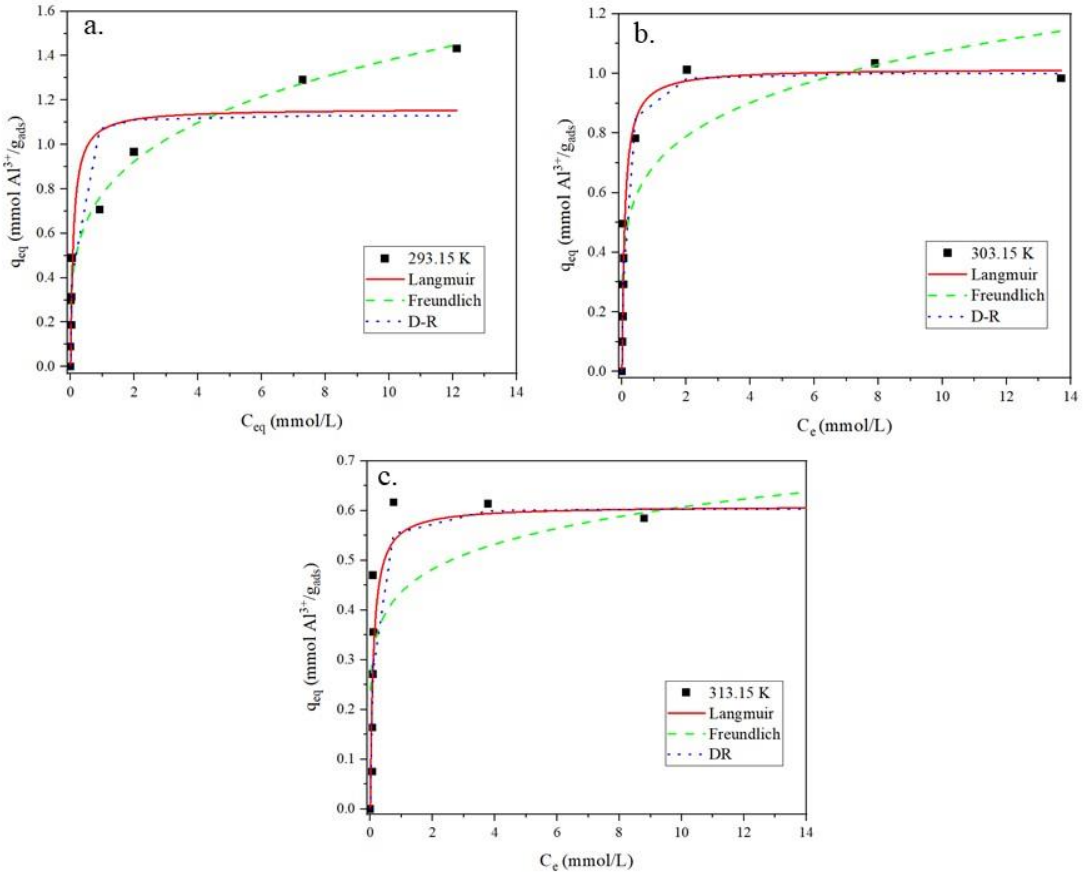

Table 4.4 shows the best fitting of Freundlich model at the lowest temperature (293.15 K) considering all adjustment parameters (R^2, AICc, RMD and w_a). For higher temperatures (303.15 and 313.15 K), good adjustments were obtained with two models, Langmuir and D-R. In this case, the Akaike wight (Eq. 4.13) was applied and the ratio between the w_a for both models were calculated. For 303.15 K the ratio of evidence was 1.059 for the Langmuir model, which indicates that this model is 1.059 times more representative than the D-R adjustment at this temperature. For 313.15 K, D-R model

revealed to describe the equilibrium data 1.195 times better than Langmuir. However, according to Santos et al. (2019) , such a low ratio of evidence is not significant, therefore, both models may be adequate to describe the system in 303.15 and 313.15 K. Although, Langmuir model assumes that the biosorbent surface is composed by active sites energetically homogeneous, whilst D-R and Freundlich describe adsorption in multilayers, i.e., on a heterogeneous surface. That said, considering the excellent fitting of Freundlich model to describe equilibrium data at 293.15 K, it can be considered that the surface of RES is predominantly heterogeneous. The results analyzed for isosteric heat, further discussed in this section, helps to stand this hypothesis.

Analyzing the variable E, associated to the energy of sorption, obtained through the D-R model, it is observed that the biosorption mechanisms in this system are predominantly physical in the entire temperature range studied (E = 5.50 – 5.62 kJ/mol). A similar result reported by Nishikawa et al. (2018) using the same biomaterial for the removal of cadmium. In addition, the values of parameter n of the Freundlich model, which represents the adsorption intensity, are greater than a unity, which suggests the favorability of the biosorption. Also, K_f increases proportional to the adsorption capacity since this parameter is related to electrostatic attraction force (Shaaban et al. 2017).

Table 8.4 Equilibrium model adjustments for Al(III) biosorption at different temperatures

Model	**Parameters**	**Temperature (K)**		
		293.15	**303.15**	**313.5**
Experimental	$\mathbf{q_{max}}$ (mmol/g)	**1.4317**	**1.0337**	**0.6137**
Langmuir	q_{max} (mmol/g)	1.1618	1.0164	0.6094
	K_L (L/mmol)	11.2876	11.6058	10.1475
	R^2	0.8576	0.9465	0.8186
	RMD (%)	31.89%	21.31%	41.69%
	AICc	-18.6639	-32.3661	-28.9440
	w_a	0.000	0.514	0.440
Freundlich	K_F [(mmol/g).(L/mmol)$^{1/n}$]	0.7776	0.6905	0.4366
	n	4.0099	5.2018	6.9881
	R^2	0.9762	0.8078	0.5311
	RMD (%)	23.10%	48.19%	56.16%

	AICc	-34.7619	-20.8533	-23.7930
	w_a	0.999	0.002	0.034
D-R	q_{max} (mmol/g)	1.1304	1.0009	0.6036
	E (kJ/mol)	5.5047	5.6249	5.5516
	R^2	0.8460	0.9458	0.7457
	RMD (%)	31.55%	21.13%	39.89%
	AICc	-17.9641	-32.2485	-29.3010
	w_a	0.000	0.485	0.526

Within the Langmuir model the K_L parameters indicates the affinity between Al(III) ions and the residue, its value tends to increase with q_{max} values. As expected, the highest K_L was found associated with the higher q_{max}, at 293.15. The decrease in this parameter with the temperature increasement also reveals an exothermic pattern.

Table 4.5 presents a comparison between q_{max} values in aluminum biosorption using different types of algae and using the residue studied in this work. It is possible to observe that the waste has an interesting performance, and its maximum adsorptive capacity value is very close to the values presented for other biomasses. The main advantage of RES is that it is a waste, which is normally disposed and has no added value. Additionally, its raw material (*S. filipendula)* is found in abundance in nature, thus making it even more attractive for the biosorption process.

For comparison with well-established sorbents materials, Lobo-Recio and coworkers (Lobo-Recio et al. 2021) obtained a maximum removal capacity around 0.71 mmol/g using Linde type-A zeolite to treat aluminum in a synthetic solution, whereas Ates and Basak (Ates and Basak 2021) investigated the adsorption of aluminum in real effluent using a clinoptilolite-rich zeolite and obtained a maximum removal capacity of 0.13 mmol/g. For activated carbon, studies report adsorptive capacities ranging from 0.11 mmol/g (Mahdavi et al. 2018) to 3.94 mmol/g (Goher et al. 2015), these results show that this traditional adsorbent has the highest removal capacity. However, commercial activated carbons have an estimated cost of approximately US $ 21/kg (de Andrade et al.

2018), while natural zeolites can cost from US $ 0.05/kg up to US $ 0.3/kg (U.S. Geological Survey 2020). Even though they are cost-effective materials, zeolites presents lower aluminum removal results than those obtained with the studied residue. Considering that the biosorbent has no commercial value, these results confirm that it is a material with great viability for application in aluminum removal systems.

Table 4.9 Maximum adsorption capacity (q_{max}) for Al^{3+} uptake by different algae biosorbents

Biosorbent	**Experimental conditions**	**q_{max} (mmol/g)**	**Reference**
Beach-cast seaweed	C_0 = 0.18-18.5; D = 2.5; T = 298; pH 4	0.833	(Lodeiro et al. 2010)
Turbinaria conoides	C_0 = 18.3-36.6; D = 2; T = 295; pH 4	2.592	(Vijayaraghavan et al. 2012)
Gelidium latifolium	C_0 = 0.018-37.06; D = 1; T = 298; pH 4	2.060	(Shaaban et al. 2017)
Ulva lactuca	C_0 = 0.018-37.06; D = 1; T = 298; pH 4	2.082	(Shaaban et al. 2017)
Colpomenia sinuosa	C_0 = 0.018-37.06; D = 1; T = 298; pH 4	2.116	(Shaaban et al. 2017)
Padina pavonica	C_0 = 0.37-14.82; D = 8; T = 323; pH 4.5	2.864	(Sari and Tuzen 2009)
RES	C_0 = 0.2-20; D = 2; T = 293; pH 4	1.431	This work

*C_0 = Initial concentration (mg/L); D = biosorbent dosage (g/L); T = temperature (K).

4.3.4 Thermodynamics analysis

Figure 4.4S (Supplementary Material) shows the graph of ln (K) versus 1/T. The calculation of the K_d constant was performed in the region of infinite dilution of the isotherms for the three temperatures analyzed. The value of the coefficient for determining the linear regression of the graph was 0.9822, so its linear and angular coefficients were used to calculate the thermodynamic parameters (ΔH and ΔS) according to Eq. 4.5. The thermodynamics parameters obtained are given in Table 4.6.

Table 10 Thermodynamic parameters for Al(III) biosorption using RES

T (K)	ΔG (kJ.mol^{-1})	ΔH (kJ.mol^{-1})	ΔS (J.mol^{-1}.K^{-1})
293.15	-11.385		
303.15	-9.659	-61.991	-0.172
313.15	-7.932		

Negative values for ΔG demonstrate that Al(III) uptake using RES is a spontaneous process within the studied temperature range. ΔG increases with temperature increasement indicating that lower temperatures favor the process. The negative value of ΔH confirms exothermicity of the process of biosorption of Al(III) using RES. The absolute value of ΔH can also assist in defining the nature of the process. In physisorption, absolute values of ΔH ranging from 2.1 to 20.9 kJ.mol^{-1}, while ΔH values in the range of 80-200 kJ.mol^{-1} are configured as chemical processes (Saha and Chowdhury 2011). In this study, the value is in the range for chemical processes, which indicates that instead of being a purely physical process as pointed out by D-R model, chemical interactions may also be involved in its removal mechanism.

The negative ΔS value obtained reveals a decrease in the system disorder, that is, the adsorbate changes from a less organized state, in the liquid phase, to a more organized state when adsorbed to the surface of the biosorbent, decreasing the entropy variation, reflecting that the Al molecules were orderly adsorbed (Djeribi and Hamdaoui 2008). In addition, negative entropy values also indicate that the process has associative mechanisms, that is, the system disorder tends to decrease and no considerable modification happens in the internal structure of the biomaterial (Saha and Chowdhury 2011; Sotirelis and Chrysikopoulos 2015).

Figure 4.4 illustrates the isosteres (plots of ln C_e vs 1/T) for the selected equilibrium capacities (q_e = 0.96, 0.95, 0.93 mmol/g), all plots were linear, with $R^2 > 0.9$. Isosteric heat was calculated from the angular coefficients. Table 4.7 summarizes the results obtained.

Fig 4.4 Adsorption isosteres for Al^{3+} biosorption onto RES

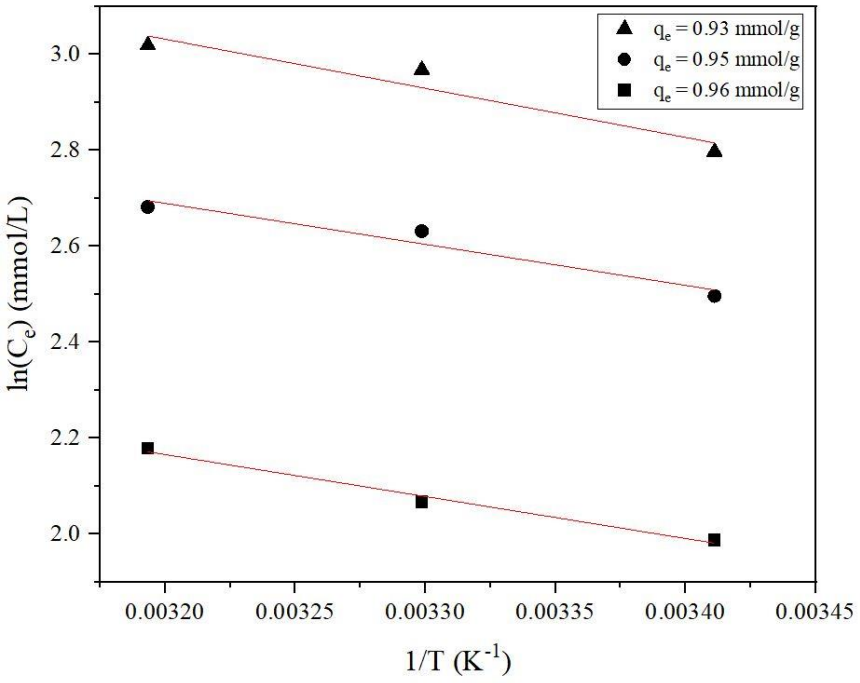

Table 4.11 Isosteric heat for different equilibrium capacities

q_e (mmol/g)	ΔH_{st} (kJ/mol)	R^2
0.96	-7.11	0.9871
0.95	-7.27	0.9437
0.93	-8.51	0.9222

The values of ΔH_{st} vary proportionally with the values of q_e. This behavior can be associated with adsorbents with an energetically heterogeneous surface (Erbil 2009), suggesting that the surface of RES is composed of different energetically active sites. Relatively low values obtained for ΔH_{st} are directly linked to the low q_e range studied, since low q values imply strong sorbate-sorbate interactions which results in low isosteric heat (Chowdhury et al. 2011). The magnitude of the isosteric value provides information on the nature of the adsorption mechanisms involved in the process. Isosteric heat values below 80 kJ/mol indicates the occurrence of physisorption mechanisms, as in the case of this study. This result is also in line with the mean adsorption energy (E) values obtained through the D-R model, presented in the previous section. It is possible to conclude that the RES-Al uptake occurs mainly by physical interactions with participation of chemisorption mechanisms such as ion exchange in the rate limiting step of the process,

as shown in Section 4.3.2. This result was expected considering the complex matrix of this biosorbent.

4.3.5 Simplified batch design

Figure 4.5 shows the amount of RES necessary to achieve removals of 40, 60 and 90% by volume ranging from 1 to 10 L for a solution with an initial concentration of 1.0 mmol/L Al. It is possible to observe that the amount of residue required increases with increasing volume and desired removal percentage. Despite this, to treat 10 L of solution with 90% removal, only 15 g of RES are needed. Comparatively, in the study performed by Moino et al. (2020) for the removal of Ni (II) using this same biosorbent, under the same conditions studied here, about 140 g of RES were taken to achieve 90% of removal in 10 L of 1 mmol/L Ni solution. In this work, the low amount of waste required to treat large volumes satisfactorily has a direct impact on the viability of the system, in addition to being an important feature for the process scale-up.

Fig 4.5 Simplified batch design for the RES amount required to obtain 40, 60 and 90 % removal of Al(III) at 1 mmol/L

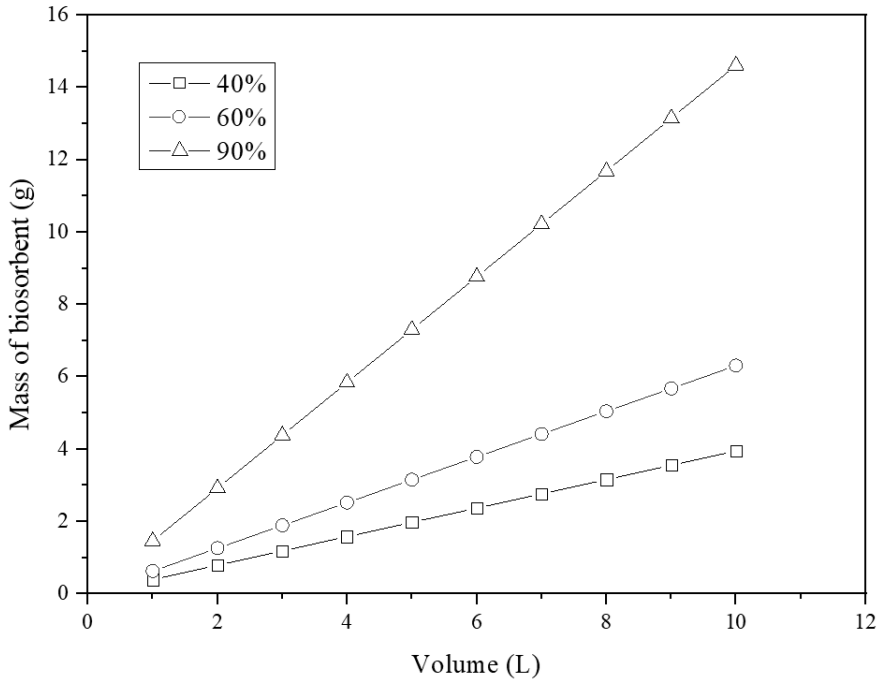

4.3.6 Biosorbent characterization

4.3.6.1 Structural properties

Table 4.8 presents the results obtained in the characterization of the porous structure of the biosorbent by mercury porosimetry and helium gas pycnometry. It can be

seen that the apparent density decreases slightly after the biosorption process. This may suggest that the metal is mostly adsorbed on the surface of the residue and not just in its pores, thus causing an increase in the volume of the material and a decrease in apparent density. The same behavior was also observed for the true density of RES, which value is slightly higher than those obtained for RES-Al. Worth mentioning that the apparent density is calculated through the relationship between the mass of the solid and the total volume, that is, the real volume of the adsorbent added to the volume occupied by Hg filling in the pores of the solid. The true density, on the other hand, is calculated using the real volume, that is, the total solid volume without the volume of empty pores. Thus, the increase in the total volume caused by the adsorption of metal ions on the surface of the material also leads to a decrease in its value.

Table 4.12 Structural properties of the biosorbent before (RES) and after (RES-Al) Al(III) biosorption

	RES	**RES-Al**
Apparent density (g/cm³)	0.9826	0.9783
True density (g/cm³)	1.4820	1.4500
Porosity (%)	33.70	32.53

Porosity, calculated using Eq. 4.15 also showed a decrease in its value, being an indication of the possible filling of empty pores. However, as pointed out by Freitas et al. (2019), this low variation indicates that aluminum has no influence on the pore filling of the biosorbent.

In summary, it is possible to note that the values obtained for the residue prior and post the adsorption of Al(III), despite the decreasing in general, the variations were minimal, revealing that the filling of pores may not be part of the mechanism of Al(III) removal by RES. In fact, these results agree with that observed in the kinetic analysis (Section 4.3.2), showing that external diffusion is the controlling step of the biosorption process.

Mercury intrusion porosimetry also provides data regarding the pore size distribution, as illustrated in Figure 4.6.

Fig 4.6 Pore size distribution of raw biosorbent and Al-contaminated

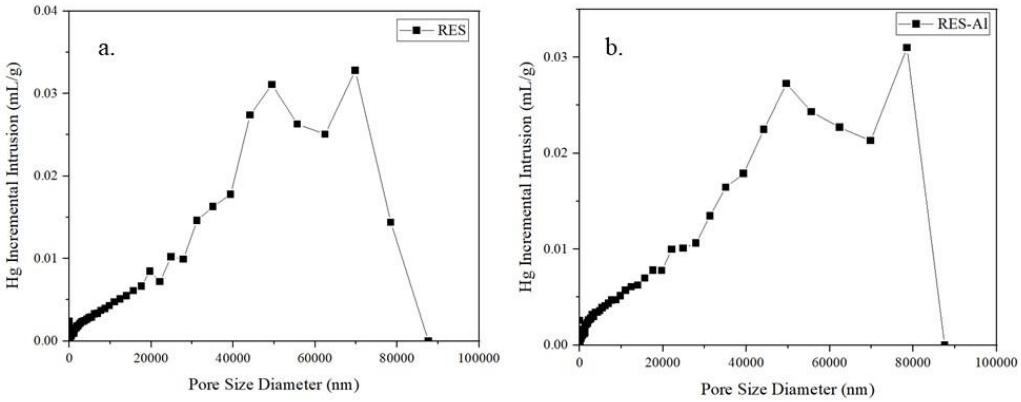

The pore diameter range remained the same after the biosorption process, corroborating with the result of the low variation in the porosity of the adsorbent analyzed previously. In physisorption, IUPAC classifies adsorbents according to their pore size (Sing 1985; Thommes et al. 2015). According to this classification and analyzing the profile shown in Figure 6, the residue can be determined as a macroporous material. Despite this, the RES has several pores with diameter significantly larger than the minimum determined for macropores. In previous works Cardoso et al. (2020) and Moino et al. (2020) obtained similar results and associate that this much larger pore width range is linked to cavities caused by the extraction process alginate, which leads the residue to have a predominantly rough surface instead of macroporous.

Figure 4.7 presents the isotherms of adsorption and desorption of nitrogen realized by BET method for RES and RES-Al. According to IUPAC classification, isotherms for RES (Fig 7a) and for RES-Al (Fig 7b) are type II with a more gradual curvature. Type II isotherms are characteristics of nonporous or macroporous biosorbents, which corroborates with the results obtained from pore size distribution analysis. A minor curvature is related to overlap of monolayer coverage and the beginning of multilayer adsorption (Thommes et al. 2015).

Fig 4.7 N_2 adsorption and desorption isotherms for RES and RES-Al

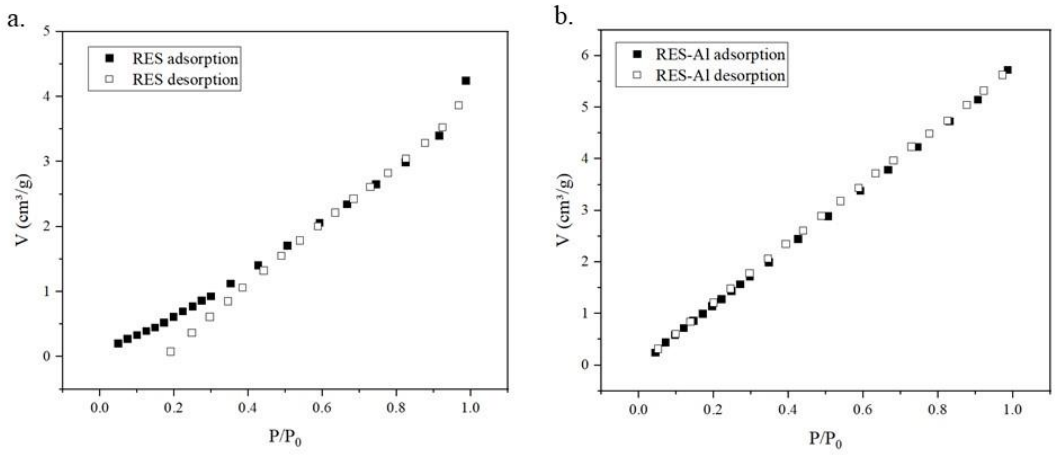

4.3.6.2 Thermogravimetric analysis (TGA)

Thermogravimetric analyzes help to characterize the thermal resistance of the material. Figure 4.8 presents the TG, DTG (thermogravimetric analysis) and DTA (thermodifferential analysis) curves obtained for RES and RES-Al.

It can be seen from the TG curves for RES and RES-Al that the mass of the biosorbent decreases with heating. Both curves show a similar decay at the beginning of the process, this loss of initial mass is associated with dehydration of the material (Kalderis et al. 2008). The mass loss equilibrium is reached at 800 ºC for RES and 600 ºC for RES-Al. RES curve shows the first decrease between 250 and 350 ºC, the loss of mass in this range is associated with the degradation of cellulosic compounds (330 ºC) and the remaining alginic acid (200 ºC). Alginate also usually presents another peak of degradation around 550 ºC, but this behavior was not obtained for both RES and RES-Al (Soares et al. 1995, 2004). RES-Al curve presents a milder loss of mass profile, but a main point can be identified between 200 and 350 ºC, as well as for RES, associated with the decomposition of cellulose and alginate present in the material structure. The total loss of mass for RES was of 91% and for the contaminated residue of 67.5%, which confirms the greater thermal stability of the latter.

Fig 4.8 Thermal analysis curves for: (a) RES, and (b) RES-Al

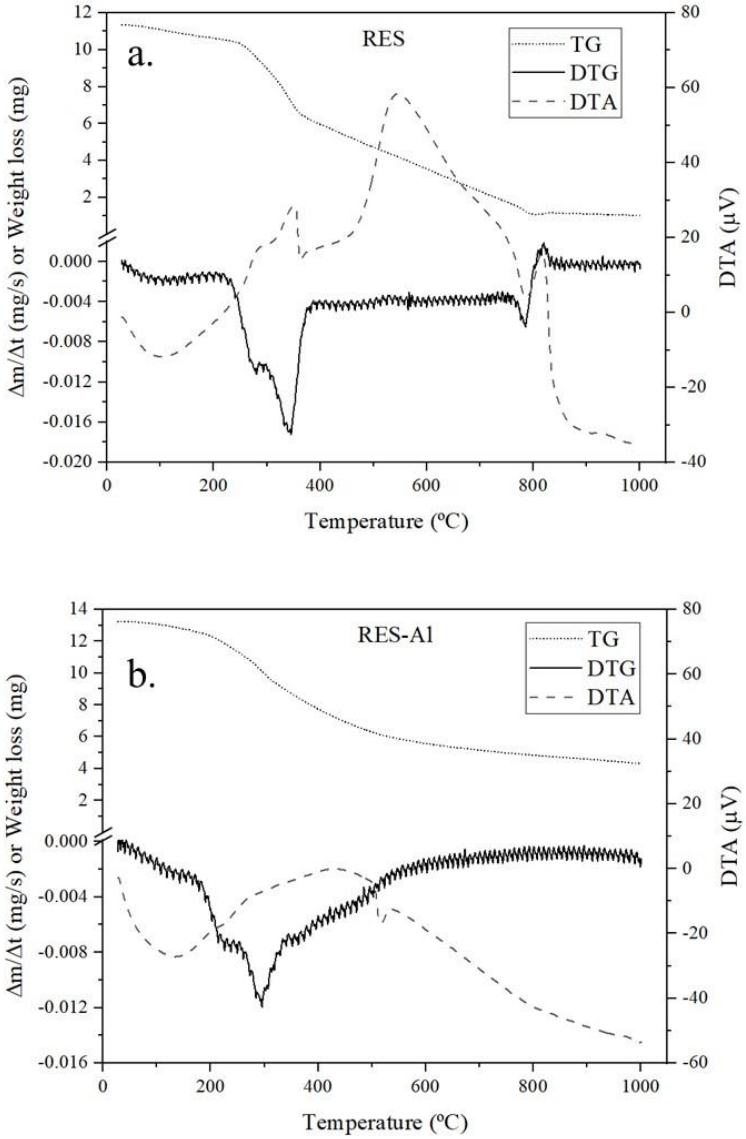

All these factors reveal that the residue contaminated by aluminum has greater stability than the waste prior process. This indicates that the binding of Al(III) ions to the functional groups on the surface of the biosorbent increases the thermal stability of the intermediates formed by the heating process. Herewith, it can be concluded that the residue presents considerable stability when heated to temperatures around 150 ºC, thus being able to be applied to processes that use higher temperatures. Despite this, as observed in the equilibrium study, higher temperatures disadvantage the uptake capacity for aluminum removal, so the application of this system at high temperatures would be unfeasible.

DTA curves identify the occurrence of endothermic and exothermic events. Endothermic peaks are observed at around 100 ºC for both materials, these peaks are

related to water evaporation. In RES it is possible to notice the presence of a peak related to an endothermic event (330 ºC) and immediately afterwards an exothermic peak (350 ºC), both are associated with the degradation of alginic compounds (Soares et al. 2004). Exothermic events between 200 and 400 ºC also represent the decomposition of the protein fraction of the material and are related to a great loss of mass, which can be confirmed by observing the pattern of TG curves (Yu et al. 2008; Biswas et al. 2017). Above 400 ºC exothermic events are linked to the occurrence of char formation. The endothermic peak observed at 380 ºC for RES may be related to the depolymerization of cellulose (Soares et al. 1995).

For RES-Al, as in TG, a more attenuated DTA curve pattern, with less evident peaks, was obtained. Cardoso et al. (2020) found a similar behavior in the DTA curves obtained for the same residue contaminated with Zn ions. The authors associate this behavior with the presence of metal ions in the material. Although attenuated, the endothermic and exothermic peaks presented for RES-Al after 500ºC may be related to the combustion of remaining metallic compounds (Do Nascimento et al. 2021).

4.4 Conclusions

This work evaluated the removal of aluminum ions through biosorption employing the waste originated from alginate extraction from *S. filipendula* algae. The pH presented significant influence in the process and pH 4 favored the uptake of Al(III) by RES. The kinetic study showed that the residue removes more than 90% of Al^{3+} ions in about 60 min of the process, in all concentrations tested. The PSO and EMTR models better described the kinetic behavior, demonstrating that the process is predominantly controlled by external diffusion. In equilibrium assays it was found that the increase in temperature decreases the biosorption capacity. In equilibrium data modeling, the 293.15 K isotherm was better described through the Freundlich model, whereas Langmuir and D-R models better fitted the isotherms at 303.15 and 313.15 K with the same representativity for both curves. The values of free adsorption energy (E = 5.50 – 5.62 $kJ.mol^{-1}$), obtained by the DR model, indicates that the biosorption of aluminum by RES has characteristics of a physical process. The maximum adsorption capacity obtained was of 1.431 mmol/g at 293.15 K, a very encouraging value when comparing to other low-cost adsorbents. The biosorption of Al(III) is an exothermic (ΔH = -61.991 $kJ.mol^{-1}$) and spontaneous process (ΔG = -11.385 to -7.932 $kJ.mol^{-1}$). The biosorbent surface is heterogeneous with the occurrence of physical mechanisms during the removal process.

The characterizations performed on the material prior (RES) and post aluminum biosorption (RES-Al) indicated that the residue has a macroporous structure, low porosity and considerable resistance to mass loss at temperatures up to 150 ºC (423.15 K). The findings in this article demonstrate that the removal of aluminum using this biosorbent is a complex system, with the involvement of physisorption and chemisorption related mechanisms like ion exchange, which is for the most part associated to the nature and composition of the biomaterial.

Acknowledgments

The authors thank the Coordination Office for the Improvement of Higher Education Personnel (CAPES), Brazilian Council for Scientific and Technological Development (CNPq) (Grant # 308046/2019-6) and São Paulo Research Foundation (FAPESP) (Grants # 2017/18236-1 and # 2019/11353-8) for the financial support.

APPENDIX 4.A Supplementary Material

Figure 4.1S. Adjustments of the experimental data for the initial Al concentration of 1 mmol/L by the kinetic models: a) Pseudo-first order and Pseudo-second order; b) Intraparticle diffusion; c) Boyd model and d) EMTR

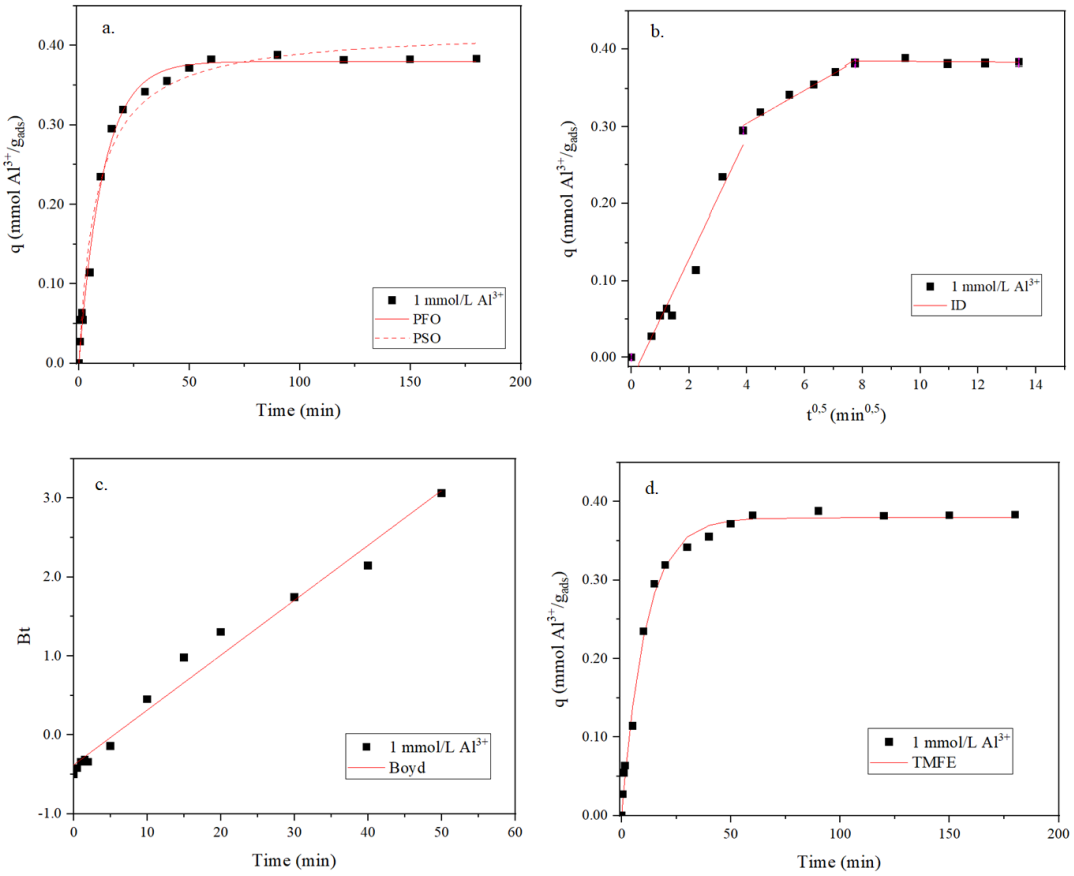

Figure 4.2S. Adjustments of the experimental data for the initial Al concentration of 2 mmol/L by the kinetic models: a) Pseudo-first order and Pseudo-second order; b) Intraparticle diffusion; c) Boyd model and d) EMTR

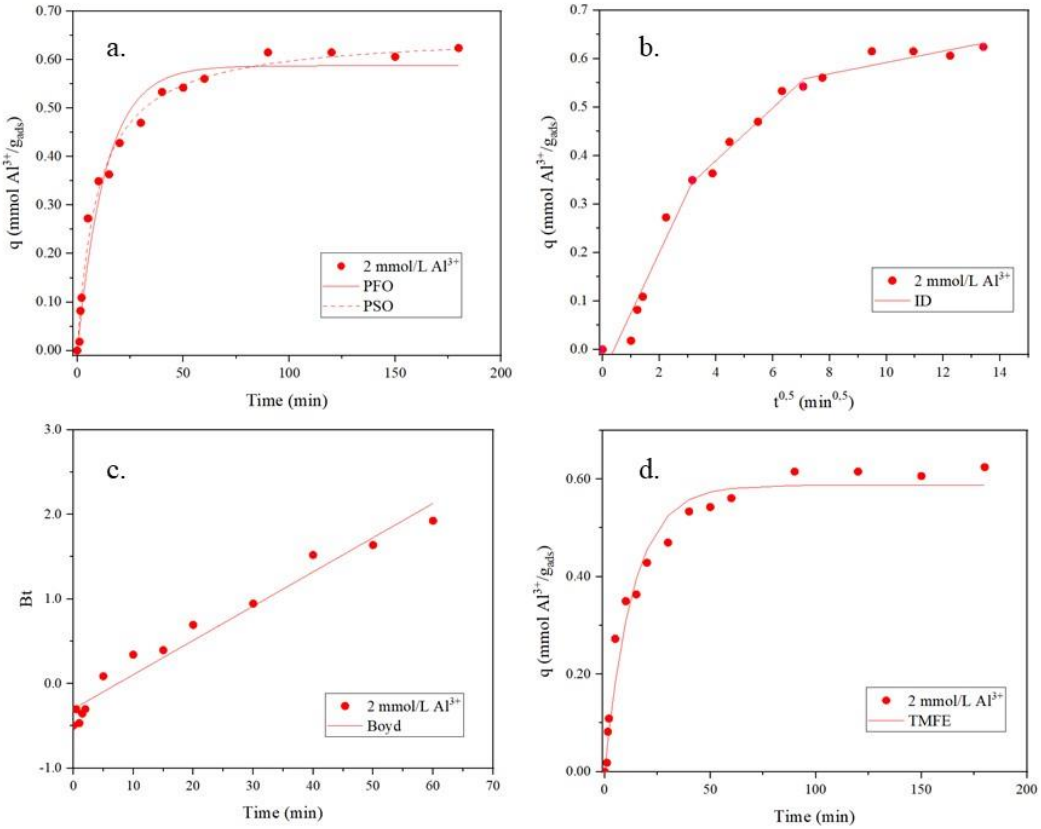

Figure 4.3S. Adjustments of the experimental data for the initial Al concentration of 3 mmol/L by the kinetic models: a) Pseudo-first order and Pseudo-second order; b) Intraparticle diffusion; c) Boyd model and d) EMTR

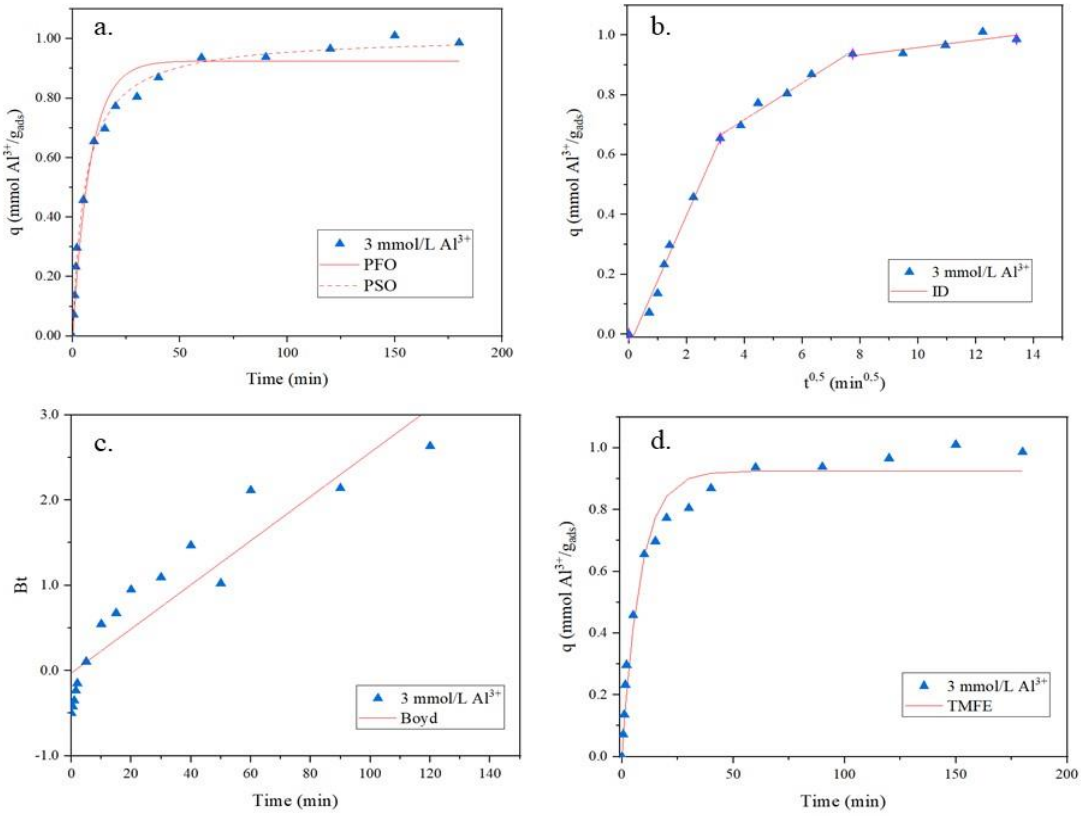

Figure 4.4S. Plot of ln (K) versus 1/T to obtain the thermodynamic parameters

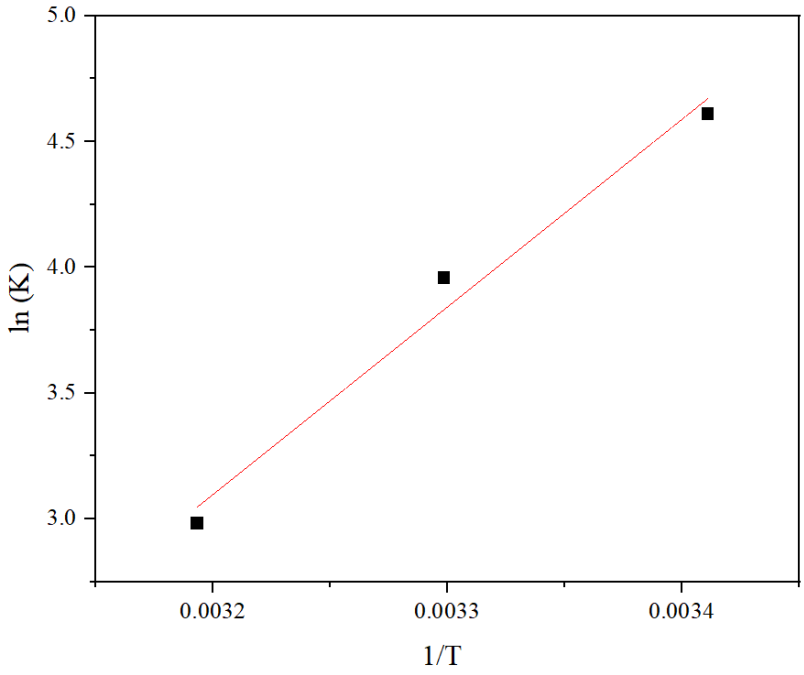

References

Agarwal A, Upadhyay U, Sreedhar I, et al (2020) A review on valorization of biomass in heavy metal removal from wastewater. J Water Process Eng 38:101602. https://doi.org/10.1016/j.jwpe.2020.101602

Akaike H (1998) Information Theory and an Extension of the Maximum Likelihood Principle. pp 199–213

Aravindhan R, Rao JR, Nair BU (2007) Removal of basic yellow dye from aqueous solution by sorption on green alga Caulerpa scalpelliformis. J Hazard Mater 142:68–76. https://doi.org/10.1016/j.jhazmat.2006.07.058

Ates N, Basak A (2021) Selective removal of aluminum, nickel and chromium ions by polymeric resins and natural zeolite from anodic plating wastewater. Int J Environ Health Res 31:102–119. https://doi.org/10.1080/09603123.2019.1631263

Biswas B, Arun Kumar A, Bisht Y, et al (2017) Effects of temperature and solvent on hydrothermal liquefaction of Sargassum tenerrimum algae. Bioresour Technol 242:344–350. https://doi.org/10.1016/j.biortech.2017.03.045

Boeris PS, Agustín M del R, Acevedo DF, Lucchesi GI (2016) Biosorption of aluminum through the use of non-viable biomass of Pseudomonas putida. J Biotechnol 236:57–63. https://doi.org/10.1016/j.jbiotec.2016.07.026

Boyd GE, Adamson AW, Myers LS (1947) The Exchange Adsorption of Ions from Aqueous Solutions by Organic Zeolites. II. Kinetics 1. J Am Chem Soc 69:2836–2848. https://doi.org/10.1021/ja01203a066

Bulgariu L, Bulgariu D, Rusu C (2015) Marine Algae Biomass for Removal of Heavy Metal Ions. In: Hb25_Springer Handbook of Marine Biotechnology. Springer Berlin Heidelberg, Berlin, Heidelberg, pp 611–648

Cardoso SL, Costa CSD, Da Silva MGC, Vieira MGA (2020) Insight into zinc(II) biosorption on alginate extraction residue: Kinetics, isotherm and thermodynamics. J Environ Chem Eng 8:103629. https://doi.org/10.1016/j.jece.2019.103629

Cardoso SL, Costa CSD, Nishikawa E, et al (2017) Biosorption of toxic metals using the alginate extraction residue from the brown algae Sargassum filipendula as a natural ion-exchanger. J Clean Prod 165:491–499. https://doi.org/10.1016/j.jclepro.2017.07.114

Cayllahua JEB, Torem ML (2010) Biosorption of aluminum ions onto Rhodococcus opacus from wastewaters. Chem Eng J 161:1–8. https://doi.org/10.1016/j.cej.2010.03.025

Chen JP, Wu S, Chong K-H (2003) Surface modification of a granular activated carbon by citric acid for enhancement of copper adsorption. Carbon N Y 41:1979–1986. https://doi.org/10.1016/S0008-6223(03)00197-0

Chowdhury S, Mishra R, Saha P, Kushwaha P (2011) Adsorption thermodynamics, kinetics and isosteric heat of adsorption of malachite green onto chemically modified rice husk. Desalination 265:159–168. https://doi.org/10.1016/j.desal.2010.07.047

Coelho CM, de Andrade JR, da Silva MGC, Vieira MGA (2020) Removal of propranolol

hydrochloride by batch biosorption using remaining biomass of alginate extraction from Sargassum filipendula algae. Environ Sci Pollut Res 27:16599–16611. https://doi.org/10.1007/s11356-020-08109-4

Costa CSD, Bertagnolli C, Boos A, et al (2020) Application of a dealginated seaweed derivative for the simultaneous metal ions removal from real and synthetic effluents. J Water Process Eng 37:. https://doi.org/10.1016/j.jwpe.2020.101546

Costa CSD, Cardoso SL, Nishikawa E, et al (2016) Characterization of the residue from double alginate extraction from sargassum filipendula seaweed. Chem Eng Trans 52:133–138. https://doi.org/10.3303/CET1652023

Costa HP de S, da Silva MGC, Vieira MGA (2021) Biosorption of aluminum ions from aqueous solutions using non-conventional low-cost materials: A review. J Water Process Eng 40:101925. https://doi.org/10.1016/j.jwpe.2021.101925

Daneshvar E, Vazirzadeh A, Niazi A, et al (2017) A comparative study of methylene blue biosorption using different modified brown, red and green macroalgae – Effect of pretreatment. Chem Eng J 307:435–446. https://doi.org/10.1016/j.cej.2016.08.093

Davis TA, Volesky B, Mucci A (2003) A review of the biochemistry of heavy metal biosorption by brown algae. Water Res 37:4311–4330. https://doi.org/10.1016/S0043-1354(03)00293-8

de Andrade JR, Oliveira MF, da Silva MGC, Vieira MGA (2018) Adsorption of Pharmaceuticals from Water and Wastewater Using Nonconventional Low-Cost Materials: A Review. Ind Eng Chem Res 57:3103–3127. https://doi.org/10.1021/acs.iecr.7b05137

Dermience M, Lognay G, Mathieu F, Goyens P (2015) Effects of thirty elements on bone metabolism. J Trace Elem Med Biol 32:86–106. https://doi.org/10.1016/j.jtemb.2015.06.005

Djeribi R, Hamdaoui O (2008) Sorption of copper(II) from aqueous solutions by cedar sawdust and crushed brick. Desalination 225:95–112. https://doi.org/10.1016/j.desal.2007.04.091

Do Nascimento WJ, Landers R, Gurgel Carlos da Silva M, Vieira MGA (2021) Equilibrium and desorption studies of the competitive binary biosorption of silver(I) and copper(II) ions on brown algae waste. J Environ Chem Eng 9:104840. https://doi.org/10.1016/j.jece.2020.104840

Dubinin MM, Radushkevitch L V (1947) The equation of the characteristic curve of activated charcoal. Proc Acad Sci USSR 55:

El Houda Larbi N, Merouani DR, Aguedal H, et al (2019) Removal of heavy metals Cd(II) and Al(III) from aqueous solutions by an eco-friendly biosorbent. Key Eng Mater 800 KEM:181–186. https://doi.org/10.4028/www.scientific.net/KEM.800.181

Erbil HY (2009) Solid Surfaces. In: Surface Chemistry of Solid and Liquid Interfaces. Blackwell Publishing, p 368

Farooq U, Kozinski JA, Khan MA, Athar M (2010) Biosorption of heavy metal ions using wheat based biosorbents - A review of the recent literature. Bioresour Technol 101:5043–5053. https://doi.org/10.1016/j.biortech.2010.02.030

Foo KY, Hameed BH (2010) Insights into the modeling of adsorption isotherm systems. Chem Eng J 156:2–10. https://doi.org/10.1016/j.cej.2009.09.013

Freda J (1991) The effects of aluminum and other metals on amphibians. Environ Pollut 71:305–328. https://doi.org/10.1016/0269-7491(91)90035-U

Freitas GR, Vieira MGA, da Silva MGC (2019) Fixed bed biosorption of silver and investigation of functional groups on acidified biosorbent from algae biomass. Environ Sci Pollut Res 26:36354–36366. https://doi.org/10.1007/s11356-019-06731-5

Freitas GR, Vieira MGA, Da Silva MGC (2018) Batch and Fixed Bed Biosorption of Copper by Acidified Algae Waste Biomass. Ind Eng Chem Res 57:11767–11777. https://doi.org/10.1021/acs.iecr.8b02541

Freitas GR, Vieira MGA, Silva MGC (2017) Kinetic adsorption of copper ions by the residue of alginate extraction from the seaweed Sargassum filipendula. Chem Eng Trans 57:655–660. https://doi.org/10.3303/CET1757110

Freundlich H (1907) Über die Adsorption in Lösungen. Zeitschrift für Phys Chemie 57U: https://doi.org/10.1515/zpch-1907-5723

Gensemer RW, Playle RC (1999) The bioavailability and toxicity of aluminum in aquatic environments. Crit Rev Environ Sci Technol 29:315–450. https://doi.org/10.1080/10643389991259245

Gibbs JW (1873) Graphical Methods in the Thermodynamics of Fluids. Trans Connect Acad Arts Sci 2:309–342

Giles CH, MacEwan TH, Nakhwa SN, Smith D (1960) 786. Studies in adsorption. Part XI. A system of classification of solution adsorption isotherms, and its use in diagnosis of adsorption mechanisms and in measurement of specific surface areas of solids. J Chem Soc 3973. https://doi.org/10.1039/jr9600003973

Goher ME, Hassan AM, Abdel-Moniem IA, et al (2015) Removal of aluminum, iron and manganese ions from industrial wastes using granular activated carbon and Amberlite IR-120H. Egypt J Aquat Res 41:155–164. https://doi.org/10.1016/j.ejar.2015.04.002

Halim AA, Ezani E, Othman MS, et al (2012) Adsorption study of aluminium onto Curcuma longa. Nat Environ Pollut Technol 11:193–197

Hartzog DG, Sircar S (1995) Sensitivity of PSA process performance to input variables. Adsorption 1:133–151. https://doi.org/10.1007/BF00705001

He J, Chen JP (2014) A comprehensive review on biosorption of heavy metals by algal biomass: Materials, performances, chemistry, and modeling simulation tools. Bioresour Technol 160:67–78. https://doi.org/10.1016/j.biortech.2014.01.068

Ho Y., McKay G (1999) Pseudo-second order model for sorption processes. Process Biochem 34:451–465. https://doi.org/10.1016/S0032-9592(98)00112-5

Irannajad M, Kamran Haghighi H (2021) Removal of Heavy Metals from Polluted Solutions by Zeolitic Adsorbents: a Review. Environ Process 8:7–35. https://doi.org/10.1007/s40710-020-00476-x

Kalderis D, Bethanis S, Paraskeva P, Diamadopoulos E (2008) Production of activated

carbon from bagasse and rice husk by a single-stage chemical activation method at low retention times. Bioresour Technol 99:6809–6816. https://doi.org/10.1016/j.biortech.2008.01.041

Krewski D, Yokel R a, Nieboer E, et al (2007) KREWSKI, D. et al. Human Health Risk Assessment For Aluminium, Aluminium Oxide, and Aluminium Hydroxide. [s.l: s.n.]. v. 10Human Health Risk Assessment For Aluminium, Aluminium Oxide, and Aluminium Hydroxide

Lagergren S (1898) Zur theorie Der Sogenannten adsorption geloster stoffe, Kungliga Svenska Vetenskapsakademiens. Handlingar 24:1–39. https://doi.org/10.1007/BF01501332

Langmuir I (1918) THE ADSORPTION OF GASES ON PLANE SURFACES OF GLASS, MICA AND PLATINUM. J Am Chem Soc 40:1361–1403. https://doi.org/10.1021/ja02242a004

Lee HS, Suh JH, Kim IB, Yoon T (2004) Effect of aluminum in two-metal biosorption by an algal biosorbent. Miner Eng 17:487–493. https://doi.org/10.1016/j.mineng.2004.01.002

Lobo-Recio MÁ, Rodrigues C, Custódio Jeremias T, et al (2021) Highly efficient removal of aluminum, iron, and manganese ions using Linde type-A zeolite obtained from hazardous waste. Chemosphere 267:128919. https://doi.org/10.1016/j.chemosphere.2020.128919

Lodeiro P, Gudiña Á, Herrero L, et al (2010) Aluminium removal from wastewater by refused beach cast seaweed. Equilibrium and dynamic studies. J Hazard Mater 178:861–866. https://doi.org/10.1016/j.jhazmat.2010.02.017

Mahdavi M, Ebrahimi A, Mahvi AH, et al (2018) Experimental data for aluminum removal from aqueous solution by raw and iron-modified granular activated carbon. Data Br 17:731–738. https://doi.org/10.1016/j.dib.2018.01.063

McHugh DJ (1987) FAO Fisheries Technical Paper 288. In: Chapter 2 - Prod. Prop. uses alginates. http://www.fao.org/3/x5822e04.htm#chapter

Merian E, Anke M, Ihnat M, Stoeppler M (2004) Elements and Their Compounds in the Environment Edited by Related Titles Joachim Nölte Bernhard Welz , Michael Sperling Handbook of Elemental Speciation Markus Stoeppler , Wayne R . Wolf , Peter J . Jenks (eds) Reference Materials for Chemical Analysis

Milonjic S (2007) A consideration of the correct calculation of thermodynamic parameters of adsorption. J Serbian Chem Soc 72:1363–1367. https://doi.org/10.2298/JSC0712363M

Moino BP, Costa CSD, Carlos da Silva MG, Vieira MGA (2020) Reuse of the alginate extraction waste from Sargassum filipendula for Ni(II) biosorption. Chem Eng Commun 207:17–30. https://doi.org/10.1080/00986445.2018.1564909

Moino BP, Costa CSD, da Silva MGC, Vieira MGA (2017) Removal of nickel ions on residue of alginate extraction from Sargassum filipendula seaweed in packed bed. Can J Chem Eng 95:2120–2128. https://doi.org/10.1002/cjce.22859

Naeemullah N, Tuzen M, Sari A, Mendil D (2017) Biosorption of aluminum from aqueous solutions by using macrofungus (Cortinarius armillatus): Equilibrium,

Kinetic, and Thermodynamic Studies and Determination by GFAAS. At Spectrosc 38:149–157. https://doi.org/10.46770/as.2017.05.005

Nishikawa E, da Silva MGC, Vieira MGA (2018) Cadmium biosorption by alginate extraction waste and process overview in Life Cycle Assessment context. J Clean Prod 178:166–175. https://doi.org/10.1016/j.jclepro.2018.01.025

Otunola BO, Ololade OO (2020) A review on the application of clay minerals as heavy metal adsorbents for remediation purposes. Environ Technol Innov 18:100692. https://doi.org/10.1016/j.eti.2020.100692

Ozdemir G, Baysal SH (2004) Chromium and aluminum biosorption on Chryseomonas luteola TEM05. Appl Microbiol Biotechnol 64:599–603. https://doi.org/10.1007/s00253-003-1479-0

Pagnanelli F (2011) Equilibrium, Kinetic and Dynamic Modelling of Biosorption Processes. In: Microbial Biosorption of Metals. Springer Netherlands, Dordrecht, pp 59–120

Puranik P., Modak J., Paknikar K. (1999) A comparative study of the mass transfer kinetics of metal biosorption by microbial biomass. Hydrometallurgy 52:189–197. https://doi.org/10.1016/S0304-386X(99)00017-1

Rajamohan N, Rajasimman M, Rajeshkannan R, Saravanan V (2014) Equilibrium, kinetic and thermodynamic studies on the removal of Aluminum by modified Eucalyptus camaldulensis barks. Alexandria Eng J 53:409–415. https://doi.org/10.1016/j.aej.2014.01.007

Rocha Freitas G, Adeodato Vieira MG, Carlos da Silva MG (2020) Characterization and biosorption of silver by biomass waste from the alginate industry. J Clean Prod 271:122588. https://doi.org/10.1016/j.jclepro.2020.122588

Rosa LMT, Botero WG, Santos JCC, et al (2018) Natural organic matter residue as a low cost adsorbent for aluminum. J Environ Manage 215:91–99. https://doi.org/10.1016/j.jenvman.2018.03.048

Ruthven DM (1984) Principles of Adsorption and Adsorption Processes. Wiley

Saha P, Chowdhury S (2011) Insight Into Adsorption Thermodynamics. In: Tadashi M (ed) Thermodynamics. InTech, pp 349–364

Santos NT das G, da Silva MGC, Vieira MGA (2019) Development of novel sericin and alginate-based biosorbents for precious metal removal from wastewater. Environ Sci Pollut Res 26:28455–28469. https://doi.org/10.1007/s11356-018-3378-z

Santos NT das G, Moraes LF, da Silva MGC, Vieira MGA (2020) Recovery of gold through adsorption onto sericin and alginate particles chemically crosslinked by proanthocyanidins. J Clean Prod 253:119925. https://doi.org/10.1016/j.jclepro.2019.119925

Sari A, Tuzen M (2009) Equilibrium, thermodynamic and kinetic studies on aluminum biosorption from aqueous solution by brown algae (Padina pavonica) biomass. J Hazard Mater 171:973–979. https://doi.org/10.1016/j.jhazmat.2009.06.101

Shaaban AESM, Badawy RK, Mansour HA, et al (2017) Competitive algal biosorption of Al3+, Fe3+, and Zn2+ and treatment application of some industrial effluents from

Borg El-Arab region, Egypt. J Appl Phycol 29:3221–3234. https://doi.org/10.1007/s10811-017-1185-4

Sing KSW (1985) Reporting physisorption data for gas/solid systems with special reference to the determination of surface area and porosity (Recommendations 1984). Pure Appl Chem 57:603–619. https://doi.org/10.1351/pac198557040603

Singh KK, Rastogi R, Hasan SH (2005) Removal of Cr(VI) from wastewater using rice bran. J Colloid Interface Sci 290:61–68. https://doi.org/10.1016/j.jcis.2005.04.011

Skibniewska E, Skibniewski M (2019) Aluminum, Al. In: Mammals and Birds as Bioindicators of Trace Element Contaminations in Terrestrial Environments. Springer International Publishing, Cham, pp 413–462

Soares JP, Santos JE, Chierice GO, Cavalheiro ETG (2004) Thermal behavior of alginic acid and its sodium salt. Eclética Química 29:57–64. https://doi.org/10.1590/S0100-46702004000200009

Soares S, Camino G, Levchik S (1995) Comparative study of the thermal decomposition of pure cellulose and pulp paper. Polym Degrad Stab 49:275–283. https://doi.org/10.1016/0141-3910(95)87009-1

Sotirelis NP, Chrysikopoulos C V. (2015) Interaction Between Graphene Oxide Nanoparticles and Quartz Sand. Environ Sci Technol 49:13413–13421. https://doi.org/10.1021/acs.est.5b03496

Srivastava SK, Tyagi R, Pant N (1989) Adsorption of heavy metal ions on carbonaceous material developed from the waste slurry generated in local fertilizer plants. Water Res 23:1161–1165. https://doi.org/10.1016/0043-1354(89)90160-7

Stephens BR, Jolliff JS (2015) Aluminum and Alzheimer's Disease. Elsevier Inc.

Tassist A, Lounici H, Abdi N, Mameri N (2010) Equilibrium, kinetic and thermodynamic studies on aluminum biosorption by a mycelial biomass (Streptomyces rimosus). J Hazard Mater 183:35–43. https://doi.org/10.1016/j.jhazmat.2010.06.078

Thommes M, Kaneko K, Neimark A V., et al (2015) Physisorption of gases, with special reference to the evaluation of surface area and pore size distribution (IUPAC Technical Report). Pure Appl Chem 87:1051–1069. https://doi.org/10.1515/pac-2014-1117

Titah HS, Purwanti IF, Tangahu BV, et al (2019) Kinetics of aluminium removal by locally isolated Brochothrix thermosphacta and Vibrio alginolyticus. J Environ Manage 238:194–200. https://doi.org/10.1016/j.jenvman.2019.03.011

U.S. Geological Survey (2020) Mineral Commodity Summaries - Zeolites (Natural)

Vijayaraghavan K, Gupta S, Joshi UM (2012) Comparative assessment of Al(III) and Cd(II) biosorption onto turbinaria conoides in single and binary systems. Water Air Soil Pollut 223:2923–2931. https://doi.org/10.1007/s11270-012-1075-y

Wagenmakers E-J, Farrell S (2004) AIC model selection using Akaike weights. Psychon Bull Rev 11:192–196. https://doi.org/10.3758/BF03206482

Walton JR (2011) Bioavailable Aluminum: Its Metabolism and Effects on the Environment. In: Encyclopedia of Environmental Health. Elsevier, pp 343–352

Weber WJ, Morris CJ (1963) Kinetics of Adsorption on Carbon from Solution. J Sanit Eng Div 89:31–60

Young DM, Crowell AD (1962) Physical Adsorption of Gases. Butterworths, London

Yu LJ, Wang S, Jiang XM, et al (2008) Thermal analysis studies on combustion characteristics of seaweed. J Therm Anal Calorim 93:611–617. https://doi.org/10.1007/s10973-007-8274-6

Yurtsever M, Nalçak M (2019) Al(III) removal from wastewater by natural clay and coconut shell. Glob Nest J 21:477–483. https://doi.org/10.30955/gnj.002566

Zhu B, Xia P, Ho W, Yu J (2015) Isoelectric point and adsorption activity of porous g-C3N4. Appl Surf Sci 344:188–195. https://doi.org/10.1016/j.apsusc.2015.03.086

5. Bioadsorção de Alumínio utilizando resíduo da extração de alginato da alga *S. filipendula* em Leito Fixo

Fixed bed biosorption and ionic exchange of aluminum by brown algae residual biomass***

Heloisa Pereira de Sá Costa[1], Meuris Gurgel Carlos da Silva[1], Melissa Gurgel Adeodato Vieira[1]

[1]Department of Processes and Products Design, School of Chemical Engineering, University of Campinas, Albert Einstein Av., 500, Campinas, São Paulo, 13083-852, Brazil

ABSTRACT

This study aimed to evaluate the ion exchange and biosorption of aluminum using as biosorbent material a residual biomass generated in the alginate extraction process from the brown algae *S. filipendula* (named RES). The dynamic system in a fixed packed bed column and the reuse/regeneration of the biosorbent was assessed by breakthrough method. The batch mode results showed that ion exchange, mainly with Na^+ ions, has an important participation on the removal of Al^{3+} ions by RES. Characterization analyses and blocking assays indicated that carboxylic, amino and sulfonate functional groups play a key role on the aluminum biosorption. Fixed bed experiments pointed that higher aluminum removal was achieved at 0.5 mL/min and 1 mmol/L. DualSD and Yan et al. models showed superior prediction of experimental data. Biosorption/Desorption cycles demonstrated the reuse feasibility of the biosorbent, which maintained a considerable adsorption capacity in all cycles performed.

Keywords: Biosorption; aluminum; residue; brown algae; fixed bed.

*** Manuscript published in *Journal of Water Process Engineering* 42 (2021) 102117. DOI: 10.1016/j.jwpe.2021.102117. Reprinted with permission from *Journal of Water Process Engineering.*

5.1 Introduction

In view of the current scenario of constant industrial expansion and, consequently, the increase in the pollution of water bodies by the discharge of contaminated effluents, processes for the removal of pollutants have been increasingly investigated. Among the processes most used nowadays by the industry for the treatment of contaminated wastewaters, generally chemical precipitation is the most applied, mainly due to its operational simplicity. Nevertheless, this method generates large amounts of highly contaminated sludge, thus leading to the occurrence of secondary pollution.

Therefore, advanced methods with redefined approaches are necessary in search for a sustainable development of industrial expansion. Biosorption is an adsorption process that uses materials of biological origin as adsorbents (biosorbents) to remove various types of contaminants, especially toxic metals [1,2]. This technology stands out for being simple, eco-friendly, inexpensive and at the same time flexible for scale up, that is, for the continuous treatment of large amounts of effluents contaminated with mild concentrations of metals.

Aluminum is a hazardous metal widely used in several industrial processes, e.g., mining, metallurgic, smelting and electroplating, hence large amounts of wastewaters are found with significant concentrations of this metal [3,4]. Once they are generated quickly and in large quantities, the treatment of these effluents requires a fast, cheap and simple method, such as biosorption and, in this case, the properties of the biosorbent material must also meet requirements such as having high availability and the lowest commercial value as possible. There are several studies reported in the literature that uses different biomaterials for the removal of Al^{3+} such as microorganisms, agro-industrial residues and seaweeds [5–10].

Algae are known as promisors biosorbents for the removal of toxic metals due to their great affinity [11], especially brown algae stands out for having satisfactory Al^{3+} removal percentages when compared to green and red algae [9]. The system studied in this research consists on the biosorption of Al^{3+} ions in an aqueous medium using as biosorbent the residue from the alginate extraction from the brown alga *Sargassum filipendula*. This biomaterial, in addition to meeting the requirements previously mentioned, is also considered promising for the uptake of toxic metals for having in its composition functional groups directly associated to the mechanism of toxic metals removal [12]. Previously studies highlighted the effectiveness of this biosorbent for

removing metals such as cadmium, zinc, chromium and nickel [13–15]. Since it has no added value, this waste, here termed as RES, is usually discarded in the sea.

Compared to other toxic metals, a lack in literature for in-depth investigations on Al^{3+} biosorption systems is found [16]. In addition to that, in previous works this residue showed a remarkable affinity for Al^{3+} ions, however, this system was not completely studied [17]. Thus, this metal was selected for this study. This work has the objective to advance in understanding the mechanism of ion exchange involved in the biosorption of Al^{3+} using the residue through batch studies and characterizations of the biosorbent material before and after the process. Furthermore, the viability/efficiency of the process and the biosorbent regeneration in continuous system was also investigated. All objectives meet at the point of explore an innovative, accessible and feasible technology to remove Al^{3+} ions present in aqueous media, in addition to helping to fill the niche found in the literature concerning Al^{3+} biosorption studies in a fixed-bed dynamic system.

5.2 Material and Methods

5.2.1 Aluminum solution

Al^{3+} solutions were prepared using analytical nonahydrate Al^{3+} nitrate ($Al(NO_3)_3.9H_2O$, Dinâmica) dissolved in deionized water at required concentrations and molar proportions.

5.2.2 Biosorbent obtainment

The raw biomass of *S. filipendula* was gathered at Cigarra's beach, on the north coast of São Paulo, Brazil. The seaweed was rinsed with deionized water repetitively and dried at 333.15 K for 24 h and refined at particles with diameter around 1 mm. Alginate removal was performed according to McHugh's methodology [18]. The dealginated residue, here termed as RES, generated from extraction operation was washed and dried (333.15 K, 24 h). In order to obtain fractions with diameter about 0.737 mm, the biosorbent was sieved through #12, #16 and #32 mesh screens.

5.2.3 Biosorbent characterization

Characterization analyses were carried out on the residue before (RES) and after (RES-Al) biosorption, in order to elucidate the mechanisms involved in the Al^{3+} uptake using this biomaterial. To analyze the morphology and chemical composition of the

biosorbent, scanning electron microscopy with X-ray dispersive energy (SEM-EDX, Leo 440i / 6070, England) was conducted. The biosorbent was overlaid with a gold film (~ 200 A°) before scanning. The micrographs were obtained with 1000x magnification and the operating conditions were 50 pA and 15 kV for SEM, and 800 pA and 20 kV for EDX analysis.

Fourier Transform Infrared spectroscopy (FTIR) was conducted to obtain information about the functional groups present on the surface of the biosorbent. The analysis was performed in a spectrum range of 4000 to 500 cm^{-1} with scan resolution of 4 cm^{-1} using a Nicolet 6700 spectrometer (ThermoScientific).

5.2.4 Ion-exchange study

The occurrence of ion exchange mechanisms is a characteristic of seaweed biomasses and are frequently involved on toxic metal removal [19]. In view of the possible participation of these mechanisms in Al^{3+} biosorption, the occurrence of this phenomenon was evaluated in kinetic studies that were conducted in order to determine the concentration profiles of the main light cations (Ca^{2+}, K^{+}, Mg^{2+} and Na^{+}) involved in the removal of toxic metals using this biosorbent [13]. For this purpose, 1000 mL of a 3 mmol/L Al^{3+} solution was treated with 2 g of residue at room temperature (298.15 K), for 3 hours, under constant agitation (250 rpm). Aiming to avoid metal precipitation, the solution pH was fixed at 4 and controlled using HNO_3 solutions (0.1 and 0.5 mmol/L). Samples were collected at regular time intervals and the metal concentration was measured by Atomic Absorption Spectrometry, AAS (Shimadzu, Japan).

5.2.5 Esterification of functional groups

To evaluate the participation of the main functional groups in the removal of Al^{3+} ions by the residue, the esterification of these groups was performed. The blocked functional groups were the carboxyl and sulfonate groups, as they are notably the most involved in biosorption processes using algae-derived biomasses [11]. The esterification of the carboxylic groups was performed according to the methodology established by Gardea-Torresdey et al. [20] where 4 g of residue were added to a solution of 260 mL of methanol and 2.4 mL of concentrated hydrochloric acid in constant agitation for 6 hours at 298.15 K. Subsequently, the biosorbent was rinsed with deionized water and dried at 333.15 K for 12 hours. This residue was named esterified waste (RES-EST). For the esterification of sulfonate groups, 1 g of the residue was put in contact to a mixture of 50

mL of methanol and 0.5 mL of hydrochloric acid under constant stirring for 48 hours, divided into 4 cycles where the methanol and HCl solution was replaced between cycles. The residue, termed blocked esterified residue (RES-EST-BLK), was washed with deionized water and dried for 12 hours at 333.15 K [21].

Blocking experiments were conducted in batch mode, in an orbital shaker (JeioTech, SI-600R) with constant agitation (250 rpm) and controlled temperature (298.15 K), for 6 hours. The dosage of biosorbent was 2 g/L for both biomasses. In order to respect the acid constant (pKa) of each group, the tests were conducted at different pH for RES-EST and RES-EST-BLK. According to Sheng et al. [22], brown algae carboxylic groups have pKa in range of 3.5 to 5, whereas for sulfonate groups this value is between 1 and 2.5, so tests with the esterified residue were performed at pH 5, while for the esterified and blocked residue pH 2 was chosen. To evaluate the adsorptive capacity of the residues in equilibrium (q_{eq}, mmol/g) and the percentage of Al^{3+} removal (%R) Equations 5.1 and 5.2 were applied, respectively.

$$q_{eq} = \frac{(C_0 - C_{eq})V}{w} \tag{5.1}$$

$$\%R = \left(\frac{C_0 - C_{eq}}{C_0}\right).100 \tag{5.2}$$

Where, C_0 represents the initial metal concentration in solution (mmol/L); C_{eq} is the metal concentration at equilibrium (mmol/L), V is the volume of the solution (L) and w is the residue dry weight (g).

5.2.6 Desorption study

In order to select the most suitable eluent solution for the system, 1.5 g of residue was contaminated in 750 mL of Al^{3+} solution (1 mmol/L), in batch mode, with pH fixed in 4, for 3 hours with constant agitation of 250 rpm. The contaminated residue was dried at 333.15 K for 24 hours. The metal concentration was measured before and after this process to ensure that the residue was properly contaminated. The eluents tested were chosen based on the efficiency reported in other works in the literature[10,23,24], a total of five eluents were tested: a) $CaCl_2$ (0.5 mol/L); b) Na_2EDTA (0.005 mol/L); c) HNO_3 (0.1 mol/L); d) HCl (0.1 mol/L); e) H_2O. The batch desorption was carried out in a shaker with constant agitation and temperature (250 rpm and 298.15 K) adding 0.1 g of Al-

loaded residue (RES-Al) to 50 mL of eluent solution. The mixture was stirred for 4 hours. At the end of the process, Al^{3+} concentration in the solution was measured by AAS. The elution efficiency (%EE) was calculated by Equation 5.3. To evaluate the mass loss, the desorbed residue was dried at 333.15 K for 24 h and weighed.

$$\%EE = \frac{C_d\, V_d}{q_{eq}\, w} x100 \tag{5.3}$$

In Equation 3, C_d represents the Al^{3+} concentration in the desorption system (mmol/L) and V_d is the volume of the desorption medium (L).

5.2.7 Evaluation of Al^{3+} biosorption in dynamic system

Fixed bed assays were carried out in a glass column with 0.7 cm internal diameter and 7 cm height that was coupled to an automatic aliquot collector and to a peristaltic pump, according to the diagram shown in Figure 5.1S (see Supplementary Material). The experiments were made with 0.3 g of the biosorbent, hydrated and expanded for 12 hours in ultrapure MilliQ water and then used to fill the glass column. The Al^{3+} solution was fed in ascending flow through the bed using the peristaltic pump (Masterflex). The automatic collector (FC 203, Gilson) was programmed to withdraw samples at regular intervals of time, aiming to obtain the rupture curves (C/C_0 vs. t). The Al^{3+} concentration was determined by AAS. All dynamic assays were conducted at 298.15 K.

5.2.7.1 Effect of flow rate and inlet concentration

The fluid dynamic study was performed aiming to assay the flow rate where the greatest ion biosorption occurs. Al^{3+} solution (1 mmol/L) was fed at flows 0.5, 0.8 and 1 mL/min. In this study, parameters that are directly influenced by the process flow rate were analyzed, which are: useful amount removed up to the breaking point (q_r) and until saturation (q_s), length of the mass transfer zone (MTZ), percentage of total removal until breaking point (% R_r) and saturation (%R_s), presented by Equations 5.4-5.8.

$$q_r = \frac{C_0 Q}{w} \int_0^{t_r} \left(1 - \frac{C}{C_0}\right) dt \tag{5.4}$$

$$q_s = \frac{C_0 Q}{w} \int_0^{t_s} \left(1 - \frac{C}{C_0}\right) dt \tag{5.5}$$

$$MTZ = \left(1 - \frac{q_u}{q_s}\right).H_t \tag{5.6}$$

$$\%R_r = \frac{q_u\, m}{C_0\, Q\, t_r} \quad (5.7)$$

$$\%R_s = \frac{q_s\, m}{C_0\, Q\, t_s} \quad (5.8)$$

In which, Q is the flow rate (L/min); C denotes the Al^{3+} concentration at time t (mmol/L); t_r and t_s represents, respectively, the breakthrough and saturation time (min); and H_t stands for the bed height (cm).

In the next step, with the flow previously defined, different inlet concentrations (0.8, 1 and 1.5 mmol/L) of Al^{3+} solution were tested in order to define the one that most favors the Al^{3+} removal process. For this purpose, the same parameters as the previous step (q_r, q_s, ZTM, $\%R_r$ and $\%R_s$) were evaluated.

5.2.7.2 Biosorption/Desorption cycles

Once the optimal conditions were determined, four sorption/desorption cycles were conducted aiming to investigate the biomaterial regeneration potential. The eluent solution was selected based on results from assays described in section 5.2.6. Between each cycle, the residue was washed in a continuous flow of deionized water for 1 hour. Fixed bed parameters, i.e. q_r, q_s, ZTM, $\%R_r$ and $\%R_s$, were calculated aiming to compare with results previously obtained.

5.2.7.3 Model evaluation

Mathematical modeling is used to describe the behavior of breakthrough curves, assisting in the understanding and scale-up of the system. Five different column adsorption models were adjusted to breakthrough curves data to explain the process of Al^{3+} biosorption by RES in fixed bed configuration, as follows: Yoon-Nelson [25], Thomas [26], Clark [27], Yan et al. [28] and DualSD [29]. The mathematical models of Yoon-Nelson, Thomas, Clark and Yan et al. are well established in the literature and the most commonly found to predict the dynamic behavior of biosorption systems, while the DualSD model is more recent and based on the law of mass conservation [29].

The Yoon-Nelson model undertakes that the adsorption rate decreases proportionally to the removal of adsorbate and the rupture curve of the adsorbent, disregarding information such as adsorbate properties, type of adsorbent and specifications about the adsorption column. Thomas' mathematical model presumes that

intraparticle diffusion and external resistance to mass transfer are low, therefore, negligible and that the adsorption process is governed by the reversible kinetic model of pseudo-second order, with equilibrium described by the Langmuir model. While Clark's model is based on the concepts of mass transfer and the Freundlich isotherm, in addition to assuming that the flow of the solution in the column behaves like a piston and discards the occurrence of dispersion [30]. The empirical model proposed by Yan et al. minimizes possible errors in the application of the Thomas model. The DualSD model is based on linear driving force models and assumes that the biosorbent surface is formed by different types of adsorption sites, therefore different kinetics behaviors can govern the process. The equations for each model are listed in Table 1. Models' adjustment to the experimental data were performed using Maple® 17 and Origin® 8.

Table 13. Models' equations applied to the breakthrough curves of $^{Al3+}$ removal by RES in a fixed bed system.

Model	Equation
Yoon-Nelson	$\frac{C}{C_0} = \frac{1}{1 + \exp(k_{YN}(\tau - t))}$ $q_{YN} = \frac{\tau C_0 Q}{w}$
Thomas	$\frac{C}{C_0} = \frac{1}{1 + \exp\left(\frac{K_{TH}}{Q}(q_{TM} w - C_0 Q t)\right)}$
Clark	$\frac{C}{C_0} = \frac{1}{(1 + A_c . \exp(-r . t))^{\frac{1}{n-1}}}$
Yan et al.	$\frac{C}{C_0} = 1 - \frac{1}{1 + \left(\frac{Q^2 t}{k_y q_y w}\right)^{\frac{k_y C_0}{Q}}}$
DualSD	$D_a = u_0 d_p \left(\frac{20}{\varepsilon}\frac{D_m}{u_0 d_p} + \frac{1}{2}\right)$

Parameters: C is the Al^{3+} concentration at the column outlet (mmol/L); C_0 is the metal initial concentration (mmol/L); t is the time (h); q_{TH} is RES adsorption capacity (mmol/g); K_{YN} is the Yoon and Nelson constant (1/h); τ is the time demanded for the system to reach $C_t/C_0 = 0.50$ (h); K_{TH} is Thomas rate constant (L/mg.h); Q represents the flow rate (L/h); w is the weight of RES packed (0.3 g); A_C is the Clark constant; r_C is the mass transfer coefficient (1/h); n is the heterogeneity factor obtained from the adjustment of the Freundlich isotherm model to the equilibrium data; q_γ is the RES maximum adsorption capacity (mmol/g), k_γ is the Yan constant

model; D_a is the axial dispersion coefficient (cm²/min); u_0 is the interstitial velocity (cm/min); d_p represents the RES particles diameter (cm); ε is the void fraction and D_m is the molecular diffusivity (cm²/min).

5.2.7.4 Error analysis

Models' adjustments were analyzed using the determination coefficients (R^2) (Equation 5.9) and the corrected Akaike Information Criteria (AICc) (Equation 5.10).

$$RMD = \frac{1}{N}\sum_{i=1}^{N}\left|\frac{q_{exp} - q_{pred}}{q_{exp}}\right| x100 \quad (5.9)$$

$$AICc = N.ln\left(\frac{\sum_{i=1}^{N}(q_{exp}-q_{pred})^2}{N}\right) + 2p + \frac{2p(p+1)}{N-p-1} \quad \text{when } \frac{N}{p} < 40 \quad (5.10)$$

The predicted and experimental points are represented by q_{exp} and q_{pred}, respectively, N is the number of experimental points and p is the number of model parameters.

5.3 Results and Discussion

5.3.1 Biosorbent characterization

5.3.1.1 FTIR

The understanding of functional groups involved in the biosorption of toxic metals is essential to elucidate the mechanism of this process. Groups such as carboxylic, sulfonate, hydroxyl and amine are among the major responsible for the metal uptake by algae biomaterials [31]. In the case of the residue studied here, its composition is very similar to the *Sargassum filipendula* seaweed [12]. In order to analyze the functional groups involved in the removal of Al^{3+} ions by RES, Figure 5.1 shows the infrared spectrum of the unloaded (a) and Al-loaded (b) residue.

According to Sheng et al. [22], the broadband at 3000-3600 cm^{-1} corresponds to bindings related to the -OH and -NH groups. The change observed in the peak of 3420 cm^{-1} of RES to 3440 cm^{-1} in RES-Al indicates that these groups have an active participation in the bonding with Al^{3+} ions. The variation of bands from 1538 cm^{-1} to 1548 cm^{-1} after biosorption confirms the amino groups participation in the process. The peaks identified in the region of 1639 cm^{-1} and 1404 cm^{-1} represent the COO-M

carboxylic salts, where M refers to light metals as Na^{+}, K^{+}, Mg^{2+} and Ca^{2+} [21], the change to 1643 and 1462 cm^{-1} suggests that these metals are being exchanged for the metal of interest, in this case Al^{3+}, pointing to the occurrence of ion exchange mechanisms. This result is confirmed by the ion exchange evaluation experiment discussed further in section 5.3.2.

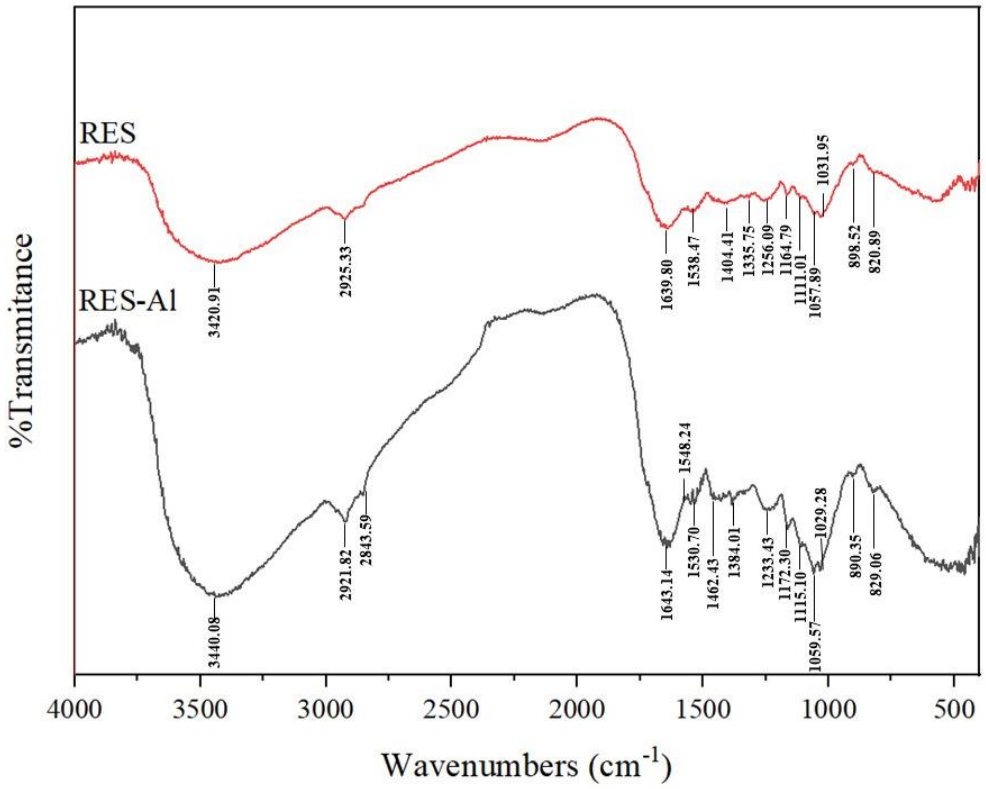

Figure 5.3 FTIR spectra for a) RES and b) RES-Al.

The peaks at 1057 and 1031 cm^{-1} are ascribed to C-O bonds of the alcoholic groups. After the removal of Al^{3+} these values changed to 1059 and 1029 cm^{-1}, respectively, this subtle shift may reveal that coordination with the metal ions has minor participation in the mechanism of Al^{3+} uptake by RES. The band at 1111.01 cm^{-1} is related to the stretching of C-O of ether groups, the variation to 1115.10 cm^{-1} after biosorption indicates that these bindings also have trivial participation in this system. The band at 1164 cm^{-1} (RES) and 1172 cm^{-1} (RES-Al) is associated with sulfonic groups (S=O and C-S-O) of fucoidan, one of the main compounds of the brown alga *S. filipendula* [32]. The changes in peaks at 1256 cm^{-1} in RES to 1233 cm^{-1} in RES-Al are also linked to sulfonic functions. The significant changes noted in these bands after the biosorption process point that sulfonic groups actively take part in the Al^{3+} complexation by RES.

Thus, it can be inferred that carboxylic, amino and sulfates groups are predominantly participating in the process of Al^{3+} removal using the residue. The sharp peaks at 820 cm^{-1} (RES) and 829 cm^{-1} (RES-Al) are related to the participation of mannuronic groups, which indicates the presence of remaining alginate from the extraction process [33]. Overall, similar results are reported in the literature for RES in the uptake of other toxic metals, as for other biosorbents algae-derived in the removal of Al^{3+} ions [1,9,10,34,35].

5.3.1.2 SEM-EDX

Figure 5.2 depicts the micrographs obtained for the residue before (a) and after (b) the biosorption of Al^{3+}, in addition to showing the distribution of this metal on the surface of the biosorbent (c). Moreover, Table 5.2 summarizes the chemical composition obtained by EDX also for raw and Al-contaminated RES.

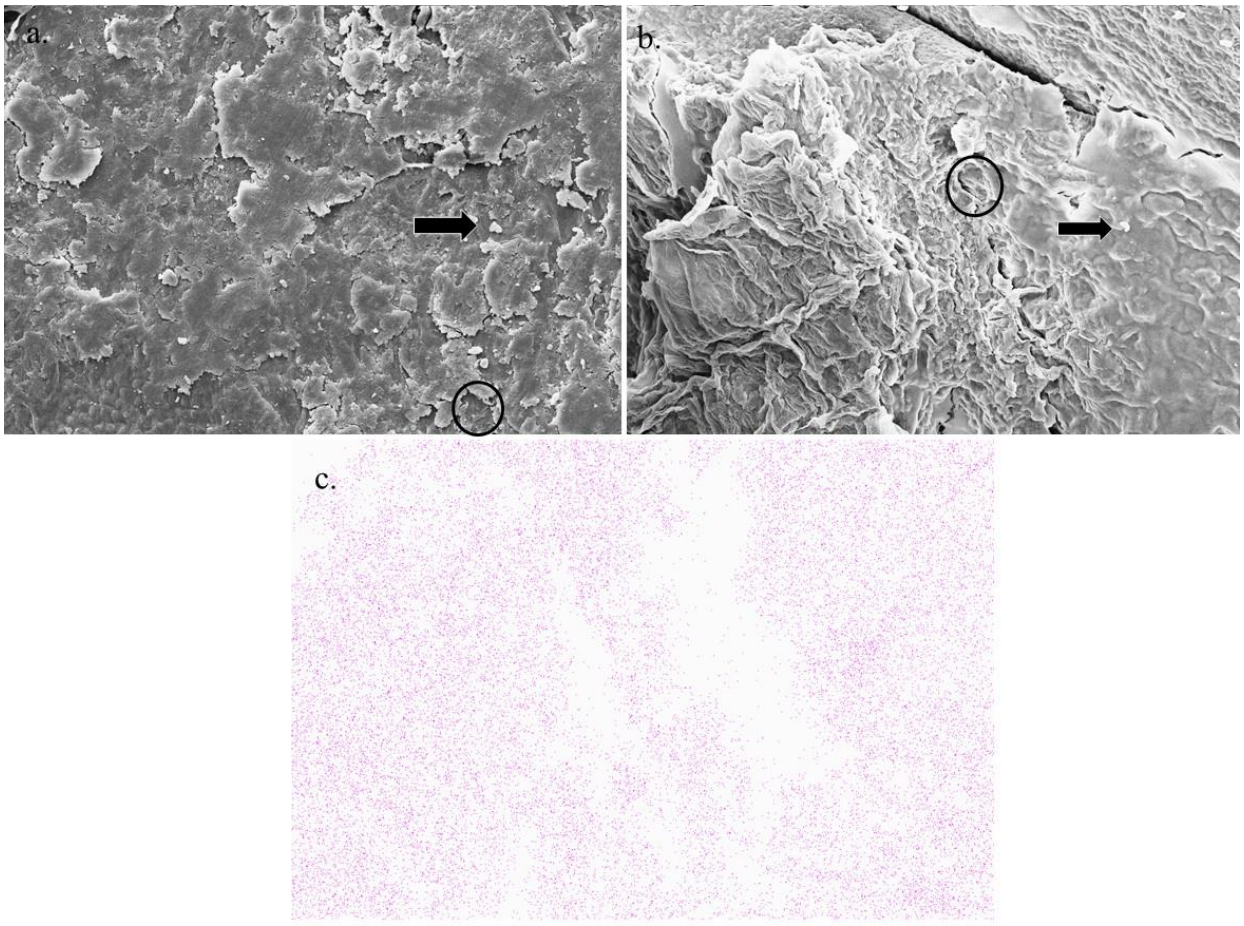

Figure 5.4 SEM images obtained for RES (a) before and (b) after Al^{3+} biosorption; and (c) Al^{3+} ions distribution on the residue surface.

From Figure 5.2 (a and b), it can be noted that the biosorbent before and after biosorption has a very irregular rough surface, with macropores and cracks. Many of these irregularities can be associated with damages caused by the process of alginate extraction,

since it is present in large percentage on the algal cell wall. The presence of whitish spots (pointed by the black arrows) is associated with the phenomenon called "calcium flowers" covering the surface of the biomaterial that are remaining after removal of Al, confirming what can be seen in Table 2, where the percentage of calcium in the residue decreases after biosorption, but does not reach zero.

Furthermore, it is also possible to notice the presence of diatom shells, indicated by black circles in the images, these organisms are commonly found in seaweed and contain elements such as Al, S and, mainly, Si, the latter being responsible for the rigidity of the wall cell [36], thus it may justify the presence of these elements in the residue composition presented in Table 2. In Figure 5.2(c) it is possible to evaluate that the Al^{3+} ions are apparently distributed homogeneously on the surface of the biosorbent, a result similar to that reported in other studies of literature [37,38].

Table 5.14. Estimation of chemical composition of unloaded and Al-loaded RES (%Atomic).

Element	**Biosorbent**	
	RES	**RES-Al**
C	47.94	43.34
O	47.27	53.49
Na	3.25	0.19
S	0.53	0.39
Si	0.35	0.23
Ca	0.34	0.07
Mg	0.23	-
Al	0.15	2.36

Analyzing Table 5.2, it is possible to verify that, in addition to C and O, the element with the greatest presence in the composition of pure waste is sodium (Na^{+}), the notable decrease in its percentage after the Al^{3+} biosorption process indicates the involvement of a mechanism ion exchange in removing the metal of interest. In contrast to this behavior, after biosorption, an increase in the percentage of Al^{3+} is noted, as expected, indicating the possible participation of ion exchange mechanisms in Al^{3+} uptake by RES. Ion exchange is usually identified as the main mechanism for the biosorption of metals in biosorbents derived from brown algae [11].

In addition to that, it is observed that despite the remarkable percentage of S and Si these two elements appear to have little participation in the ion exchange mechanism. The opposite is observed for Mg^{2+} and Ca^{2+}, where after biosorption the presence of these elements was reduced substantially to almost zero. Similar results were obtained by

Freitas et al. [38] and Costa et al. [12] analyzing the biosorption of other toxic metals by this same biomaterial. Other paper works also report the presence of other elements such as Fe, P and K that were not found by EDX analysis in this study. However, Bertagnolli et al. [34] highlight that the composition of the alga is affected by factors such as the season of the year in which it was collected or the stage of its life cycle.

5.3.2 Investigation of ion-exchange mechanism

Considering the results obtained by analyzing the chemical composition of the biosorbent, experiments were carried out to evaluate the ion exchange between Al^{3+} and light metals such as Na^{+}, Mg^{2+}, K^{+} and Ca^{2+}, in the biosorption process using RES. The investigated metals were selected based on previously reports in the literature. Figure 5.3 shows the kinetic profile of ion exchange behavior obtained using a solution with an initial Al^{3+} concentration of 3 mmol/L.

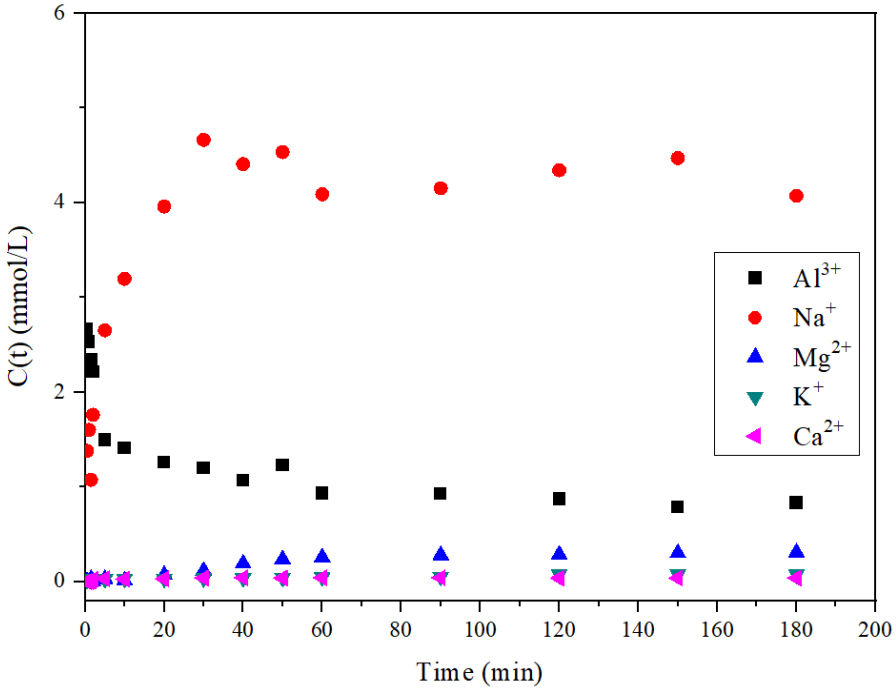

Figure 5.5 Kinetic profile of ion exchange behavior with light metals during Al^{3+} biosorption in RES.

Figure 5.3 makes explicit the exchange behavior between Al^{3+} ions and light metals linked to the functional groups on the biosorbent surface. It can be observed that Na^{+} ions concentration remarkable increase in the medium while Al^{3+} ions decrease rapidly, indicating that Na^{+} ions were exchanged for Al^{3+} in the active sites on biosorbent surface. Hence, Na^{+} stands out as the main exchangeable metal in the system, followed by Mg^{2+} and Ca^{2+}, this pattern is in accordance with that observed in Table 5.2 of the

previous section (5.3.1.2). Although K^+ was not presented in the quantification by EDX, it also seems to have such a small participation in the system's ion exchange mechanism. The major exchange between Na^+ and Al^{3+} ions is also commonly observed in the biosorption of other metals by algae-derived biosorbents [32,38,39].

Also, the hard-soft-acid-base (HSBA) principle helps to clarify the connection between metals, according to this theory metals like Al^{3+}, Na^+, Ca^{2+}, K^+ and Mg^{2+} are classified as hard acids [40]. According to Gadd [40], hard cations exhibit greater electronegativity and low polarization and, therefore, tend to participate in electrostatic bonds with ligands of functional groups. Still following this theory, Al^{3+} would form more stable complexes with hard binders, that is, oxygen containing ligands such as OH^-- and CO_3^{2-}.

5.3.3 Effect of functional groups esterification

Given the confirmation in the preceding section (5.3.1.1) of the broad participation of carboxylic and sulfonate groups in Al^{3+} biosorption using RES and aiming to evaluate the influence of each one in the bonding of the metal in the biosorbent surface, assays were carried out using RES with these groups esterified. Table 5.3 presents the results obtained for the tests using the residue without modifications (RES) at pH 4 and 2; for esterified residue (RES-EST) at pH 4; and for esterified and blocked residue (RES-EST-BLK) at pH 2. As aforementioned, the pH values of the experiments were chosen based on the pKa, pH where the group has more active participation in the removal of metals, of each blocked functional group.

Table 5.15. Al^{3+} removal parameters for the unmodified biosorbent and for the carboxylic and sulfonate blocked biosorbents.

Biosorbent	**pH**	**q_{eq} (mmol Al^{3+}/g_{ads})**	**%R**
RES	4	0.473	92.14
RES	2	0.198	38.54
RES-EST	4	0.325	63.31
RES-EST-BLK	2	0.030	6.02

It is well established in the literature that there is a great influence of pH in the adsorptive capacity and in the percentage of removal in biosorption processes. This is confirmed by observing the results obtained for biosorption at pH 4 and pH 2 using the residue without modifications. It is noted that there was a significant drop in the efficiency of the system when the pH was lowered to 2. This is associated to the fact that at low pH

values the concentration of H^+ ions in the aqueous medium tends to increase, increasing the competition for active sites with Al^{3+} ions and, consequently, decreasing their removal effectiveness.

For the biosorbent with blocked carboxylic groups, it is possible to notice a significant reduction in the percentage of Al^{3+} removal in relation to the percentage obtained in the test performed with RES at pH 4, confirming that this group has an important role in the mechanism of Al^{3+} removal. Yet, this percentage, as well as the removal capacity, remains relatively high. Costa et al. [41] achieved similar results for the removal of Cr^{3+} ions in their study of blocking functional groups of the same biosorbent applied here. These results suggest that the mechanism of removal of trivalent ions can occur, mostly, by coordination with hydroxyl groups instead of ion exchange with carboxylic functions [22].

On the other hand, in the process using the residue with blocked sulfate groups, removal percentages of around 6% were obtained. Given the pH of the test, a low removal value was already expected, but the pronounced reduction in the biosorption efficiency in relation to the test at pH 2 with RES reinforces that sulfonic functions have a great involvement in the removal of Al^{3+} ions using this material, as observed in the results discussed in the previous section (5.3.1.1).

5.3.4 Desorption Experiments

The results of the eluent selection assays are shown in Figure 5.4. It can be noted that acidic eluents showed better performance in desorption of Al^{3+} ions. This result is in agreement with what is normally observed in the literature for the elution of other toxic metals such as Ag and Cu in RES [23,24], as for the biosorption of Al^{3+} using different algae-derived biosorbents, e.g., beach-cast seaweed and *Turbinaria conoides* biomass [4,42]. As expected, the water did not show significant percentages of elution, which indicates that the bonds between the metal and the biosorbent are strong and may be mostly chemical in nature [43].

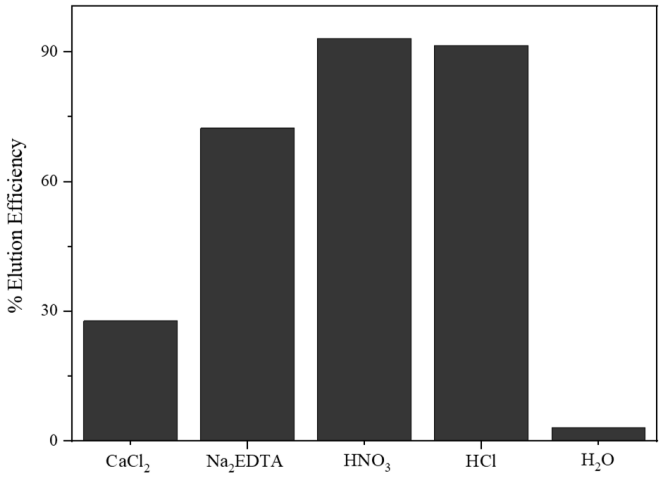

Figure 5.6 Elution efficiencies using different desorbing solutions.

Vijayaraghavan and Yun [44] point out that in order to select the most suitable eluent for the system, several factors, besides its effectiveness, must be evaluated, such as the damages caused to the biosorbent as even as to the ecosystem. Thus, Table 5.4 presents the data of mass loss as well as the risks to human health and to the environment for each eluent tested.

Table 5.16. Mass loss and toxic classification of the eluent solutions assessed in the desorption study.

Eluent	IMAP designation – Human Health	IMAP designation – Environment	Mass loss (%)
$CaCl_2$	HH II	E I	7.10
Na_2EDTA	HH I	E I	26.97
HNO_3	HH II	E I	15.40
HCl	HH III	E I	20.18
H_2O	-	-	8.97

Established by the Australian government, The Inventory Multi-Tiered Assessment and Prioritization (IMAP) is a classification of chemicals products based on its hazardous potential in different levels. Concerning human health risk categories, HH I classification indicates substances that are not considered to present an unreasonable danger to human health and the environment in industrial applications. HH Tier II represents chemicals industrially applied that have potential to cause some harm and need additional examination. While EI classification indicates that the chemical is a reactive substance with rapidly conversion into species of low ecotoxicological concern, therefore poses no unreasonable risk to the environment [45].

Regarding the mass loss, the basic eluent $CaCl_2$ was the one that most preserved the biosorbent, being followed by H_2O. However, at the same time, these two eluents also had the two worst elution percentages of Al^{3+}. Na_2EDTA, on the other hand, presented the highest mass loss of the biosorbent. As previously mentioned, the acid eluents showed elution percentages greater than 90%. Concerning mass loss, the acidic HNO_3 solution seems to be less prejudicial to the biosorbent when compared to results obtained for the HCl solution. In addition, HNO_3 also presents a lower risk to human health and to the environment, according to IMAP. Taking all these factors into account, nitric acid was the eluting agent selected for the regeneration studies of the biosorbent, presented in section 5.3.5.2.

5.3.5 Al^{3+} biosorption in fixed bed column system

5.3.5.1 Effect of flow rate and inlet concentration

Influence of factors such as bed height, flow rate and metal inlet concentration on breakthrough curves have been extensively studied by several researchers. Kumar et al. [46] suggests that, between factors frequently studied for dynamic systems, flow rate and initial concentration are decisive parameters, since it determines, respectively, the duration of the metal-biosorbent contact and the potential driving force for the biosorption process. Figure 5.5 shows the breakthrough curves obtained for the fluid dynamic study (a) and for the analysis of the inlet concentration effect (b) for the Al^{3+} biosorption system using RES in continuous mode.

It can be seen from Figure 5.5a that high flow rates caused a decrease in the breakthrough time. This behavior is related to the fact that higher flow rates results in a faster column saturation [23]. The flow rate 0.5 mL/min is the most suitable for the system, since its breakthrough curve has a shape close to a step function, indicating that in this flow there is less resistance to mass transfer, leading to a smaller mass transfer zone (MTZ), as can be seen in the parameters presented in Table 5.5. Regarding parameters such as adsorptive capacities (q_r and q_s) and removal percentages (%R_r and% R_s), in general, the flow rate of 0.5 mL/min also presented superior results compared to the other studied flows. Hence, this feed flow rate was chosen for the subsequent tests. This result agrees with most articles related to biosorption in dynamic systems found in the literature. Moino et al. [47] performed the removal of Ni^{2+} ions in a continuous system using RES and also obtained the best efficiency of the system at the lowest flow rate (0.5 mL/min).

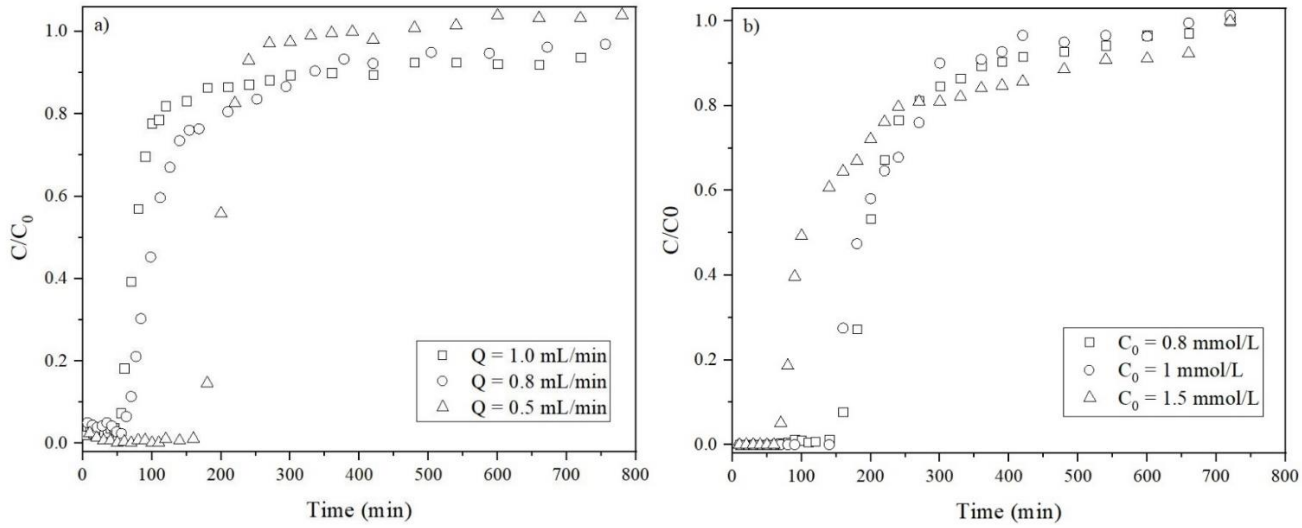

Figure 5.7 Breakthrough curves for a) feed flow rate (C_0 = 1 mmol/L) and b) inlet concentration assessments (Q = 0.5 mL/min) for Al^{3+} biosorption by RES in fixed-bed column.

Table 5.17. Experimental efficiency parameters calculated for the breakthrough curves at different operational conditions.

Feed flow rate (mL/min)	**1.0**	**0.8**	**0.5**	**0.5**	**0.5**
Inlet concentration (mmol/L)	**1.0**	**1.0**	**1.0**	**0.8**	**1.5**
q_r	0.165	0.162	0.302	0.184	0.141
q_s	0.349	0.412	0.372	0.285	0.412
MTZ (cm)	3.68	4.26	1.32	2.48	4.59
$\%R_r$	90.47	88.00	93.46	92.69	85.31
$\%R_s$	33.91	35.88	70.66	54.58	32.04

Concerning the effect of inlet concentration, it can be seen from Figure 5.5b that the breaking point is very close to the concentrations of 1 and 0.8 mmol/L, while a more pronounced difference can be noted for the 1.5 mmol/L curve, where the latter reaches the rupture point more quickly than at the other two concentrations studied. The minor difference between 1 and 0.8 mmol/L breakthrough curves indicates that at lower concentrations the diffusion becomes less influenced by the inlet concentration of the metallic solution. However, in relation to the shape of the curve, it can be noted that 1 mmol/L is closer to a step function than the curves of other concentrations. Assessing the efficiency parameters presented in Table 5.5 for the three concentrations studied, it is noted that the mass transfer zone is significantly lower at the inlet concentration of 1 mmol/L. The MTZ calculated in this condition is smaller than values normally observed

for toxic metal removal systems using this residue, Freitas et al. [23] obtained MTZ of 2.84 cm in optimized conditions for the removal of Cu^{2+} ions, while Nishikawa et al. [37] found a minor influence of the concentration variation on the efficiency parameters for Cd^{2+} uptake, where the obtained MTZ values ranged from 2.56 to 2.33 cm (both studies using the same column configuration). Furthermore, the 1.0 mmol/L concentration also presented better results for the parameters of removal capacity at rupture and for the percentage of removal at rupture and saturation points. Hence, evaluating in general, this concentration reaches the objective of optimization of the dynamic system for the removal of Al^{3+} ions. Thus, the subsequent assessments were performed under the optimized conditions, being: C_0 = 1 mmol/L and Q = 0.5 mL/min.

5.3.5.2 Biosorption/Desorption cycles

After the operational conditions optimization (Q = 0.5 mL/min; C0 = 1.0 mmol/L), four cycles of Al^{3+} biosorption using RES in a continuous system were performed aiming to evaluate the biosorbent regeneration and reuse potential. Between each biosorption cycle, a desorption cycle was performed using a 0.1 mol/L HNO_3 solution, totalizing four desorption cycles. Figure 6 exhibits the breakthrough curves obtained for the biosorption (a) and desorption (b) cycles.

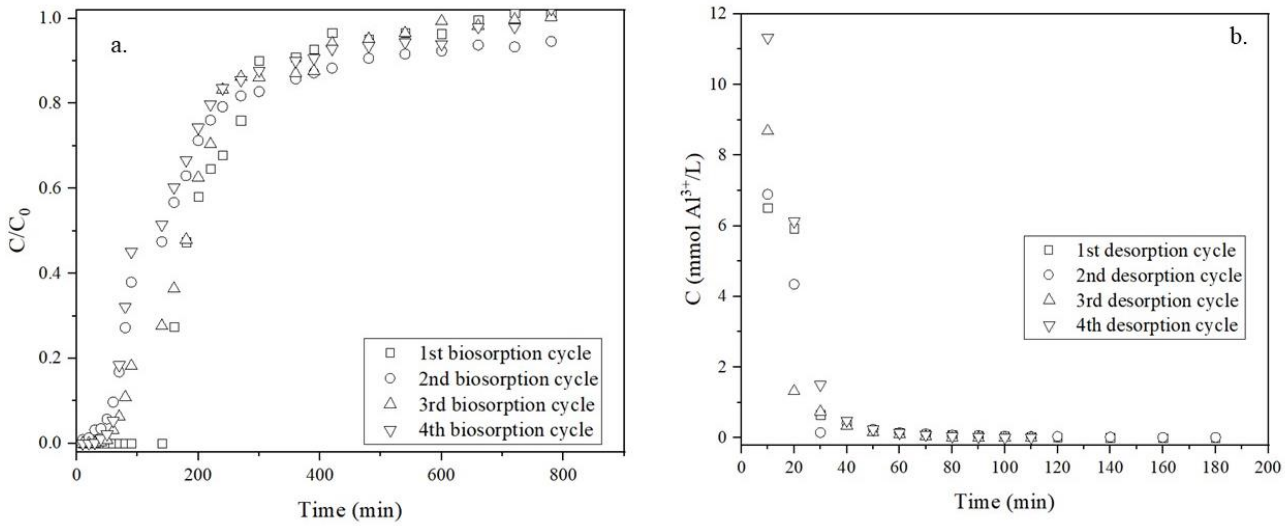

Figure 5.8 Breakthrough curves for four Al^{3+} biosorption (a) and desorption (b) cycles.

Figure 5.6a reveals that the biosorbent has satisfactory regeneration potential, removing Al^{3+} ions up to four cycles satisfactorily. This result is interesting to this biosorbent, since previous studies indicated that in the removal of other toxic metals, the biomass became unviable as of the second cycle of biosorption [15,35]. Although the

rupture time decreased substantially from the first (143 min) to the second cycle (46 min), it remained considerably stable in the other cycles, with 66 and 59 min for the third and fourth, respectively. From Figure 5.6a, it is also observed that the cycles, with the exception of the first, are similar in relation to their profile, however the efficiency parameters must be analyzed to evaluate them individually, as well as the viability of each one. Table 5.6 presents the parameters obtained for the breakthrough curves of the regeneration cycles.

Table 5.18. Efficiency parameters obtained for Al^{3+} biosorption cycles.

Parameters	1st biosorption cycle	2nd biosorption cycle	3rd biosorption cycle	4th biosorption cycle
q_r	0.256	0.069	0.106	0.093
q_s	0.369	0.270	0.280	0.248
MTZ (cm)	2.48	5.22	4.34	4.38
$\%R_r$	92.97	76.63	84.11	82.12
$\%R_s$	49.28	26.15	37.48	27.03

It is possible to note that the second cycle showed an inferior performance among all, this may be linked to the fact that the Al^{3+} ions were not fully eluted in the first desorption cycle. The decrease in the removal capacity was already expected since the use of an acid eluting solution leads to an increase in the binding of H^+ ions in the active sites on the surface of the biosorbent, thus sites are gradually more occupied with each elution, leading to the lower availability for binding with Al^{3+} ions in the next biosorption cycle. This effect was minimized by carrying out between the desorption and biosorption cycles a step of washing the bed with deionized water passing constantly for 1 h, in order to remove the H^+ ions in excess present in the biosorbent [48–50]. However, the tendency is that at some point the effect of protonation of the active sites may be too strong to be reversed, thus collaborating to achieve the exhaustion of the biosorbent material.

The pattern observed for MTZ is also similar to that obtained for removal capabilities. At first, the MTZ value is low and satisfactory, showing viability of the column, but in the second cycle the value of this parameter increases considerably, decreases in the next cycle and increases slightly in the last cycle. This behavior converges to the fact that the first cycle of desorption was not as efficient as the successors. However, at the same time, the increment of this parameter was expected since it has a directly relation to the increase in mass transfer resistance.

As previously mentioned, results obtained in this study are a novelty for the metal removal in fixed bed system using this residue. Several previous studies have evaluated that after the second biosorption cycle the system suffers a significant loss of efficiency, not being viable to continuation. It is possible to associate this superior regeneration potential of the system presented in this research to the evaluated metal, since in general other studies evaluating the removal of Al^{3+} using different biosorbents showed good performance in multiple reuse cycles, for example, Boeris et al. [51] performed the biosorption of Al^{3+} in fixed bed using *Pseudomonas putida* immobilized on agar-agar and reached up to 12 removal cycles keeping the capacity and the percentage of removal almost constant amidst them. In addition to these, other studies evaluated the use of regenerated biosorbents Al^{3+} removal in batch mode obtaining promising results by performing several cycles without major losses in the efficiency of the system [6,9,10]. This may be associated with the properties of the bonds that Al^{3+} forms with the functional groups of the biomaterial. In this case, they may be weaker, perhaps most of a physical nature and thus easier to break, facilitating the regeneration of the biosorbent.

5.3.5.3 Biosorption modeling

Studies on the biosorption of Al^{3+} ions in fixed bed columns are not abundant in the literature, although this is a topic of great interest since this is the configuration that most closely matches the process scale-up, aiming the industrial application. That said, the application of mathematical and phenomenological models helps to predict the breakthrough curves and the systems' maximum capacity. Figure 5.2S (see Supplementary Material) presents the mathematical modeling of curves obtained for the feed flow rate and inlet concentration studies applying Yoon-Nelson, Yan et al., Thomas, Clark and DualSD models. Adjustment parameters are shown in Table 5.7.

In general, all models presented R^2 greater than 0.95 for all breakthrough curves fit, indicating a good adherence to data. However, the model that seems to best describe the system behavior was the phenomenological model DualSD, which presented all R^2 values above 0.99, lower values for the Akaike criterion (AICc) and $q_{e,pred}$ values very close to the q_s experimental values. The best fit of this model indicates that two diffusion rates influence the rupture curves at different times in the biosorption process [29]. Regarding mathematical models, Yan et al. model also showed considerable fitting to the experimental values obtained. This model was developed aiming to reduce errors in the adjustment of the Thomas model, which in fact can be seen in Table 5.7, where the

adsorptive capacity values predicted by Yan are closer to the experimental values. This indicates that the parameters obtained from Yan et al. model could be used for the scale-up of Al^{3+} ions biosorption system using RES. In the literature, it is possible to observe that Yan et al. often tends to fit better to experimental data from biosorption systems using RES for the uptake of toxic metals [15,35,37].

Except for the breakthrough curve in the optimized conditions (Q = 0.5 mL/min and C_0 = 1 mmol/L), in general, no mathematical model was able to predict assertive adsorptive capacity values with the experimental data, this is related to the fact that none of these models appears to predict satisfactorily the curves final data.

Table 5.19. Parameters obtained from the fitting of dynamic models to RES-Al breakthrough curves.

Models	**Parameters**	**Feed flow rate (mL/min)**				
		1	**0.8**	**0.5**	**0.5**	**0.5**
		Initial concentration (mmol/L)				
		1.0	**1.0**	**1.0**	**0.8**	**1.5**
Experimental	**q_s (mmol/L)**	**0.346**	**0.412**	**0.372**	**0.285**	**0.412**
Yoon-Nelson	K_{YN} ($1.min^{-1}$)	0.0667	0.0357	0.0827	0.0360	0.0193
	q_{YN} (mmol/g)	0.2693	0.3000	0.3316	0.2752	0.3682
	τ (min)	80.78	112.50	198.93	206.43	147.26
	R^2	0.9552	0.9590	0.9984	0.9784	0.9057
	AICc	-127.542	-131.672	-207.473	-144.152	-111.285
Yan *et al.*	α_Y	4.5179	3.2344	16.2484	6.3415	2.2146
	q_Y (mmol/g)	0.2125	0.2935	0.3309	0.2743	0.3363
	R^2	0.9658	0.9777	0.9987	0.9854	0.9630
	AICc	-134.897	-148.196	-215.391	-154.886	-136.56
Thomas	K_{TH} ($L.mmol^{-1}.min^{-1}$)	0.0667	0.0357	0.0827	0.0450	0.013
	q_{TH} (mmol/g)	0.2154	0.3000	0.3316	0.2752	0.2303
	R^2	0.9552	0.9589	0.9983	0.9783	0.8322
	AICc	-127.542	-131.672	-207.473	-144.152	-84.080
Clark	A	161208.00	10268.60	2858030	2375950	1180.03
	r (mg^{-1})	0.1236	0.0643	0.0652	0.0617	0.0347
	R^2	0.9423	0.9427	0.9789	0.9679	0.8755
	AICc	-124.75	-126.696	-142.293	-137.562	-107.85
DualSD	D_a	0.11972	0.09956	0.06932	0.06931	0.06931
	α	0.222	0.2584	0.3244	0.2535	0.2394
	$K_{S,1}$	0.05594	0.02572	0.05295	0.03012	0.0190
	$K_{S,2}$	$5.92x10^{-4}$	$3.89x10^{-4}$	$6.26x10^{-4}$	$1.65x10^{-4}$	$5.52x10^{-4}$

$q_{s,pred}$ (mmol/g)	0.4683	0.3574	0.379	0.2882	0.5679
R^2	0.9979	0.9924	0.9993	0.9817	0.9832
AICc	-207.601	-174.601	-227.192	-208.189	-155.22

Nonetheless, due to the good fit of the models, the parameters obtained by them can also be considered for the analysis of the system. Apart from the curve for the highest concentration (1.5 mmol/L), it can be noted that some parameters of the Yoon-Nelson and Thomas model are equal, as well as the values of R^2 and AICc. This is due to the mathematical equivalence between both models, whatever has been commonly reported in other studies [29,52]. Analyzing the τ parameter of the Yoon-Nelson model, which is related to the time to reach 50% of the saturation of the biosorbent, the values decreased in higher flows and concentrations, since a higher flow leads to a greater amount of solution to be treated inducing a faster saturation of the adsorbent material, that also occurs at higher concentrations. In Clark model, parameter A improved with decreasing flow and reduced with increasing initial concentration, although this parameter has no physical significance [53], this behavior indicates that the removal of Al^{3+} ions by RES in fixed bed is favored by lower flows and concentrations.

Figure 5.3S (see Supplementary Material) and Table 5.8 present, respectively, the rupture curves and adjustment parameters obtained for the performed biosorption cycles.

It is possible to verify from Table 5.8 that the adsorption capacity values predicted by all models decreased over the cycles, following the behavior of the experimental data. This result is expected, since the tendency of the biosorbent to lose its effectiveness was already observed in the breakthrough parameters, previously discussed in section 5.3.5.2. It can be also observed that models' constants follow a general tendency to increase from the first to the last cycle. Regarding models' adjustment, results similar to those observed in the evaluation of the flow and initial concentration were obtained, the DualSD model presented better fitting, with R^2 closer to a unity and lower AICc values. In this case, among the mathematical models, Yan et al. also seems to describe the data of the cycle's breakthrough curves, where the adsorption capacities values predicted by the model are closer to those obtained experimentally.

Table 5.20. Parameters obtained from the fitting of dynamic models for breakthrough curves of biosorption cycles.

Models	Parameters	Biosorption cycle			
		1st	2nd	3rd	4th
Experimental	**q_s (mmol/L)**	**0.3691**	**0.2702**	**0.2798**	**0.2483**
Yoon-Nelson	K_{YN} (1.min^{-1})	0.0260	0.0173	0.0344	0.0401
	q_Y (mmol/g)	0.3822	0.2954	0.2478	0.1970
	τ (min)	201.14	155.46	30.44	103.70
	R^2	0.9822	0.9562	0.9750	0.9649
	AICc	-148.359	-134.48	-142.56	-133.47
Yan *et al.*	a_Y	4.8185	2.0676	3.3737	3.0745
	q_Y (mmol/g)	0.3750	0.2621	02490	0.1958
	R^2	0.9896	0.9914	0.9915	0.9816
	AICc	-162.95	-178.73	-171.70	-154.52
Thomas	K_{TH} (L.mmol^{-1}.min^{-1})	0.0288	0.0150	0.0302	0.0352
	q_{TH} (mmol.g^{-1})	0.3822	0.2954	0.2479	0.1970
	R^2	0.9822	0.8610	0.9750	0.9599
	AICc	-148.359	-103.35	-142.56	-133.47
Clark	A	75458	913.90	52655.4	12201.6
	r (mg^{-1})	0.0457	0.0309	0.0691	0.0718
	R^2	0.9708	0.9357	0.9653	0.9447
	AICc	-139.00	-128.19	-137.73	-128.80
DualSD	D_a	0.06931	0.06931	0.06931	0.06931
	α	0.3734	0.2537	0.2447	0.1791
	$K_{S,1}$	0.01612	0.0106	0.0169	0.0236
	$K_{S,2}$	7.50x10^{-5}	2.11x10^{-4}	1.07x10^{-4}	1.67x10^{-4}
	$q_{e,pred}$ (mmol/L)	0.3931	0.3264	0.2706	0.2165
	R^2	0.9942	0.9947	0.9953	0.9931
	AICc	-168.25	-180.69	-176.86	-170.21

5.6 Conclusions

In this work, the ion exchange involved in the Al^{3+} biosorption process using residue derived from the brown alga *S. filipendula* was evaluated. Batch mode tests alongside with SEM/EDX analysis showed that ion exchange mechanisms are involved in the removal of Al^{3+} by RES. Among the light metals' ions analyzed (Na^+, K^+, Mg^{2+} and Ca^{2+}), Na^+ ions have major participation in the exchange of Al^{3+}, whereas Mg^{2+} and

K^+ ions present minor roles. FTIR analysis and blocking assays indicated that carboxylic, amino and sulfonate functional groups play a key role on the Al^{3+} biosorption. HNO_3 solution presented the best result for the recovery of the contaminated residue and caused fewer damages on the biosorbent. In fixed bed system, the most suitable condition was the flow rate of 0.5 mL/min and initial Al^{3+} concentration of 1 mmol/L. Biosorbent regenerating and reusing studies showed that the removal capacity remained satisfactory in the four performed cycles. The modeling indicated that the phenomenological model DualSD best described the breakthrough data. In summary, the residue seems to be a promising alternative biosorbent for the removal of Al^{3+} ions in a dynamic system. Future studies on larger scales aiming at industrial application should be performed, since this biosorbent presents, besides to the good adsorption capacity, several advantages such as low cost, high availability and promising regeneration/reutilization.

Acknowledgments

The authors are grateful for the financial support provided by the Coordination Office for the Improvement of Higher Education Personnel (CAPES), Brazilian Council for Scientific and Technological Development (CNPq) (Grant # 308046/2019-6) and São Paulo Research Foundation (FAPESP) (Grants # 2017/18236-1 and # 2019/11353-8).

APPENDIX 5.A Supplementary Material

Figure 5.1S Schema of experimental set-up for fixed bed assays.

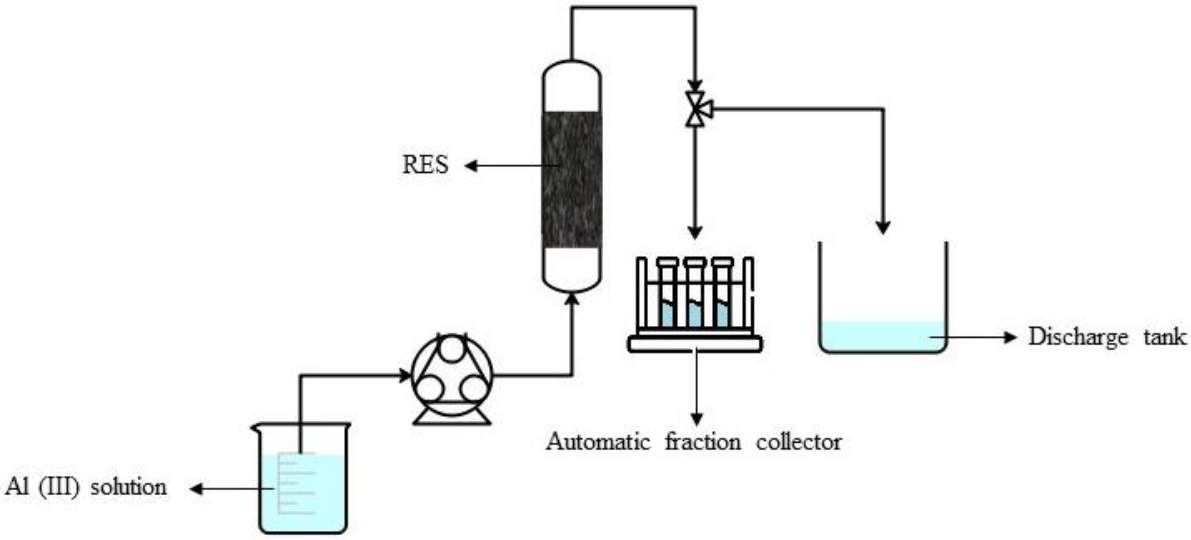

Figure 5.2S Adjustment of Yoon and Nelson, Yan et al., Thomas, Clark and DualSD models to RES-Al breakthrough curves performed at the following feed flow rates and aluminum inlet concentrations: (a) 1.00 mL/min and 1 mmol/L; (b) 0.8 mL/min and 1 mmol/L; (c) 0.5 mL/min and 1 mmol/L; (d) 0.5 mL/min and 0.8 mmol/L; and (e) 0.5 mL/min and 1.5 mmol/L.

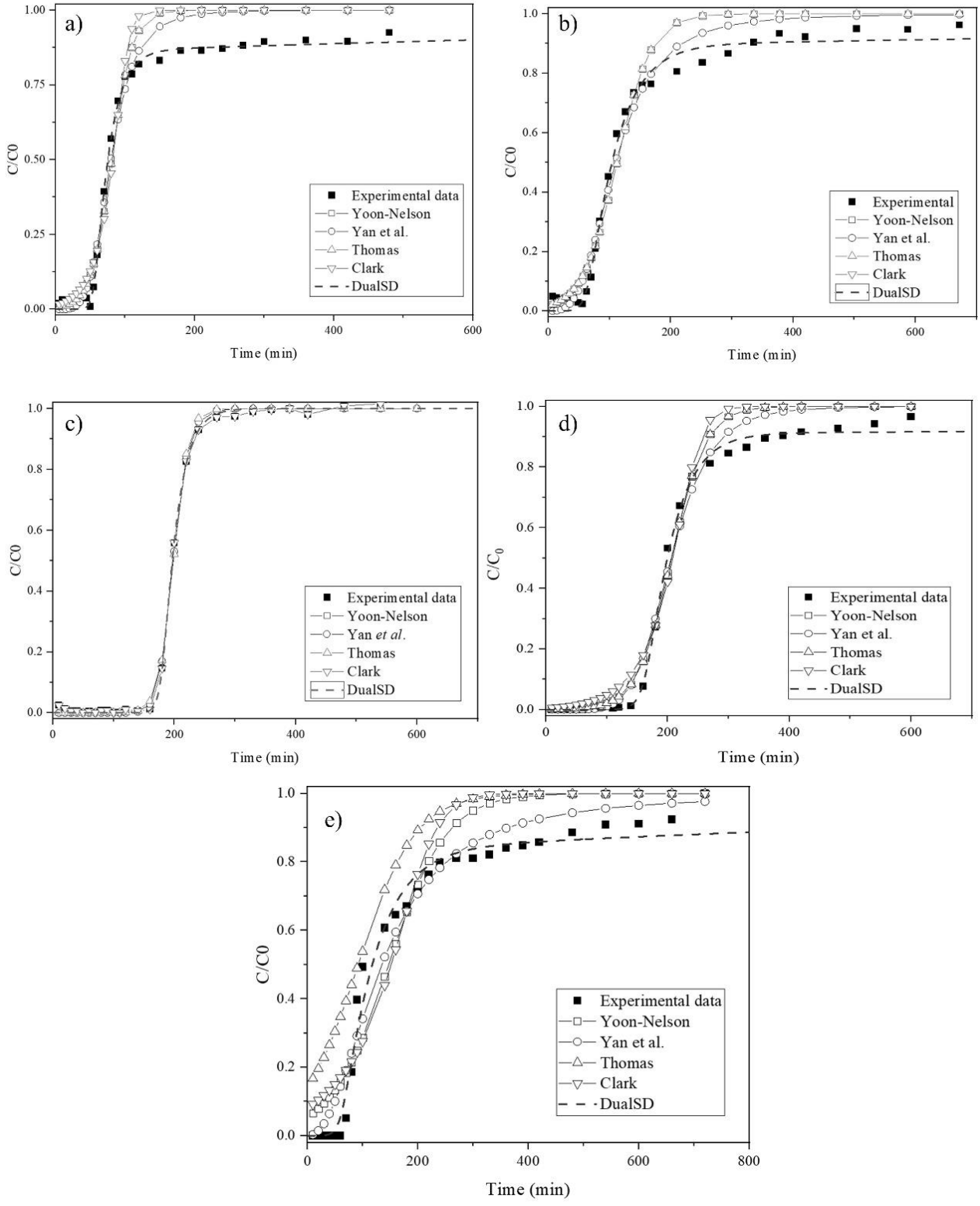

Figure 5.3S Adjustment of Yoon and Nelson, Yan et al., Thomas, Clark and DualSD models to RES-Al breakthrough curves obtained at optimized conditions (Q = 0.5 mL/min; C_0 = 1.0 mmol/L) for: a) First biosorption cycle; b) Second biosorption cycle; c) Third biosorption cycle; and d) Fourth biosorption cycle.

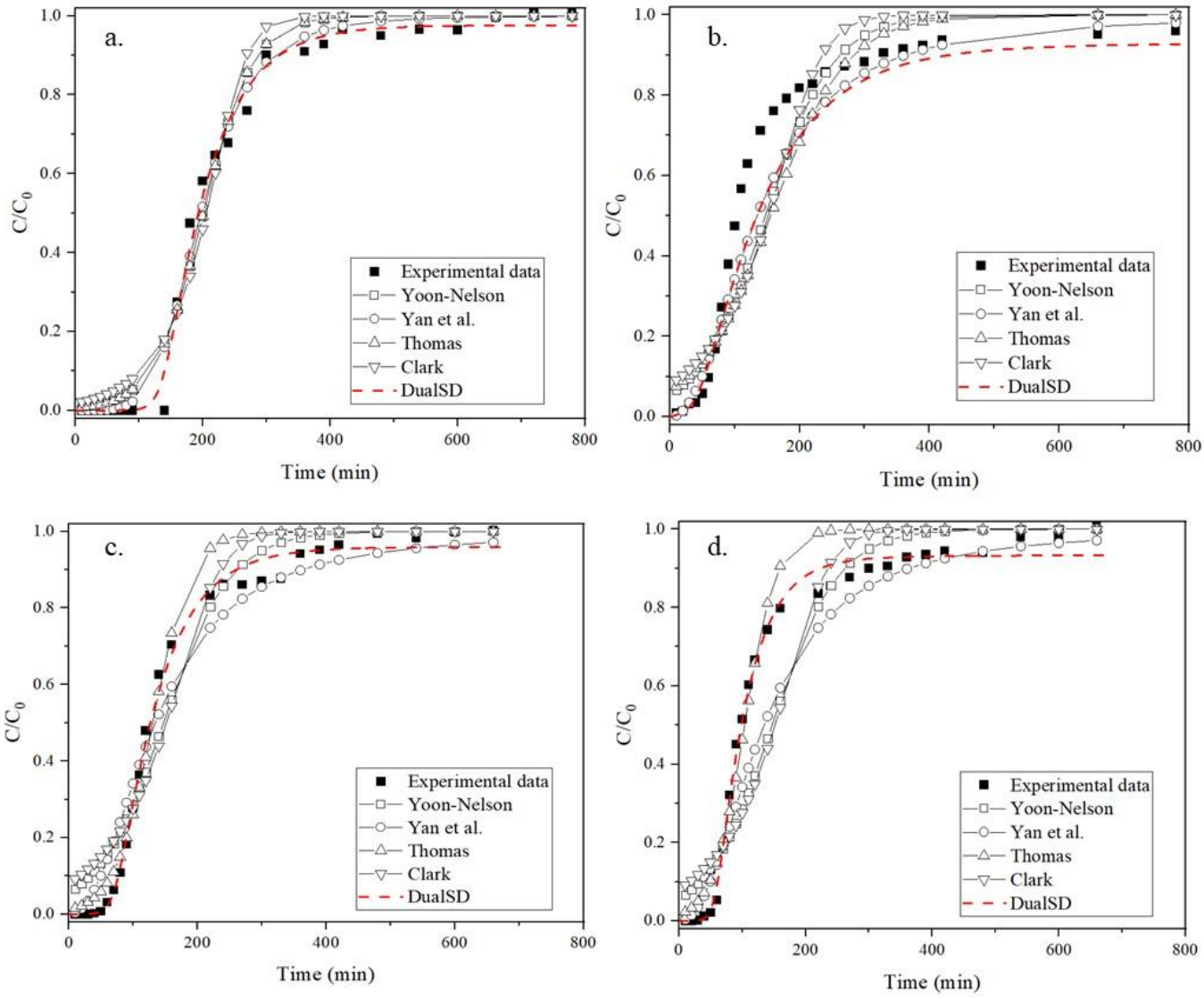

References

[1] A.A. Beni, A. Esmaeili, Biosorption, an efficient method for removing heavy metals from industrial effluents: A Review, Environ. Technol. Innov. 17 (2020) 100503. https://doi.org/10.1016/j.eti.2019.100503.

[2] B. Volesky, Biosorption of heavy metals, 1st ed., CRC Press, Boca Raton, Florida, USA., 1990.

[3] P.S. Boeris, M. del R. Agustín, D.F. Acevedo, G.I. Lucchesi, Biosorption of $^{Al3+}$ through the use of non-viable biomass of Pseudomonas putida, J. Biotechnol. 236 (2016) 57–63. https://doi.org/10.1016/j.jbiotec.2016.07.026.

[4] K. Vijayaraghavan, S. Gupta, U.M. Joshi, Comparative assessment of Al(III) and Cd(II) biosorption onto turbinaria conoides in single and binary systems, Water. Air. Soil Pollut. 223 (2012) 2923–2931. https://doi.org/10.1007/s11270-012-1075-y.

[5] A.A. Kumari, K. Ravindhranath, New Bio-Sorbents in the Removal of Aluminium (III) from Polluted Waters, J. Chem. Pharm. Sci. 10 (2017) 398–409.

[6] N. Naeemullah, M. Tuzen, A. Sari, D. Mendil, Biosorption of $^{Al3+}$ from aqueous solutions by using macrofungus (Cortinarius armillatus): Equilibrium, Kinetic, and Thermodynamic Studies and Determination by GFAAS, At. Spectrosc. 38 (2017) 149–157. https://doi.org/10.46770/as.2017.05.005.

[7] K. Boriová, S. Čerňanský, P. Matúš, M. Bujdoš, A. Šimonovičová, M. Urík, Removal of aluminium from aqueous solution by four wild-type strains of Aspergillus niger, Bioprocess Biosyst. Eng. 42 (2019) 291–296. https://doi.org/10.1007/s00449-018-2033-x.

[8] M. Yurtsever, M. Nalçak, Al(III) removal from wastewater by natural clay and coconut shell, Glob. Nest J. 21 (2019) 477–483. https://doi.org/10.30955/gnj.002566.

[9] A.E.S.M. Shaaban, R.K. Badawy, H.A. Mansour, M.E. Abdel-Rahman, Y.I.E. Aboulsoud, Competitive algal biosorption of Al3+, Fe3+, and Zn2+ and treatment application of some industrial effluents from Borg El-Arab region, Egypt, J. Appl. Phycol. 29 (2017) 3221–3234. https://doi.org/10.1007/s10811-017-1185-4.

[10] A. Sari, M. Tuzen, Equilibrium, thermodynamic and kinetic studies on $^{Al3+}$ biosorption from aqueous solution by brown algae (Padina pavonica) biomass, J. Hazard. Mater. 171 (2009) 973–979.

https://doi.org/10.1016/j.jhazmat.2009.06.101.

[11] T.A. Davis, B. Volesky, A. Mucci, A review of the biochemistry of heavy metal biosorption by brown algae, Water Res. 37 (2003) 4311–4330. https://doi.org/10.1016/S0043-1354(03)00293-8.

[12] C.S.D. Costa, S.L. Cardoso, E. Nishikawa, M.G.A. Vieira, M.G.C. Da Silva, Characterization of the residue from double alginate extraction from sargassum filipendula seaweed, Chem. Eng. Trans. 52 (2016) 133–138. https://doi.org/10.3303/CET1652023.

[13] S.L. Cardoso, C.S.D. Costa, E. Nishikawa, M.G.C. da Silva, M.G.A. Vieira, Biosorption of toxic metals using the alginate extraction residue from the brown algae Sargassum filipendula as a natural ion-exchanger, J. Clean. Prod. 165 (2017) 491–499. https://doi.org/10.1016/j.jclepro.2017.07.114.

[14] E. Nishikawa, M.G.C. da Silva, M.G.A. Vieira, Cadmium biosorption by alginate extraction waste and process overview in Life Cycle Assessment context, J. Clean. Prod. 178 (2018) 166–175. https://doi.org/10.1016/j.jclepro.2018.01.025.

[15] B.P. Moino, C.S.D. Costa, M.G.C. da Silva, M.G.A. Vieira, Removal of nickel ions on residue of alginate extraction from Sargassum f ilipendula seaweed in packed bed, Can. J. Chem. Eng. 95 (2017) 2120–2128. https://doi.org/10.1002/cjce.22859.

[16] H.P. de S. Costa, M.G.C. da Silva, M.G.A. Vieira, Biosorption of $^{Al3+}$ ions from aqueous solutions using non-conventional low-cost materials: A review, J. Water Process Eng. 40 (2021) 101925. https://doi.org/10.1016/j.jwpe.2021.101925.

[17] C.S.D. Costa, C. Bertagnolli, A. Boos, M.G.C. da Silva, M.G.A. Vieira, Application of a dealginated seaweed derivative for the simultaneous metal ions removal from real and synthetic effluents, J. Water Process Eng. 37 (2020) 101546. https://doi.org/10.1016/j.jwpe.2020.101546.

[18] D.J. McHugh, Production, properties and uses of alginates, in: FAO Fish. Tech. Pap. - T288, Rome, 1987: pp. 58–115.

[19] S. Schiewer, B. Volesky, Modeling Multi-Metal Ion Exchange in Biosorption, Environ. Sci. Technol. 30 (1996) 2921–2927. https://doi.org/10.1021/es950800n.

[20] J.L. Gardea-Torresdey, M.K. Becker-Hapak, J.M. Hosea, D.W. Darnall, Effect of chemical modification of algal carboxyl groups on metal ion binding, Environ. Sci. Technol. 24 (1990) 1372–1378. https://doi.org/10.1021/es00079a011.

[21] E. Fourest, B. Volesky, Contribution of Sulfonate Groups and Alginate to Heavy

Metal Biosorption by the Dry Biomass of Sargassum fluitans, Environ. Sci. Technol. 30 (1996) 277–282. https://doi.org/10.1021/es950315s.

[22] P.X. Sheng, Y.-P. Ting, J.P. Chen, L. Hong, Sorption of lead, copper, cadmium, zinc, and nickel by marine algal biomass: characterization of biosorptive capacity and investigation of mechanisms, J. Colloid Interface Sci. 275 (2004) 131–141. https://doi.org/10.1016/j.jcis.2004.01.036.

[23] G.R. Freitas, M.G.A. Vieira, M.G.C. Da Silva, Batch and Fixed Bed Biosorption of Copper by Acidified Algae Waste Biomass, Ind. Eng. Chem. Res. 57 (2018) 11767–11777. https://doi.org/10.1021/acs.iecr.8b02541.

[24] W.J. Do Nascimento, R. Landers, M. Gurgel Carlos da Silva, M.G.A. Vieira, Equilibrium and desorption studies of the competitive binary biosorption of silver(I) and copper(II) ions on brown algae waste, J. Environ. Chem. Eng. 9 (2021) 104840. https://doi.org/10.1016/j.jece.2020.104840.

[25] Y.H. Yoon, J.H. Nelson, Application of Gas Adsorption Kinetics I. A Theoretical Model for Respirator Cartridge Service Life, Am. Ind. Hyg. Assoc. J. 45 (1984) 509–516. https://doi.org/10.1080/15298668491400197.

[26] H.C. Thomas, Heterogeneous Ion Exchange in a Flowing System, J. Am. Chem. Soc. 66 (1944) 1664–1666. https://doi.org/10.1021/ja01238a017.

[27] R.M. Clark, Evaluating the cost and performance of field-scale granular activated carbon systems, Environ. Sci. Technol. 21 (1987) 573–580. https://doi.org/10.1021/es00160a008.

[28] G. Yan, T. Viraraghavan, M. Chen, A New Model for Heavy Metal Removal in a Biosorption Column, Adsorpt. Sci. Technol. 19 (2001) 25–43. https://doi.org/10.1260/0263617011493953.

[29] J.R. de Andrade, M.F. Oliveira, R.L.S. Canevesi, R. Landers, M.G.C. da Silva, M.G.A. Vieira, Comparative adsorption of diclofenac sodium and losartan potassium in organophilic clay-packed fixed-bed: X-ray photoelectron spectroscopy characterization, experimental tests and theoretical study on DFT-based chemical descriptors, J. Mol. Liq. 312 (2020) 113427. https://doi.org/10.1016/j.molliq.2020.113427.

[30] H. Patel, Fixed-bed column adsorption study: a comprehensive review, Appl. Water Sci. 9 (2019) 45. https://doi.org/10.1007/s13201-019-0927-7.

[31] V. Murphy, H. Hughes, P. McLoughlin, Cu(II) binding by dried biomass of red, green and brown macroalgae, Water Res. 41 (2007) 731–740.

https://doi.org/10.1016/j.watres.2006.11.032.

[32] A. Bhatnagar, V.J.P. Vilar, C. Ferreira, C.M.S. Botelho, R.A.R. Boaventura, Optimization of nickel biosorption by chemically modified brown macroalgae (Pelvetia canaliculata), Chem. Eng. J. 193–194 (2012) 256–266. https://doi.org/10.1016/j.cej.2012.04.037.

[33] W.J. do Nascimento Júnior, M.G.C. da Silva, M.G.A. Vieira, Competitive biosorption of Cu2+ and Ag+ ions on brown macro-algae waste: kinetic and ion-exchange studies, Environ. Sci. Pollut. Res. 26 (2019) 23416–23428. https://doi.org/10.1007/s11356-019-05471-w.

[34] C. Bertagnolli, A.P.D.M. Espindola, S.J. Kleinübing, L. Tasic, M.G.C. da Silva, Sargassum filipendula alginate from Brazil: Seasonal influence and characteristics, Carbohydr. Polym. 111 (2014) 619–623. https://doi.org/10.1016/j.carbpol.2014.05.024.

[35] S.L. Cardoso, C.S.D. Costa, M.G.C. da Silva, M.G.A. Vieira, Dealginated seaweed waste for Zn(II) continuous removal from aqueous solution on fixed-bed column, J. Chem. Technol. Biotechnol. 93 (2018) 1183–1189. https://doi.org/10.1002/jctb.5479.

[36] B. Tesson, M.J. Genet, V. Fernandez, S. Degand, P.G. Rouxhet, V. Martin-Jézéquel, Surface Chemical Composition of Diatoms, ChemBioChem. 10 (2009) 2011–2024. https://doi.org/10.1002/cbic.200800811.

[37] E. Nishikawa, S.L. Cardoso, C.S.D. Costa, M.G.C. da Silva, M.G.A. Vieira, New perception of the continuous biosorption of cadmium on a seaweed derivative waste, J. Water Process Eng. 36 (2020) 101322. https://doi.org/10.1016/j.jwpe.2020.101322.

[38] G. Rocha Freitas, M.G. Adeodato Vieira, M.G. Carlos da Silva, Characterization and biosorption of silver by biomass waste from the alginate industry, J. Clean. Prod. 271 (2020) 122588. https://doi.org/10.1016/j.jclepro.2020.122588.

[39] S.L. Cardoso, C.S.D. Costa, E. Nishikawa, M.G.C. da Silva, M.G.A. Vieira, Biosorption of toxic metals using the alginate extraction residue from the brown algae Sargassum filipendula as a natural ion-exchanger, J. Clean. Prod. 165 (2017) 491–499. https://doi.org/10.1016/j.jclepro.2017.07.114.

[40] G.M. Gadd, Metals and microorganisms: A problem of definition, FEMS Microbiol. Lett. 100 (1992) 197–203. https://doi.org/10.1016/0378-1097(92)90209-7.

[41] C.S.D. Costa, M.G.C. da Silva, M.G.A. Vieira, Investigation of the simultaneous biosorption of toxic metals through a mixture design application, J. Clean. Prod. 200 (2018) 890–899. https://doi.org/10.1016/j.jclepro.2018.07.314.

[42] P. Lodeiro, Á. Gudiña, L. Herrero, R. Herrero, M.E. Sastre de Vicente, Aluminium removal from wastewater by refused beach cast seaweed. Equilibrium and dynamic studies, J. Hazard. Mater. 178 (2010) 861–866. https://doi.org/10.1016/j.jhazmat.2010.02.017.

[43] L. Fang, C. Zhou, P. Cai, W. Chen, X. Rong, K. Dai, W. Liang, J.-D. Gu, Q. Huang, Binding characteristics of copper and cadmium by cyanobacterium Spirulina platensis, J. Hazard. Mater. 190 (2011) 810–815. https://doi.org/10.1016/j.jhazmat.2011.03.122.

[44] K. Vijayaraghavan, Y.S. Yun, Bacterial biosorbents and biosorption, Biotechnol. Adv. 26 (2008) 266–291. https://doi.org/10.1016/j.biotechadv.2008.02.002.

[45] Australian Government (Deptartment of Health), Australian Industrial Chemicals Introduction Scheme, (n.d.). industrialchemicals.gov.au/chemical-information.

[46] D. Kumar, L.K. Pandey, J.P. Gaur, Metal sorption by algal biomass: From batch to continuous system, Algal Res. 18 (2016) 95–109. https://doi.org/10.1016/j.algal.2016.05.026.

[47] B.P. Moino, C.S.D. Costa, M.G.C. da Silva, M.G.A. Vieira, Removal of nickel ions on residue of alginate extraction from Sargassum filipendula seaweed in packed bed, Can. J. Chem. Eng. 95 (2017) 2120–2128. https://doi.org/10.1002/cjce.22859.

[48] Y.-F. Zhou, R.J. Haynes, A Comparison of Inorganic Solid Wastes as Adsorbents of Heavy Metal Cations in Aqueous Solution and Their Capacity for Desorption and Regeneration, Water, Air, Soil Pollut. 218 (2011) 457–470. https://doi.org/10.1007/s11270-010-0659-7.

[49] M. Jain, V.K. Garg, K. Kadirvelu, Cadmium(II) sorption and desorption in a fixed bed column using sunflower waste carbon calcium–alginate beads, Bioresour. Technol. 129 (2013) 242–248. https://doi.org/10.1016/j.biortech.2012.11.036.

[50] G. Yan, T. Viraraghavan, Heavy metal removal in a biosorption column by immobilized M. rouxii biomass, Bioresour. Technol. 78 (2001) 243–249. https://doi.org/10.1016/S0960-8524(01)00020-7.

[51] P.S. Boeris, A.S. Liffourrena, G.I. Lucchesi, $^{Al3+}$ biosorption using non-viable biomass of Pseudomonas putida immobilized in agar–agar: Performance in batch

and in fixed-bed column, Environ. Technol. Innov. 11 (2018) 105–115. https://doi.org/10.1016/j.eti.2018.05.003.

[52] N.T. das G. Santos, L.F. Moraes, M.G.C. da Silva, M.G.A. Vieira, Recovery of gold through adsorption onto sericin and alginate particles chemically crosslinked by proanthocyanidins, J. Clean. Prod. 253 (2020) 119925. https://doi.org/10.1016/j.jclepro.2019.119925.

[53] W. Zhang, L. Dong, H. Yan, H. Li, Z. Jiang, X. Kan, H. Yang, A. Li, R. Cheng, Removal of methylene blue from aqueous solutions by straw based adsorbent in a fixed-bed column, Chem. Eng. J. 173 (2011) 429–436. https://doi.org/10.1016/j.cej.2011.08.001.

5. Discussão geral

Na presente dissertação foi investigada a bioadsorção de alumínio em meio aquoso utilizando como material adsorvente alternativo o resíduo originado da extração de alginato da alga marrom *Sargassum filipendula.* Neste capítulo tem-se por objetivo relacionar, sumarizar e discutir de forma síncrona os resultados obtidos apresentados nos capítulos anteriores.

Em primeiro momento, no Capítulo 2 abordou-se a problemática em que se insere a poluição ambiental causada pela contaminação de corpos hídricos, em especial por alumínio. Neste capítulo mostrou-se a grande efetividade e diversas vantagens em processos de bioadsorção aplicando bioadsorventes alternativos de baixo custo para o tratamento de efluentes contaminados por este metal, reforçando, assim, a viabilidade do sistema estudado nesta pesquisa. No que se refere ao processo adsortivo, a influência das condições operacionais nos resultados de remoção foi reportada, enfatizando, com isso, a importância da execução do planejamento experimental apresentado no Capítulo 3, onde os efeitos das principais variáveis envolvidas no processo foram avaliados. A dosagem do bioadsorvente demonstrou ter grande influência nos resultados do sistema, bem como a concentração inicial da solução metálica. Esta última, no entanto, não influenciou de forma significativa a cinética e o tempo de equilíbrio do processo, conforme demonstrado no Capítulo 4. A agitação do sistema também não mostrou impacto na eficiência da bioadsorção para a faixa estudada. Assim, o Capítulo 3 auxiliou na definição das condições operacionais dos experimentos realizados nas fases subsequentes da pesquisa, apresentadas nos Capítulos 4 e 5. Nestes dois capítulos buscou-se avaliar a viabilidade do sistema em diferentes configurações (Banho Finito e Leito Fixo), além de investigar os mecanismos de remoção envolvidos na bioadsorção de Al (III) por RES, de forma que ambos os estudos, complementando-se entre si, buscam elucidar o processo e almejar a aplicação deste sistema em maior escala.

O resíduo estudado no presente trabalho é derivado da alga marrom brasileira *Sargassum filipendula* e o seu potencial adsortivo para a remoção de metais tóxicos e poluentes emergentes vem sendo amplamente explorado e consolidado em diversos estudos conduzidos pelo grupo de pesquisa LEA/LEPA na FEQ/Unicamp. Entretanto, a viabilidade do sistema para a remoção de Alumínio ainda não havia sido amplamente explorada. A afinidade deste metal com o bioadsorvente estudado foi descoberta por Costa [20], egressa do mesmo grupo de pesquisa. Este resíduo se insere na categoria de

bioadsorvente derivados de algas marinhas, conforme estabelecido no Capítulo 2. Estes bioadsorventes, especialmente os derivados de algas marrons, são de fato conhecidos por possuírem alta afinidade com metais tóxicos e se destacam na remoção de alumínio quando comparados aos bioadsorventes de outros grupos, i.e., microrganismos e resíduos agroindustriais.

Uma vez estabelecida a afinidade significativa entre o metal e o adsorvente, e definidas no Capítulo 3 as condições de concentração inicial, dosagem da biomassa e agitação do sistema, os estudos em Banho finito apresentados no Capítulo 4 auxiliaram na investigação aprofundada das condições operacionais bem como dos possíveis mecanismos de remoção envolvidos no processo. Conforme observado na seção 4.3.1 deste capítulo, o pH é uma variável que influencia o processo de maneira majoritária, não sendo recomendada a utilização de valores acima de 5,5, de forma a evitar a precipitação dos íons Al^{3+}. É importante destacar que o estudo do pH foi realizada antes da etapa de planejamento experimental, pois para a realização deste último era fundamental que se definisse o pH dos experimentos. Dentre a faixa de valores analisada, melhores resultados de remoção foram obtidos em sistema com pH 4, conforme observado nos resultados apresentados na Figura 4.1 do Capítulo 4. Assim, esta foi a condição selecionada para a realização dos experimentos subsequentes. É possível observar no Capítulo 2 que, em sua maioria, os estudos que apresentam a bioadsorção de alumínio por materiais alternativos também operam em pH semelhante ao definido nesta pesquisa. Uma vez definida estas condições, os estudos cinéticos conduzidos, com resultados apresentados na seção 4.2.3, indicam que a etapa controladora do sistema é de natureza química devido ao melhor ajuste ao modelo matemático de pseudossegunda ordem. Este comportamento é condizente com a maior parte dos trabalhos apresentados na seção 2.4.3 do Capítulo 2. Além disso, ainda na modelagem cinética foi possível avaliar que a bioadsorção de alumínio utilizando este resíduo ocorre predominantemente por transferência de massa em filme externo.

Em relação ao estudo termodinâmico do sistema, verificou-se que o processo é de natureza exotérmica, sendo favorecido com a diminuição da temperatura. Conforme destacado, esse comportamento não é comumente observado em sistemas de bioadsorção de alumínio ou mesmo na bioadsorção de outros metais tóxicos utilizando este mesmo material bioadsorvente. Além disso, o ajuste dos modelos matemáticos de equilíbrio às isotermas obtidas em diversas temperaturas mostrou que a superfície do adsorvente é

composta por sítios ativos energeticamente heterogêneos, o que foi corroborando por análises de caracterização da superfície do bioadsorvente. O estudo de equilíbrio apontou ainda a participação de mecanismos de natureza física na remoção de alumínio pelo RES. Por outro lado, na seção 5.3.2 do Capítulo 5 foi possível verificar que o mecanismo de troca iônica também está envolvido neste processo de bioadsorção. Estes resultados indicam que nesse sistema há grande envolvimento de ligações tanto de quimissorção quanto de fisissorção, sendo que a troca iônica ocorre majoritariamente com íons Na^{+}, conforme confirmado pela análise de EDX. Entretanto, interações eletrostáticas não parecem ter grande envolvimento neste sistema, levando em conta que a superfície do bioadsorvente está carregada positivamente no pH de estudo, o que desfavoreceria a bioadsorção de cátions por este mecanismo. Os mecanismos envolvidos no processo estão esquematicamente representados na Figura 6.1.

Figura 6.1 Mecanismos de remoção envolvidos no processo da bioadsorção de íons Al^{3+} por RES.

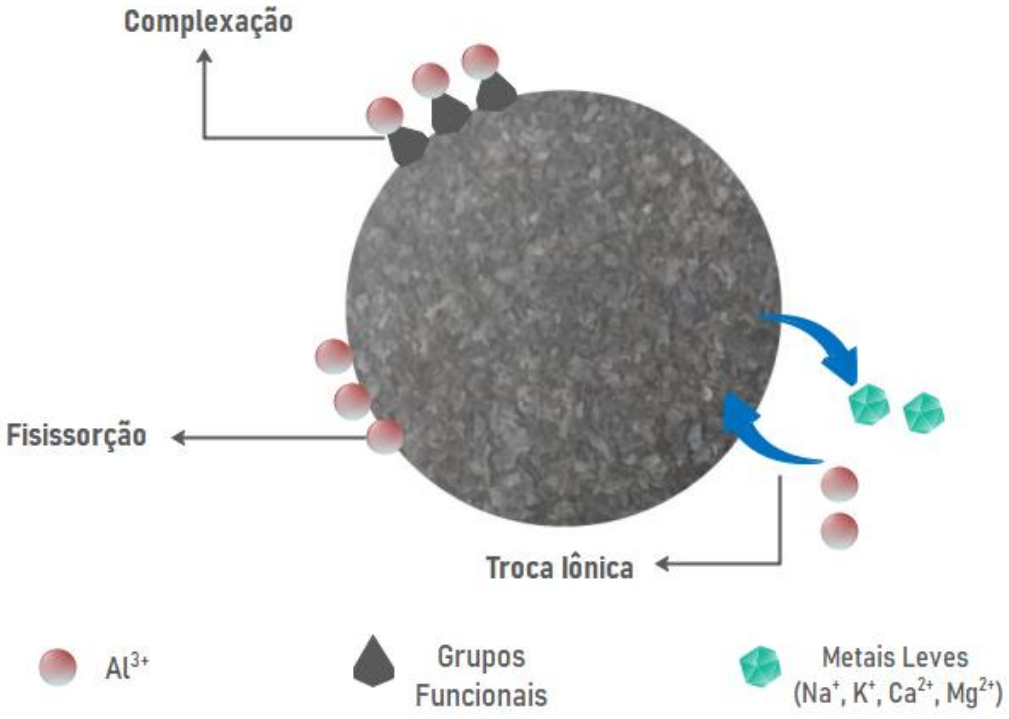

Fonte: Adaptado de Costa et al., 2021

Em relação à estrutura do biomaterial, as caracterizações de picnometria, porosimetria e BET revelaram a estrutura macroporosa do bioadsorvente, sendo este resultado confirmado posteriormente pelas micrografias obtidas pela análise de MEV, apresentadas no Capítulo 5 (seção 5.3.1.2). Além disso, esta análise de caracterização

associada ao EDX também confirmou a natureza irregular e complexa do adsorvente. A análise de FTIR explicitou a participação de grupos funcionais carboxílicos, sulfatos e aminos na bioadsorção de alumínio pelo RES. Estes grupos são frequentemente associados ao mecanismo de remoção de metais, conforme apontado no Capítulo 2. Os experimentos de esterificação dos grupos carboxílicos e sulfatos apresentados na seção 5.3.3 ratificaram este resultado.

A regeneração do bioadsorvente reportada na seção 5.3.4 do Capítulo 5 mostra que a eluição utilizando soluções ácidas é mais eficiente para a quebra das ligações adsorbato-adsorvente neste sistema. O HNO_3 foi escolhido avaliando-se uma série de fatores como a perda de massa e o seu impacto ambiental. Neste cenário, esse reagente se mostrou eficaz tanto nos ensaios em banho finito quanto nos ensaios em sistema contínuo apresentados na seção 5.3.5.2 deste mesmo capítulo, sendo que neste último o bioadsorvente manteve sua capacidade adsortiva durante os 4 ciclos de bioadsorção/dessorção realizados. Esse potencial de regenerabilidade demonstra a viabilidade do biomaterial para a execução de ciclos contínuos de adsorção.

A bioadsorção de Al (III) por RES em sistema dinâmico foi realizada em leito fixo visando à avaliação do efeito da vazão e da concentração de alimentação em parâmetros de transferência de massa e de eficiência da coluna, resultados apresentados na seção 5.3.5.1. Neste estudo foi possível constatar que o sistema contínuo é favorecido por baixas vazões e que concentrações inferiores a 1 mmol/L não apresentaram mudanças expressivas nos perfis das curvas de ruptura obtidas. Este resultado novamente mostra que a concentração da solução de alumínio, na faixa de estudo, não impactou sobremaneira este processo. A ocorrência de duas diferentes taxas de difusão atuando em momentos distintos do processo em modo contínuo é confirmada pela elevada correlação obtida entre os dados experimentais e o modelo fenomenológico DualSD.

Comparando os resultados de capacidade de remoção no ponto de exaustão obtida nas condições otimizadas do sistema de leito fixo (q_S = 0,412 mmol/g) e em banho finito ($q_{máx}$ = 1,431 mmol/g,), pode-se verificar que este último apresenta melhor resultado. A discrepância entre estes dois valores de capacidade adsortiva pode ser justificada por duas hipóteses. A primeira é de que o tempo de residência da solução metálica no interior da coluna não tenha sido suficiente para que a transferência de massa ocorresse de forma efetiva da fase fluida para o adsorvente. A segunda hipótese é de que ocorrência de caminhos preferenciais de escoamento no interior da coluna de leito fixo, o que também

acarreta a diminuição significativa da remoção de adsorbato pela matriz do biomaterial. Entretanto, a capacidade de regeneração de forma prática desse sistema e uso em múltiplos ciclos é uma vantagem desejada quando visada à aplicação industrial do processo. Em adição a isso, a elevada porcentagem de remoção (~93%) até o ponto de ruptura observada no estudo do sistema dinâmico consolida este bioadsorvente como um material viável para o tratamento de soluções com baixas concentrações de alumínio próximas ao encontrado em efluentes reais contaminados por este metal, conforme mostrado na seção 2.5.7. No projeto simplificado em batelada apresentado, remoções em torno de 90% podem ser alcançadas no tratamento de 10 litros de solução metálica utilizando uma baixa dosagem de bioadsorvente (14 g).

Em suma, pode-se avaliar que o sistema bioadsortivo estudado se mostrou viável, com o resíduo da alga marrom apresentando um alto potencial como material adsorvente para a remoção de alumínio em meio aquoso tanto em sistema de batelada quanto em sistema dinâmico.

6. Conclusões e perspectivas futuras

Os resultados apresentados nesta pesquisa confirmaram a viabilidade do sistema de bioadsorção de íons alumínio em solução pelo uso do resíduo derivado da extração de alginato de algas marrons. O material apresentou elevados percentuais de remoção do metal em diversas configurações e, de modo geral, os mecanismos envolvidos neste processo puderam ser elucidados. Entre os resultados dos experimentos em banho finito destaca-se a capacidade máxima de adsorção obtida (1,431 mmol/g), que é superior ao observado em trabalhos realizados anteriormente na remoção de outros metais tóxicos utilizando o mesmo bioadsorvente, e ainda é próxima aos valores obtidos para a bioadsorção de alumínio utilizando outros biomateriais com maior valor comercial agregado. Por outro lado, entre os resultados do modo contínuo a dessorção de alumínio presentes no resíduo pela solução ácida de HNO_3 a 0,1 mol/L revelou a satisfatória regenerabilidade da biomassa contaminada.

Pode-se avaliar que o sistema de bioadsorção de alumínio por RES é um processo que tem como etapa limitante a transferência de massa em filme externo, ocorrendo com o envolvimento de mecanismos de natureza tanto física quanto química, sendo que este último ocorre em maior parte pela troca iônica com íons de metais leves presentes no resíduo, principalmente íons Na^+, esse resultado corrobora com o resultado da análise da composição química do resíduo (EDX) antes e após a contaminação com íons Al (III), onde os principais metais leves trocáveis diminuíram notavelmente após o processo de bioadsorção. Os dados cinéticos foram adequadamente descritos pelo modelo de pseudossegunda ordem ou modelo de resistência à transferência de massa em filme externo. No estudo de equilíbrio, a isotermas obtida em temperatura mais baixa foi adequadamente representada pelo modelo de Freundlich enquanto as curvas obtidas em temperaturas mais elevadas foram representadas pelos modelos de Langmuir ou D-R, apesar das conclusões conflitantes destes modelos, a análise geral do sistema juntamente aos resultados obtidos no estudo do calor isostérico indicam que os sítios ativos da superfície do bioadsorvente são predominantemente heterogêneos. As caracterizações realizadas no material antes e após a bioadsorção revelaram que o resíduo possui estrutura irregular e macroporosa, com considerável resistência à perda de massa em temperaturas até 150 ºC e baixo envolvimento da transferência de massa nos poros do adsorvente. Verificou-se o envolvimento de grupos funcionais típicos de mecanismo de remoção de metais tóxicos, sendo eles os grupos carboxílicos, sulfatos e aminos. Em leito fixo, a

maior remoção de alumínio foi atingida à vazão de 0,5 mL/min e concentração de alimentação de 1 mmol/L, onde a capacidade de adsorção no ponto de saturação foi 0,372 mmol/g. Nos ciclos de bioadsorção/dessorção um comportamento inovador para este resíduo foi observado, onde o mesmo se manteve notavelmente viável em todos os quatro ciclos realizados. Em relação a modelagem matemática, todos as curvas de ruptura obtidas no estudo contínuo foram adequadamente preditas pelo modelo DualSD, indicando a participação de mecanismos de difusão diferentes em momentos distintos do processo.

Diante dos resultados obtidos, para dar continuidade às pesquisas relacionadas ao estudo deste sistema, sugere-se:

- Modificações na superfície do bioadsorvente buscando elevar sua capacidade adsortiva e regenerabilidade em ciclos contínuos;
- Estudos de bioadsorção em sistemas multicompostos contendo íons de alumínio e outros metais tóxicos e compostos orgânicos;
- Estudos aplicando o resíduo ao tratamento de efluentes reais ou águas naturais que apresentem contaminação por íons de alumínio;
- Avaliação da viabilidade econômica e do impacto ambiental do sistema comparando-o ao uso de adsorventes convencionais;
- Estudos em maior escala visando à aplicação industrial.

7. Referências

[1] J.O. Duruibe, M.O.C. Ogwuegbu, J.N. Egwurugwu, Heavy metal pollution and human biotoxic effects, Int. J. Phys. Sci. 2 (2007) 112–118.

[2] F.R. Segura, E.A. Nunes, F.P. Paniz, A.C.C. Paulelli, G.B. Rodrigues, G.Ú.L. Braga, W. dos Reis Pedreira Filho, F. Barbosa, G. Cerchiaro, F.F. Silva, B.L. Batista, Potential risks of the residue from Samarco's mine dam burst (Bento Rodrigues, Brazil), Environ. Pollut. 218 (2016) 813–825. https://doi.org/10.1016/j.envpol.2016.08.005.

[3] A. Sari, M. Tuzen, Equilibrium, thermodynamic and kinetic studies on aluminum biosorption from aqueous solution by brown algae (Padina pavonica) biomass, J. Hazard. Mater. 171 (2009) 973–979. https://doi.org/10.1016/j.jhazmat.2009.06.101.

[4] E. Merian, M. Anke, M. Ihnat, M. Stoeppler, Elements and Their Compounds in the Environment Edited by Related Titles Joachim Nölte Bernhard Welz , Michael Sperling Handbook of Elemental Speciation Markus Stoeppler , Wayne R . Wolf , Peter J . Jenks (eds) Reference Materials for Chemical Analysis, 2004.

[5] M.L.P. Antunes, G.R.B. Navarro, Caracterização da Lama Vermelha Brasileira (Resíduo do Refino da Bauxita) e Avaliação de suas Propriedades para Futuras Aplicações, 3rd Int. Work. Adsvances Clean. Prod. (2011) 10. http://www.advancesincleanerproduction.net/third/files/sessoes/6B/4/Antunes_MLP - Paper - 6B4.pdf.

[6] A.F. de A. Neto, Í.M. de A. Macena, J.S. de Oliveira, Análise da concentração de alumínio residual no Rio Gramame proveniente dos, Rev. Ambient. 2 (2016) 88–96.

[7] B. Volesky, Biosorption of heavy metals, 1990.

[8] D. Kratochvil, Advances in the biosorption of heavy metals, Trends Biotechnol. 16 (1998) 291–300. https://doi.org/10.1016/S0167-7799(98)01218-9.

[9] E. Fourest, B. Volesky, Alginate Properties and Heavy Metal Biosorption by Marine Algae, Appl. Biochem. Biotechnol. 67 (1997) 215–226. https://doi.org/10.1007/BF02788799.

[10] D.M. Ruthven, Principles of Adsorption and Adsorption Processes, Wiley, 1984.

[11] J. Wang, C. Chen, Biosorbents for heavy metals removal and their future, Biotechnol. Adv. 27 (2009) 195–226. https://doi.org/10.1016/j.biotechadv.2008.11.002.

[12] T.. Davis, B. Volesky, R.H.S.. Vieira, Sargassum seaweed as biosorbent for heavy metals, Water Res. 34 (2000) 4270–4278. https://doi.org/10.1016/S0043-1354(00)00177-9.

[13] T.A. Davis, B. Volesky, A. Mucci, A review of the biochemistry of heavy metal biosorption by brown algae, Water Res. 37 (2003) 4311–4330. https://doi.org/10.1016/S0043-1354(03)00293-8.

[14] Y. Barbot, C. Thomsen, L. Thomsen, R. Benz, Anaerobic Digestion of Laminaria japonica Waste from Industrial Production Residues in Laboratory- and Pilot-Scale, Mar. Drugs. 13 (2015) 5947–5975. https://doi.org/10.3390/md13095947.

[15] S.J. Horn, I.M. Aasen, K. Østgaard, Ethanol production from seaweed extract, J. Ind. Microbiol. Biotechnol. 25 (2000) 249–254. https://doi.org/10.1038/sj.jim.7000065.

[16] C.S.D. Costa, S.L. Cardoso, E. Nishikawa, M.G.A. Vieira, M.G.C. Da Silva, Characterization of the residue from double alginate extraction from sargassum filipendula seaweed, Chem. Eng. Trans. 52 (2016) 133–138. https://doi.org/10.3303/CET1652023.

[17] C. Bertagnolli, Bioadsorção de cromo na alga Sargassum filipendula e em seus derivados, (2013) 152.

[18] S.L. Cardoso, C.S.D. Costa, E. Nishikawa, M.G.C. da Silva, M.G.A. Vieira, Biosorption of toxic metals using the alginate extraction residue from the brown algae Sargassum filipendula as a natural ion-exchanger, J. Clean. Prod. 165 (2017) 491–499. https://doi.org/10.1016/j.jclepro.2017.07.114.

[19] P.Y.R. Suzaki, M.T. Munaro, C.C. Triques, S.J. Kleinübing, M.R. Fagundes Klen, R. Bergamasco, L.M. de Matos Jorge, Phenomenological mathematical modeling of heavy metal biosorption in fixed-bed columns, Chem. Eng. J. 326 (2017) 389–400. https://doi.org/10.1016/j.cej.2017.05.157.

[20] C.S.D. COSTA, Bioadsorção multicompostas de cromo (III), níquel (II) e zinco (II) utilizando resíduo da extração de alginato da alga Sargassum filipendula como bioadsorvente, (2019) 200.

ANEXO A. Licenças de publicação de artigos na dissertação

Autorização da Elsevier para a inclusão do artigo publicado em *Journal of Water Process Engineering* no Capítulo 2 desta Dissertação de Mestrado.

Copyright Clearance Center RightsLink®

Home | Help | Email Support | Sign in | Create Account

Biosorption of aluminum ions from aqueous solutions using non-conventional low-cost materials: A review

Author:
Heloisa Pereira de Sá Costa,Meuris Gurgel Carlos da Silva,Melissa Gurgel Adeodato Vieira

Publication: Journal of Water Process Engineering

Publisher: Elsevier

Date: April 2021

© 2021 Elsevier Ltd. All rights reserved.

Please note that, as the author of this Elsevier article, you retain the right to include it in a thesis or dissertation, provided it is not published commercially. Permission is not required, but please ensure that you reference the journal as the original source. For more information on this and on your other retained rights, please visit: https://www.elsevier.com/about/our-business/policies/copyright#Author-rights

BACK CLOSE WINDOW

© 2021 Copyright - All Rights Reserved | Copyright Clearance Center, Inc. | Privacy statement | Terms and Conditions
Comments? We would like to hear from you. E-mail us at customercare@copyright.com

Autorização da Springer Nature para a inclusão do artigo publicado em *Environmental Science and Pollution Research* no Capítulo 4 desta Dissertação de Mestrado.

Autorização da Elsevier para a inclusão do artigo publicado em *Journal of Water Process Engineering* no Capítulo 5 desta Dissertação de Mestrado.